DEVELOPMENT OF A PROCEDURE TO EVALUATE THE SHEAR MODULUS OF LAMINATED GLASS INTERLAYERS

A Thesis

by

MICHAEL SCOTT BRACKIN

Submitted to the Office of Graduate Studies of
Texas A&M University
in partial fulfillment of the requirements for the degree of

MASTER OF SCIENCE

May 2010

Major Subject: Civil Engineering

DEVELOPMENT OF A PROCEDURE TO EVALUATE THE SHEAR MODULUS OF LAMINATED GLASS INTERLAYERS

A Thesis

by

MICHAEL SCOTT BRACKIN

Submitted to the Office of Graduate Studies of
Texas A&M University
in partial fulfillment of the requirements for the degree of

MASTER OF SCIENCE

Approved by:

Chair of Committee,	W. Lynn Beason
Committee Members,	Terry L. Kohutek
	Harry A. Hogan
Head of Department,	John Niedzwecki

May 2010

Major Subject: Civil Engineering

ABSTRACT

Development of a Procedure to Evaluate the
Shear Modulus of Laminated Glass Interlayers. (May 2010)
Michael Scott Brackin, B.S., Civil Engineering, Texas A&M University
Chair of Advisory Committee: Dr. W. Lynn Beason

Laminated glass is comprised of multiple glass plates coupled together in a sandwich construction through the use of a polymorphous interlayer that acts as a bonding agent between the glass plates. Laminated glass offers several advantages over monolithic glass including the ability to resist post fracture collapse, improved sound insulation, lower ultraviolent light transmission, and improved thermal insulation. Because the stiffness of the interlayer is often many orders of magnitude less than that of the glass, plane sections prior to loading do not remain plane throughout the laminate's thickness after load is applied.

The behavior of laminated glass is controlled by the stiffness of the interlayer. This behavior rules out the use of classical theoretical formulations for thin plates. In such cases, it is necessary to use specially formulated equations or finite element analyses to evaluate the performance of laminated glass. Previous attempts have been made to develop procedures to quantify the interlayer stiffness for use in laminated glass design. However, there is no widely accepted technique that can be referenced for use.

It is known that the interlayer stiffness is a function of both temperature and load duration. The primary objective of this thesis is to formalize a standard procedure to estimate the in situ interlayer shear modulus through the use of nondestructive testing.

Physical experiments were carried out on simply supported laminated glass beams subject to three point loading in a temperature controlled environmental testing chamber. Strains and temperatures were recorded as a function of time. These data were used in combination with results from finite element analyses to quantify the variation of the interlayer stiffness as a function of temperature and load duration for a given laminated glass beam.

This procedure was applied to three common types of interlayer materials: freshly manufactured polyvinyl butyral (PVB), over a decade old PVB, and freshly manufactured SentryGlas Plus (SGP). Results from these efforts provide specific design guidance for laminated glass that incorporates these interlayer materials. Further, the procedure was applied to various data pre-

sented in open literature by previous researchers. In addition, a standardized procedure to estimate interlayer stiffness is provided for the development of additional interlayer properties as required.

DEDICATION

To the writer's parents, Regi and Sandra Brackin, for their continuous support, love, and guidance.

To Dr. W. Lynn "Beast" Beason for his influence and leadership in academics and structural engineering.

ACKNOWLEDGEMENTS

The writer would like to thank his committee chair, Dr. W. Lynn Beason, and committee members, Terry L. Kohutek, and Harry A. Hogan for their guidance and support in the preparation of this thesis. A special thanks to Mr. A. William Lingnell for his contributions and technical advice given herein.

Finally, thanks to Mr. Christopher T. White and Mark A. Russell for their contributions to the physical experiments presented herein.

NOMENCLATURE

ε	Strain
$\mu\varepsilon$	Micro-Strain
σ	Stress
σ_x	Stress in x-direction
υ	Poisson's Ratio
°C	Degree Celsius
°F	Degree Fahrenheit
b	Width
c	Distance from Neutral Axis to Extreme Fiber
E	Modulus of Elasticity
E_{glass}	Modulus of Elasticity of Soda Lime Glass
G	Shear Modulus
GF	Gage Factor (Distance from Strain Gage to Center of Span)
h	Height
I	Moment of Inertia
ID	Inner Diameter
$I_{glass\ plate}$	Moment of Inertia for a Single Glass Plate of a Laminated Glass Beam
$I_{monolithic}$	Moment of Inertia for a Monolithic Glass Beam
I_{total}	Moment of Inertia for the total thickness of a Laminated Glass Beam
I_x	Moment of Inertia in x-direction
L	Span Length
M	Moment
$M_{applied}$	Applied Moment
M_{gage}	Moment at Strain Gage Location
M_{max}	Maximum Moment
OD	Outer Diameter
P	Load
$P_{large\ brick}$	Load Applied from a Single Large Brick

R_1	Resistance of Internal Resistor 1
R_2	Resistance of Internal Resistor 2
R_3	Resistance of Internal Resistor 3
$R_{strain\ gage}$	Resistance of Strain Gage
R_{wire1}	Resistance of Wire 1
R_{wire2}	Resistance of Wire 2
R_{wire3}	Resistance of Wire 3
S_x	Section Modulus in x-direction
$t_{equivalent}$	Equivalent Thickness
T_g	Glass Transition Temperature
t_g	Thickness of Glass Plate
t_i	Thickness of Interlayer
V	Internal Voltmeter
x	Distance from Leading Edge of Plate

TABLE OF CONTENTS

LIST OF FIGURES

Page

Page

Page

Page

LIST OF TABLES

Page

CHAPTER I

INTRODUCTION

The use of laminated glass has become increasingly more common for architectural glazing applications. Laminated glass offers several advantages over monolithic glass. These advantages include the ability to resist post fracture collapse, improved sound insulation, lower ultraviolent light transmission, and improved thermal insulation (SAFLEX 1989; Behr, Minor, and Norville 1993; Edel 1997; Beason and Lingnel 2000).

Laminated glass is comprised of multiple glass plates coupled together in a sandwich construction through the use of a polymorphous interlayer (McLellan and Shand 1984). The purpose of the interlayer is to serve as an adhesive bonding agent that couples the glass plates together. In most common cases, laminated glass consists of two glass plates of equal thickness that are bonded together with a single interlayer whose thickness is much less than the thickness of the glass plates. Usually, the interlayer material is several orders of magnitude less stiff than the glass (Hooper 1973; Behr, Minor, Linden, and Vallabhan 1985; Edel 1997; Beason and Lingnel 2000).

In most theoretical formulations for thin flat plates, experiencing small displacements, Kirchoff's hypothesis is assumed. Kirchoff's hypothesis states that in plates subjected to bending, straight fibers initially normal to the middle surface of the plate remain straight and normal to that surface through the thickness of the plate (Timoshenko and Woinowsky-Krieger 1959, Chia 1980). More commonly Kirchoff's hypothesis is stated as: plane sections through the thickness of the plate, before loading, remain plane after loading (Gere and Timoshenko 1997).

Because the interlayer material incorporated into most laminated glass assemblies are much less stiff than glass, Kirchoff's hypothesis is frequently invalid for laminated glass. This situation makes the theoretical treatment of laminated glass much more difficult than is the case with thin monolithic glass plates. Hence, classical plate theory as advanced by Timoshenko and others is not necessarily applicable to laminated glass (Timoshenko and Woinowsky-Krieger 1959; Vallabhan, Das, and Ramasamudra 1992; Vallabhan, Das, Magdi, Asik, and Bailey 1993; Edel 1997; Beason and Lingnel 2000).

This thesis follows the style of *Journal of Structural Engineering*.

Based on the above discussion, it is necessary to have a good understanding of the interlayer properties to evaluate the behavior of laminated glass. In particular, the most important property is the shear modulus of the interlayer. While there have been several attempts to develop procedures to estimate the shear modulus of the interlayer, there is no widely accepted technique that can be referenced for use (Hooper 1973; Dice 1992; Vallabhan, Das, and Ramasamudra 1992; Edel 1997). To further complicate the situation, the interlayer stiffness varies significantly as a function of both temperature and load duration (Hooper 1973; Behr, Minor, and Norville 1993; Edel 1997).

The primary objective of the research presented herein is to develop and formalize a standard procedure that can be used to estimate the in situ shear modulus of laminated glass interlayers through testing of laminated glass beams. The procedure uses straight-forward nondestructive physical experiments on small representative laminated glass beams. Further, these beams were tested under stress levels that are representative of actual laminated glass installations. Then, these results coupled with finite element analyses, are used to estimate the interlayer shear modulus for various laminated glass interlayers. In addition, the procedure accounts for both the effects of temperature and load duration in estimating the interlayer shear modulus.

The procedure developed herein involved the development of a unique environmental testing chamber into which small laminated glass beams were completely enclosed and subjected to temperatures ranging from 30 to 120 °F. The beams were simply supported inside the environmental testing chamber and subjected to a three point loading. This loading was selected so that the interlayer will experience a constant shear throughout the length of the beam. The temperature of the laminated glass beam interlayer was monitored through the use of type K thermocouples. The bending performance of the beams were monitored using strain gages.

The laminated glass beams tested were stored in the environmental testing chamber and allowed ample time to reach thermal equilibrium at a predetermined temperature. Then, through the use of a special loading device, a static load was quickly applied to the center of the beam while the temperature and strain readings were monitored and recorded as a function of time. The basic experiment was conducted for temperatures ranging from 30 to 120 °F. Strain data collected from this effort were then tabulated as a function of temperature and load duration for a given laminated glass beam. Ultimately, these data were used to construct temperature transition charts, as defined previously by Edel (Edel 1997).

Once the performance of a particular type of laminated glass beam was quantified through physical experiments, finite element models were constructed so that a theoretical response could be calculated for each laminated glass beam tested. It is well known that the elastic properties of glass remain stable over the range of temperatures involved with the experiments (Beason 1980; McLellan and Shand 1984). Therefore, the variations in the structural performance of the beams are the result of changes in the interlayer stiffness as a function of temperature and load duration. Results from the finite element analyses were used to establish a relationship between the laminated glass beam performance and interlayer shear modulus. Finally, this theoretical relationship was used to relate the measured performance of laminated glass beams to the shear modulus as a function of temperature and load duration. Ultimately, the information is presented in a convenient tabular and graphical format.

The results of this effort included the development of an environmental testing chamber, the standardization of a testing procedure to estimate the shear modulus properties for various types of laminated glass interlayers, and the presentation of these results for important types of interlayer materials. Three different types of interlayers were examined using the procedure: freshly manufactured polyvinyl butyral (PVB), PVB that was manufactured and stored for more than a decade prior to testing, and freshly manufactured SentryGlas Plus (SGP). These interlayer types cover today's most commonly used interlayers for architectural glazing applications. Further, the procedure was applied to various data presented in open literature by previous researchers. These results provide design guidance for engineers involved with laminated glass that incorporate these interlayer materials. In addition, they provide a framework for the development of additional interlayer properties.

The next chapter of this thesis presents the problem statement. The problem statement describes the issues that arise in quantifying the structural performance of laminated glass. Chapter III discusses the history and background information associated with laminated glass. In addition, this chapter discusses the historical treatment of laminated glass and the various performance models used to aid in the analysis and design of laminated glass. Chapter IV outlines research conducted previously to better understand the behavior of laminated glass. This chapter also presents selected experiments conducted on behalf of various researchers. Chapter V lays the framework for the new standardized formal procedure to evaluate the shear modulus of laminated glass interlayers. This chapter includes a discussion on the experimental effort, finite element analyses, and the determination of a relationship between shear modulus and temperature

for a given laminated glass interlayer. In addition, the results obtained using this procedure, for the three different interlayers, are presented. Chapter VI discusses the application of the procedure to data presented on behalf of previous researchers. Finally, Chapter VII summarizes the results and conclusions drawn from the research conducted herein.

CHAPTER II

PROBLEM STATEMENT

Laminated glass generally consists of two glass plates that are coupled together through the use of a flexible interlayer in a sandwich construction. In most cases, the two glass plates have the same thicknesses. The stiffness of the interlayer material that is incorporated in laminated glass is usually orders of magnitude less than that of the glass. Because of this large difference in stiffness, the strength of laminated glass is highly dependent on the mechanical properties of the interlayer and the interaction between the interlayer and the adjacent glass plates. More specifically, the coupling interaction between the glass plates is dependent on the shear modulus of the interlayer. Extensive experimental results developed for the most common interlayer material, PVB, show that the PVB interlayer shear modulus is a function of both temperature and load duration (Hooper 1973; Behr, Minor, and Norville 1993; Edel 1997).

While research has been conducted to better understand the behavior of specific laminated glass constructions, there has been little effort directed toward the development of a standardized procedure that can be used to address the fundamental question of interlayer stiffness. Without such a standardized procedure, it is difficult to judge the effectiveness of various interlayer alternatives and it is difficult to design laminated glass based on stress analysis techniques. This problem is the focus of the research presented in this thesis.

The increased use of laminated glass has generally been driven by a loose coalition of interlayer manufacturers. In addition, the interlayer manufacturers have been responsible for the promulgation of most current design recommendations. There is a very limited amount of independently developed laminated glass design data and even less independent data relating to various interlayer properties.

The purpose of the research proposed herein is to develop a procedure that shear modulus of the interlayer to be deduced from relatively straight-forward physical experiments involving small representative laminated glass beams. The procedure will be adjusted to quantify the interlayer properties for stress levels and load durations that are meaningful with respect to glass plates under wind loading.

The procedure will be demonstrated on test specimens that employ three different types of interlayer materials: freshly manufactured PVB, PVB that has been fabricated for more than

10 years, and freshly manufactured SGP. In addition, the procedure will be applied to various data presented in open literature by previous researchers.

CHAPTER III

LAMINATED GLASS

Laminated glass consists of multiple glass plates that are bonded together using a polymorphous interlayer (McLellan and Shand 1984). In the manufacture of laminated glass, the glass plates are cleaned and positioned around the interlayer material as shown in Fig. 3-1. Then, heat and pressure are applied to the laminated glass assembly. This process develops a strong bond between the glass plates and interlayer (ASME 1963). Typically, the glass plates are of equal thickness. The glass plates can be annealed, heat-strengthened, or tempered depending on the application. In most cases, the conjoining polymorphous plastic interlayer is comprised of PVB for architectural glazing applications. In recent years, a more stiff interlayer material, SGP, has become increasingly available for use in architectural glazing. The stiffnesses of these interlayer materials are orders of magnitude less than the stiffness of glass. Common thicknesses for the interlayer are 0.015, 0.030, 0.060, or 0.090 in. A typical cross-section of laminated glass is shown in Fig. 3-1.

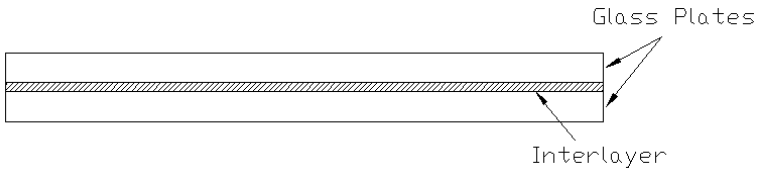

FIG. 3-1. Typical Laminated Glass Cross-Section

Historically, the purpose of laminated glass is to prevent the collapse of the laminate assembly at the time of failure. For this reason, laminated glass has gained popularity in architectural glazing applications. The polymorphous interlayer allows for fracture of either or both glass plates while maintaining adhesion to the glass shards, thus often preventing collapse (Hooper 1973; Fariss 1993). This provides added safety for laminates subjected to thermal and lateral loads. Due to the nature of the polymorphous interlayer, laminated glass can withstand impact loads much more efficiently than monolithic glass plates (Pantelides, Horst, and Minor 1991). The nature of laminated glass adds a certain level of safety and security in applications of dynamic blast loading or missile impacts from debris of hurricanes or tornadoes. It has been well

established that, these missile impacts from wind storm debris are the largest factor in glass failure (Beason, Meyers, and James 1984). Among other advantages, laminated glass offers increased thermal insulation, lower ultraviolent light transmission, and improved sound insulation (SAFLEX 1989; Behr, Minor, and Norville 1993; Edel 1997, Beason and Lingnel 2000).

Due to the interlayer incorporated into laminated glass assemblies, design complexities arise for estimating the structural performance of laminated glass. Often, the orders of magnitude difference between the stiffness of the glass and the interlayer rule out the use of traditional theoretical formulations for determining composite beam action.

More often than not, it is assumed that, for thin flat plates that undergo small displacements, Kirchoff's hypothesis is valid. Kirchoff's hypothesis states that in plates subjected to bending, straight fibers initially normal to the middle surface of the plate remain straight and normal to that surface through the thickness of the plate (Timoshenko and Woinowsky-Krieger 1959; Chia 1980). Stated in other words, Kirchoff's hypothesis says that plane sections through the thickness of the plate, before loading, remain plane after loading (Gere and Timoshenko 1997). Because the interlayer material is much less stiff than glass, Kirchoff's hypothesis cannot be automatically assumed when analyzing laminated glass. Fig. 3-2 shows the typical behavior of laminated glass beams in bending. The interlayer material allows the bottom surface of the upper glass beam to slide with respect to the top surface of the lower glass beam as shown (Gere 2006). It is this slippage that invalidates Kirchoff's hypothesis.

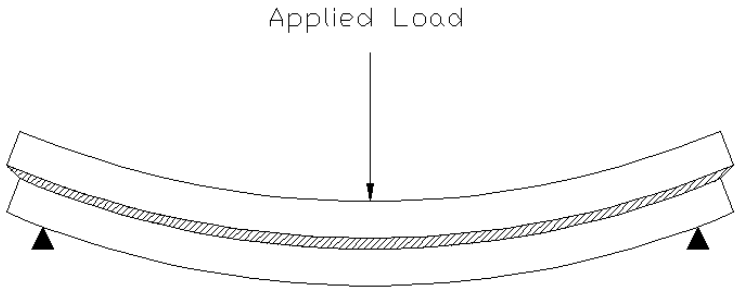

FIG. 3-2. Typical Bending Behavior of Laminated Glass

The performance of purely monolithic or layered glass plates can easily be estimated by the use of classical theoretical treatments that incorporate Kirchoff's assumption. However, when Kirchoff's assumption is violated, as in the case for laminated glass, the situation presents complexities for the use of classical theoretical treatments. Hence, classical plate theory as put forth by Timoshenko and others is not applicable for the design of laminated glass (Timoshenko and Woinowsky-Krieger 1959; Vallabhan, Das, and Ramasamudra 1992; Vallabhan, Das, Magdi, Asik, and Bailey 1993; Edel 1997; Beason and Lingnel 2000).

In addition, previous research has shown that the strength and stiffness of laminated glass varies inversely with the temperature of the laminate's interlayer (Hooper 1973; Behr, Minor, and Norville 1993; Edel 1997). Most research has shown that the structural performance of laminated glass beams, for low temperatures, can be approximated by the performance of a monolithic glass beam of the same overall thickness. In addition, research has shown that for very high temperatures, the laminated glass beam performs as two stacked glass beams with no shear transfer. In this latter case, the glass plates act independently of one another. Thus, the variation in performance between these two cases is the result of characteristic changes in the laminate's interlayer material properties. Further, the elastic properties of glass are known to be independent of temperature in the ranges of interest (Beason 1980; McLellan and Shand 1984). Therefore, the variation in the structural performance of laminated glass beams as a function of temperature must be a direct result of changes in the interlayer stiffness. It is widely accepted that the stiffnesses of the most common laminated glass interlayers are functions of both temperature and load duration (Hooper 1973; Behr, Minor, and Norville 1993; Edel 1997).

In the 1950's and 1960's, glass producers and independent consultants developed a large set of empirical glass strength data for monolithic glass subjected to uniform loadings. These uniform loadings were representative of static wind loads. These data and elementary statistical analyses were used to develop a simplified empirically based glass thickness selection chart for monolithic glass. This chart was widely circulated in glass manufacturer design literature, technical handbooks, and building codes. A technical bulletin developed by LOF presents a classic example of this simplified empirical glass thickness selection chart (LOF 1980).

For other types of glass, such as laminated, heat strengthened, tempered, insulating, etc., more limited testing was conducted. Based on the more limited set of data, basic concepts of mechanics, and engineering judgment, type factors were developed to adapt the results from the monolithic glass thickness selection chart to the other types of glass. Factors of 2.0, 4.0, 1.5, and

0.6 were commonly used for heat-strengthened, tempered, insulating, and laminated glass, respectively (UBC 1982; Boca 1984; SBC 1985). In some cases these factors were presented in tables for use by the designer and in other cases these factors were used in conjunction with the original monolithic glass thickness selection chart to produce separate charts for each of the different types of glass. It is interesting to note that the strength factor, 0.60, that was historically used for laminated glass reflected an industry wide consensus that laminated glass was not as strong as a monolithic glass of the same thickness.

At the time when the original empirical monolithic glass thickness selection charts were developed, most other structural design procedures were based on an allowable stress concept. Application of the allowable stress concept to the design of glass requires that the maximum tensile stress in the glass remain below a specified allowable stress (Beer, Johnson, and DeWolf 2002). It is known that glass is a perfectly elastic material to the point of failure (McLellan and Shand 1984; Beason and Lingnell 2000). Therefore, due to the homogeneous, elastic nature of glass prior to failure, the behavior of glass beams can be quantified using classical bending theories (Gere and Timoshenko1997).

It is believed that the origination of the 0.60 strength factor can be explained by comparing the performance of an idealized monolithic and layered glass beams of the same thickness. The idealized layered glass beam is considered to be fabricated with two identical glass beams of constant thickness, *h*. In this case it is assumed that one of the beams is simply stacked on top of the other beam so that there is zero shear transfer between the beams when a loading is applied. The total thickness of the layered beam is then equal to *2*h*. The idealized monolithic glass beam is considered to be a single glass beam with a total overall thickness of *2*h*. For each idealized model, the beams are taken to be prismatic with x as its longitudinal axis.

For the idealized monolithic glass beam acting elastically, with overall total thickness of *2*h*, the maximum bending stress, σ_x, can be calculated using the elementary flexure formula as follows:

$$\sigma_x = \frac{M_{max}}{S_x} \tag{3-1}$$

where M_{max} is the maximum moment applied to the beam and S_x is the elastic section modulus. The section modulus, S_x, is a function of the beam's cross-sectional geometry as follows:

$$S_x = \frac{b * (2 * h)^2}{6} \tag{3-2}$$

where *b* is the glass beam width and *2*h* is the total height of the monolithic beam.

The maximum bending stress in the idealized monolithic glass beam can then be calculated using the following:

$$\sigma_x = \frac{3 * M_{max}}{2 * b * h^2} \tag{3-3}$$

where all of the variables are as previously defined.

For the case of an idealized layered glass beam, where no shear is transferred between the two glass plates, the moment resisted by a single plate is equal to:

$$M = \frac{M_{max}}{2} \tag{3-4}$$

The section modulus, S_x, for a single glass beam can be calculated as follows:

$$S_x = \frac{b * h^2}{6} \tag{3-5}$$

where *b* is the glass beam width and h is the thickness of a single glass beam. Then, the maximum bending stress in the idealized layered glass beam can be calculated as follows:

$$\sigma_x = \frac{3 * M_{max}}{b * h^2} \tag{3-6}$$

where all of the variables are as previously defined.

Based on the above discussion it can be shown that the maximum bending stress in an idealized layered glass beam is exactly one half of the maximum bending stress in an idealized monolithic glass beam when they are both exposed to the same bending moment. This analysis

would support a strength factor of 0.50 for laminated glass using the traditional approach. The use of 0.50 would be based on the assumption that no shear force is transferred through the interlayer material and that the thickness of the interlayer does not affect the bending behavior. However, while it is difficult to quantify these effects, it seems clear that the interlayer would transfer some shear and that interlayer thickness would thus increase the effective section modulus of a laminated glass beam. These effects combine to increase the apparent strength of a laminated glass beam. It is believed that these observations, coupled with a small amount of experimental data, led engineers and researchers to decide on a strength reduction factor of 0.60 instead of 0.50. This factor estimates the strength of laminated glass beams to be 60 percent of the strength of an equivalent monolithic glass beam of equal thickness. This strength factor remained in use from its introduction through the early 1980's.

The American Society for Testing and Materials (ASTM) first introduced a standard for glass thickness selection in 1989. This standard began a transition for determining glass strength from glass manufacturer's recommendations, to peer reviewed independent engineers and designers. The new ASTM standard included glass thickness selection charts for monolithic annealed glass plates only. No design guidance was provided for any other type of glass including laminated glass. The ASTM glass thickness selection charts, for the first time, were based on theoretical methodologies and estimations of fundamental glass surface properties which set them apart from the empirical glass industry tradition. (ASTM 1989)

It wasn't until 1994 that ASTM first adopted a procedure for the design of laminated glass. The initial treatment of laminated glass by ASTM involved the strength concept that was initially introduced by the glass industry except that the laminated glass strength factor was taken to be 0.75 for most situations. The 0.75 strength factor was adopted for the ASTM standard with little to no supporting documentation or experimental results to quantify its use over the 0.60 strength factor. This standard clearly states that the strength factors proposed were interim values (ASTM 1994). The results of ongoing research to understand the structural behavior of laminated glass would later be used to define a more permanent methodology for estimating the strength of laminated glass. In addition, the strength factors were meant for a 60 s uniform pressure load, i.e. wind, at room temperature conditions (ASTM 1994). The standard noted that this factor probably should be reduced for elevated temperatures greater than room temperature (ASTM 1994). The use of this procedure was highly disputed between glass researchers and engineers alike.

In 2002, the ASTM standard included design charts developed for laminated glass with a variety of support conditions. These charts were not made on the basis initially set forth by the glass industry for the treatment of laminated glass using strength reduction factors. The data used to build the charts, were developed by means of theoretical methodologies and estimations of fundamental glass surface properties. The charts assume that the laminated glass has a PVB based interlayer and is exposed to a 3 s uniform pressure loading condition. This loading condition is considered by some to be representative of wind loads. In addition, it is assumed that the laminated glass is not exposed to an ambient temperature in excess of 120°F (ASTM 2002).

INTERLAYER MATERIALS

Laminated glass is fabricated with a polymorphous interlayer (McLellan and Shand 1984). This interlayer is commonly referred to as a plastic. A plastic is a synthetic or naturally organic material that softens or hardens with temperature (Somayaji 2001). Polymer describes the basic repeating unit of molecules that makeup a plastic material (Somayaji 2001).

In general terms there are two types of polymorphous plastics: thermoset and thermoplastic. A thermoset material cannot be reshaped upon being manufactured, whereas a thermoplastic material softens and melts when gradually heated (Somayaji 2001). In addition, a thermoplastic may be heated and reshaped multiple times (Somayaji 2001). Therefore, the elastic properties of a thermoplastic could undergo a transition with a change in temperature.

For thermoplastic polymers, a temperature exists at which the material experiences a marked transformation from a rubbery state to a more rigid state when cooled, or vice versa when heated (Callister 2007). This temperature is known as the glass transition temperature, T_g (Callister 2007). Unlike thermoset plastics, the physical properties of thermoplastics abruptly change at the glass transition temperature (Somayaji 2001). Properties affected include stiffness, heat capacity, and coefficient of thermal expansion (Callister 2007). The glass transition temperature is often used to define temperature bounds for the use of thermoplastics in various applications. To further complicate the situation, thermoplastic polymers that have almost identical compositions can have great variances with respect to material properties such as modulus of elasticity, ductility, and strength (Young, Mindess, Gray, and Bentur 1998). Fig. 3-3 presents an example of the variation of an elastic property, such as shear modulus, as a function of tempera-

ture (Edel 1997). The two most common types of interlayer materials used in the fabrication of laminated glass are both specified as thermoplastic polymers.

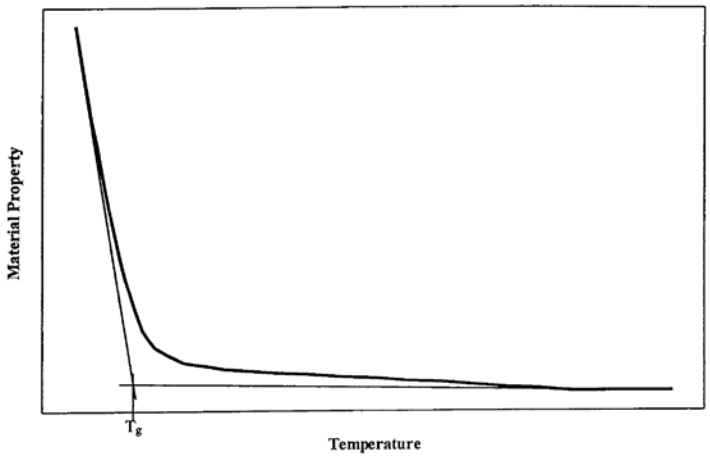

FIG. 3-3. Thermoplastic Material Property as a Function of Temperature Source: Edel 1997

As seen in Fig. 3-3, the performance of a thermoplastic polymer changes over a small range of temperatures and approaches a constant slope at both high and low temperatures. The intersection of these two slopes, seen in Fig. 3-3, is taken as the glass transition temperature (Brandrup and Immergut 1989). The rate at which a material's temperature is allowed to change can affect the glass transition temperature, however this affect may be neglected, for most polymers, that have remained at a constant temperature for a minimum of ten minutes (Brandrup and Immergut 1989).

To further complicate this issue, the glass transition temperature for thermoplastic polymers is greatly affected by the addition of plasticizers (Fariss 1993). For the case of laminated glass, the addition of plasticizer to the interlayer not only reduces the glass transition temperature, but can increase the range over which the material transitions (Edel 1997). The extent of which a plasticizer can affect the glass transition temperature is inversely related to the amount of plasticizer used, along with the type of plasticizer (Edel 1997).

Introducing plasticizers into interlayer materials can greatly affect the structural performance of laminated glass (Hooper 1973; Dice 1992; Edel 1997). Several of the advantages associated with laminated glass are achieved through the use of plasticizer mixed interlayers. Plasticizers are used to give laminated glass its compliance in safety applications, such as wind-

shields in the automotive industry, and its greater impact resistance against missile impacts and blast loadings in architectural glazing applications. These advantages are accomplished by the plasticizers ability to affect the elasticity of the interlayer material at temperatures below the glass transition temperature (Fariss 1993). In addition, the plasticizer gives stronger adhesive properties to aid in preventing post fracture collapse of the laminated glass (Fariss 1993).

An unaltered sheet of the most common interlayer material, PVB resin, has a glass transition temperature of approximately 158 °F (Fariss 1993). The addition of plasticizers to the PVB resin to produce the desired properties for laminated safety glass, reduce the glass transition temperature of the PVB resin/plasticizer mix to around 77 °F (Fariss 1993). Further research to define PVB's glass transition temperature has also shown that PVB begins to rapidly change material properties around room temperature (68 to 77 °F) (Edel 1997; Bennison, Qin, and Davies 2008). In fact, most data collected, suggests that for laminated glass with a PVB interlayer, the glass transition temperature is around room temperature. It is interesting to note, that Texas Tech's Glass Research and Testing Laboratory (GRTL) has reported that the transition in the behavior of laminated glass is not clearly defined but does not occur until temperatures around 120 °F (Behr, Minor, and Norville 1993). Alternatively, the GRTL has made claims that the performance transition occurs around 100 °F (Norville, King, and Swofford 1998). The GRTL maintains that at room temperature (75 °F) laminated glass behaves near that of monolithic glass (Behr, Minor, Linden, and Vallabhan 1985; Vallabhan, Minor, and Nagalla 1987; Minor and Reznik 1990; Behr, Minor, and Norville 1993).

It has been shown, that for laminated glass beams manufactured with a PVB based interlayer, the rate of change in interlayer material properties, at temperatures below the glass transition temperature, occur very rapidly. In contrast, the rate of change of the interlayer's material properties above the glass transition temperature occur much more gradual (Edel 1997).

Alternatively, SGP maintains a much higher glass transition temperature than that of PVB. The glass transition temperature for SGP occurs around 130 to 140 °F (Bennison, Smith, Duser, and Jagota 2002; Bennison, Qin, and Davies 2008).

Historically, PVB has been the choice interlayer material for manufacturing laminated glass. First introduced in the 1930's, laminated glass has been manufactured for more than seven decades. Since its conception, laminated glass manufactured with a PVB interlayer has been used for automotive safety glazing. Later, laminated glass became widely accepted for architectural glazing applications. Throughout this period, the PVB interlayer has been modified to en-

hance the structural performance of laminated glass. Modifications have been made for both the automotive and architectural industries. The use of a PVB interlayer make attainable, the advantages that distinguish laminated glass from other types of glass. PVB works to prevents post fracture collapse while maintaining a desired level of compliance for safety applications. In addition, PVB has improved the sound insulation, thermal insulation, and reduced ultraviolent light transmission in laminated glass.

There are several major chemical companies that produce laminated glass interlayers. Each of these companies have brand names specific to their products. While others exist, DuPont Company and Solutia are major producers of interlayer materials. DuPont Company produces a PVB interlayer known as BUTACITE and the SGP interlayer known as SentryGlas Plus. Solutia, previously Monsanto Company, produces a PVB interlayer known as SAFLEX.

The main disadvantage to the use of laminated glass with a PVB interlayer is its lower bending strength as compared to a monolithic glass of equal thickness. It has been well established that this lower performance is directly related to the PVB interlayer stiffness. Research conducted by an independent researcher, J.A. Hooper, shows that the average shear modulus for architectural grade PVB is about 90 psi for short term loadings (less than 3 minutes) at room temperature conditions (68 to 77 °F) (Hooper 1973). At the same time, GRTL researchers reported that an average shear modulus for PVB interlayer is about 300 psi (Vallabhan, Das, and Ramasamudra 1992) and 1000 psi (Behr, Minor, Linden, and Vallabhan 1985; Behr, Minor, and Linden 1986) for architectural glazing applications. The GRTL values have no defined temperature or load duration associated with them. There is a tremendous difference in the performance of laminated glass associated with variations of the interlayer shear modulus between the values of 90, 300, and 1000 psi. There exist many factors that influence the properties of PVB interlayer and its corresponding effects on the behavior of laminated glass. Therefore, the use of an average interlayer shear modulus that encompasses all conditions is not possible.

In the last decade, DuPont Company has developed and released the new interlayer material SGP for use in architectural laminated glass. SGP was developed for hurricane resistant glazing applications that cannot be accomplish with the use of common PVB based interlayers. Compared to PVB, SGP offers increased strength, improved creep response, improved durability, improved material compatibility, and a higher glass transition temperature (Bennison, Smith, Duser, and Jagota 2002; Bennison, Qin, and Davies 2008). These properties give SGP a more

stiff behavior through a larger range of elevated temperatures and longer load durations (Bennison, Smith, Duser, and Jagota 2002; Bennison, Qin, and Davies 2008).

LAMINATED GLASS PERFORMANCE MODELS

To help evaluate the structural performance of laminated glass, three simplified analytic models have been widely used. These simplified models are often used when it is more important for the results to be conservative rather than accurate. These three simplified analytical models are: the fully monolithic performance model, layered performance model, and the equivalent monolithic performance model. The models do not rigorously account for the variation in mechanical properties of the thermoplastic interlayer material. The fully monolithic performance model and the layered performance model create an upper and lower boundary for laminated glass performance. Fundamental laws of mechanics, enforce that the laminated glass behavior act within the bounds defined by these models. The layered performance model provides an absolute minimum design strength. The fully monolithic performance model is absolute maximum design strength. The equivalent monolithic model provides a compromise solution between the other two.

It is assumed that each of the simplified analytical models behaves elastically. Assumptions within each model make valid, Kirchoff's hypothesis that plane sections remain plane. Thus, the use of classical bending theory can be applied. For a prismatic beam, taking x to be its longitudinal axis, the maximum bending stresses can be calculated using the following equation:

$$\sigma_x = \frac{M * c}{I_x} \tag{3-7}$$

where M is the applied moment, I_x is the moment of inertia, and c is the distance from the neutral axis to the extreme fiber. Values for these parameters are defined specifically for each model in the following pages.

For each of these three models, the stresses are calculated as a function of loading and geometry. Thus, the stresses calculated using these methods are constant with respect to temperature.

Fully Monolithic Performance Model

The fully monolithic performance model assumes that the structural behavior of a laminated glass beam is comparable to the structural behavior of a monolithic glass beam of the total thickness of the laminated glass assembly. Thus, the thickness of the equivalent monolithic glass beam is taken to be equal to the sum of the glass plate thicknesses plus the interlayer thickness as shown in Fig. 3-4.

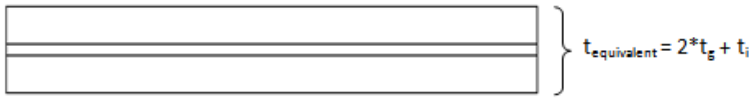

FIG. 3-4. Fully Monolithic Performance Model Equivalent Thickness

where t_g and t_i are a single glass plate thickness and the interlayer thickness, respectively.

This model assumes the interlayer is capable of transferring shear fully between the two glass beams. The mechanical properties of the interlayer are assumed to be that of glass. The bending behavior of the true monolithic performance model is taken to be as shown in Fig. 3-5. It is assumed that plane sections remain plane through the full thickness of the glass and interlayer.

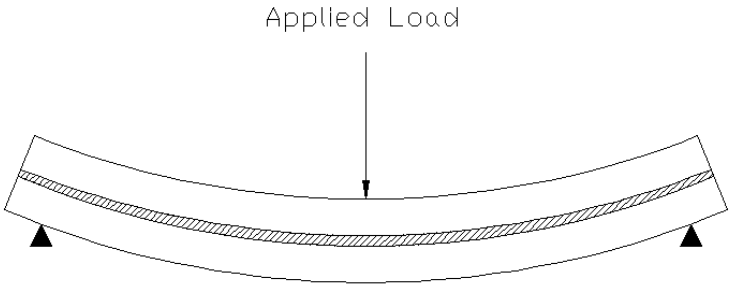

FIG. 3-5. Fully Monolithic Performance Model Bending Behavior

For the fully monolithic performance model, I_x, c, and M are as follows:

$$I_x = \frac{b * (2 * t_g + t_i)^3}{12} \tag{3-8}$$

$$c = t_g + \frac{t_i}{2} \tag{3-9}$$

$$M = M_{applied} \tag{3-10}$$

Therefore, the maximum tensile stress for the fully monolithic performance model is:

$$\sigma_x = \frac{6 * M_{applied}}{b * (2 * t_g + t_i)^2} \tag{3-11}$$

where the parameters are as defined previously.

Layered Performance Model

The second of these models is the layered performance model. The layered performance model generalizes the structural behavior of laminated glass to be an equivalent system of independent monolithic glass beams. The monolithic glass beams are stacked in layers on top of one another. It is assumed that there is no shear transfer between the glass beams. Shown in Fig. 3-6, the model is comprised of two independent glass plates lying directly on top of one another.

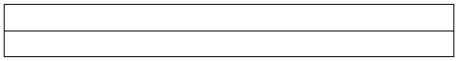

FIG. 3-6. Layered Performance Model Cross-Sectional Thickness

When load is applied, the glass beams are allowed to bend independent of one another. The interlayer's ability to transfer shear between the glass plates is assumed negligible. The bending behavior of this model is taken to be as shown in Fig. 3-7.

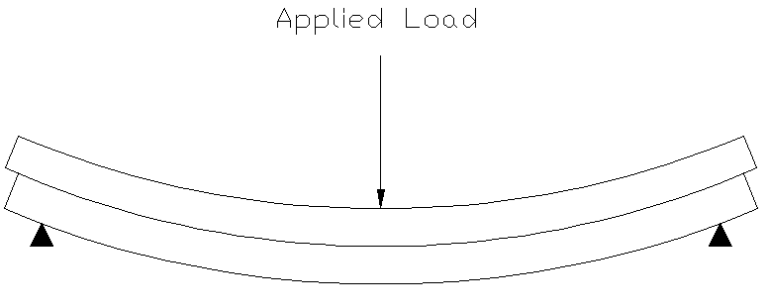

FIG. 3-7. Layered Performance Model Bending Behavior

For the layered performance model, I_x, c, and M are as follows:

$$I_x = \frac{b * {t_g}^3}{12} \tag{3-12}$$

$$c = \frac{t_g}{2} \tag{3-13}$$

$$M = \frac{M_{applied}}{2} \tag{3-14}$$

Therefore, the maximum tensile stress for the layered performance model can be calculated as follows:

$$\sigma_x = \frac{3 * M_{applied}}{b * {t_g}^2} \tag{3-15}$$

where the parameters are as defined previously.

Equivalent Monolithic Performance Model

The third model is known as the equivalent monolithic performance model. This model is similar to the fully monolithic performance model except that an equivalent monolithic thickness is used instead of the total thickness. The equivalent monolithic thickness is usually taken

to be somewhere between the thickness of a single glass plate and the total thickness of the laminated glass assembly. The GRTL suggested that the equivalent monolithic glass should be taken as the sum of the two individual glass plate thicknesses. Others have employed factors that are simply multiplied by the fully monolithic thickness of the glass. The GRTL's interpretation of the equivalent monolithic thickness is shown in Fig. 3-8.

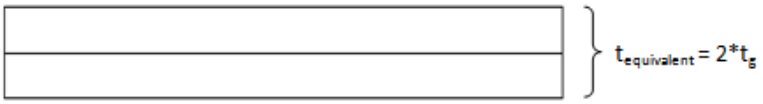

FIG. 3-8. Equivalent Monolithic Performance Model: GRTL's Equivalent Thickness

In this model it is assumed that shear is fully transferred between the glass plates. This model is analyzed as a monolithic glass plate with the specified equivalent thickness. The equivalent monolithic performance model has sometimes been called the GRTL glass only monolithic performance model.

The equivalent monolithic performance model was recommended for use in laminated glass design by the GRTL (Behr, Minor, and Norville 1993). Originally, the GRTL conducted experiments in which they reported that the behavior of laminated glass was bound by the layered performance model and fully monolithic performance model (Behr, Minor, Linden, and Vallabhan 1985; Vallabhan, Minor, and Nagalla 1987).

Later, the GRTL conducted several experiments, while under contract with Monsanto Company, to set in motion the idea that, for most boundary and load conditions, the strength of laminated glass manufactured with Monsanto's PVB interlayer was equivalent to, or exceeded that of an equivalent monolithic glass plate (Norville, King, and Swofford 1998). The GRTL stated that the interlayer thickness should not be included when calculating the equivalent monolithic thickness (Behr, Minor, and Norville 1993).

The use of this model was never fully accepted because it violates fundamental laws of mechanics and holds no relevant validity in estimating the performance of laminated glass. In addition, it requires a different equivalent thickness to model the deflections of glass than it does to model stresses.

For the equivalent monolithic performance model, I_x, c, and M are as follows:

$$I_x = \frac{2 * b * {t_g}^3}{3} \tag{3-16}$$

$$c = t_g \tag{3-17}$$

$$M = M_{applied} \tag{3-18}$$

Therefore, the maximum tensile stress for the equivalent monolithic performance model can be calculated using the following:

$$\sigma_x = \frac{3 * M_{applied}}{2 * b * {t_g}^2} \tag{3-19}$$

where the parameters are as defined previously.

CHAPTER IV

PREVIOUS RESEARCH

Previous research into the structural behavior of laminated glass has been performed by various independent researchers over the past several decades. In addition, research has been conducted to quantify interlayer material properties for laminated glass. However, there has been much debate over the structural performance of laminated glass between these various researchers.

This chapter focuses on the research conducted previously into the structural behavior of laminated glass. The results from various experiments are presented on behalf of these previous researchers.

EXPERIMENTS CONDUCTED BY HOOPER

In 1973, J. A. Hooper conducted a study into the bending of architectural laminated glass. This study was in conjunction with the construction of the Sydney Opera House in Sydney, Australia. Both theoretical and experimental studies were performed to better understand the performance of laminated glass. Individual laminated glass beams were tested in a typical four point loading device. The loading configuration for Hooper's test setup is as shown in Fig. 4-1. Each laminated glass beam had dimensions of 22 in. by 2 in. Glass and interlayer thicknesses varied for each experiment.

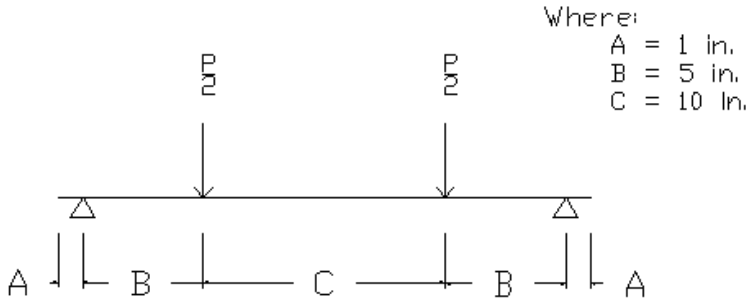

FIG. 4-1. Hooper's Four Point Loading Configuration

Hooper conducted these test with common interlayer materials used at the time. He termed the interlayer materials soft and hard. The hard interlayer was commonly used in the aircraft industry, whereas the soft was more commonly found in architectural applications and the automotive industry. The primary difference between the soft and hard interlayers was that the soft interlayer had a higher plasticizer content than did the hard interlayer.

Two series of test were conducted. The first series investigated the effects of short term loading on the bending of laminated glass beams. These tests were conducted in approximately 3 min or less at a constant ambient temperature of 70 ˚F.

For short term loading, Hooper found that a slight creep deformation occurred in the hard interlayer. This resulted in a slightly non-linear load-deformation versus strain-deformation curve. Creep was negligible in the soft interlayer. Thus, the load-deformation versus strain-deformation curves were near linear. It was determined, that at a constant temperature of 70 ˚F, the increase in proportion of plasticizer leads to a decrease in interlayer shear modulus for short term loading.

The second series of test investigated the effects of a sustained loading on the bending of laminated glass beams. These tests were conducted over various temperatures with a sustained dead load over approximately 80 days. These tests helped to determine the creep behavior of the interlayer. Deflections and ambient temperature were recorded at several intervals. Temperatures of 35, 77, and 120 ˚F were tested. For all cases the load-deflection curves were near linear.

Hooper determined that for architectural laminated glass, the bending resistance of architectural glass is primarily dependent on two things: interlayer thickness and shear modulus. Further, he found that the PVB interlayers are thermoplastic materials whose mechanical properties are affected by plasticizer content, ambient temperature, and load duration. Hooper showed that temperature has a dominate affect on the interlayer stiffness. Further, Hooper showed that the interlayer shear modulus could differ by several orders of magnitude over a narrow range of temperatures.

Hooper also determined that creep from load duration, with the exception of low temperatures, has substantially the same effect across all types of laminates independent of the interlayer type. Independent of the plasticizer proportion, creep loading of sufficient time allows the shear modulus of the interlayer to approach zero.

Hooper concluded that for sustained loads, such as snow or self weight, it would be reasonable to determine the deflections of a laminated glass beam based only on the two indepen-

dent glass layers as the interlayer contributes no coupling due to zero shear stiffness. In the case of short term loading such as wind, a reasonable shear modulus can be computed using Fig. 4-2. The information presented in Fig. 4-2 assumes a Poisson's ratio of 0.40. The selected shear modulus should be based on the maximum actual temperature of the interlayer and include the effects of solar radiation on its temperature. Once the shear modulus is defined, deflections can be estimated for the laminated glass.

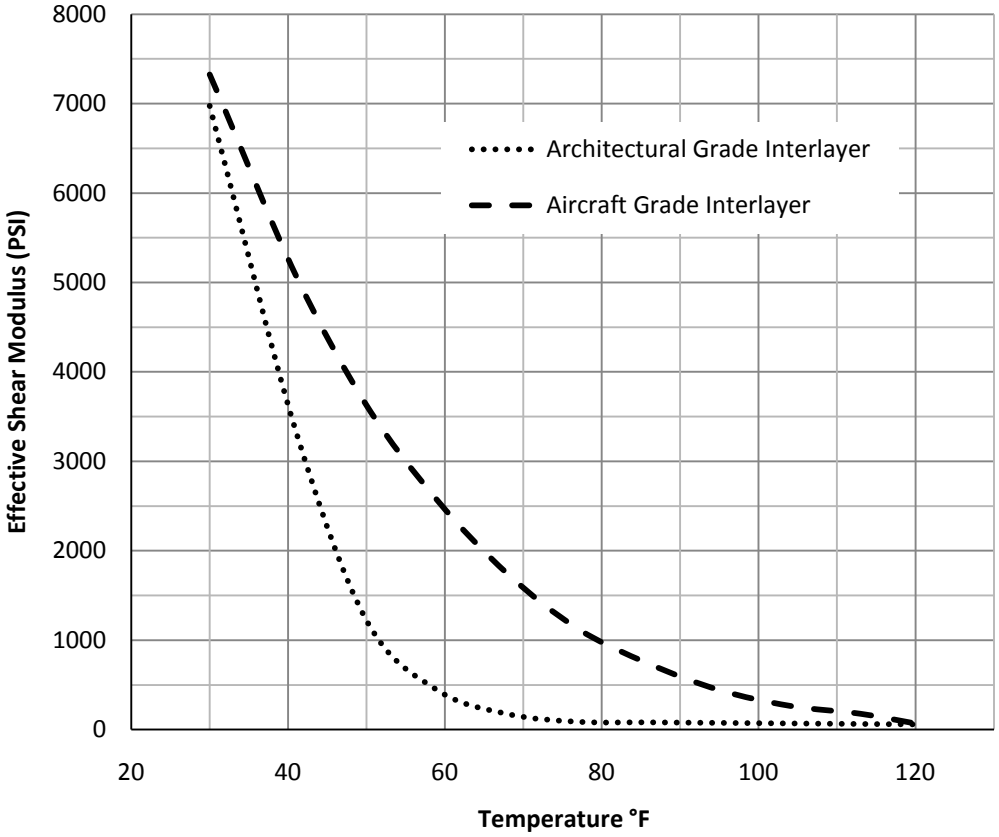

FIG. 4-2. Results from Experiments Conducted by Hooper Assuming Poisson's Ratio of 0.40

EXPERIMENTS CONDUCTED BY GRTL

Further research into the behavior of laminated glass beams has been conducted on behalf of the GRTL. Specifically, in 1993, the GRTL conducted studies to quantify the effects of

temperature on the behavior of laminated glass beams. In addition, several aspect ratios for laminated glass plates were also tested.

The laminated glass beams used in the experiments were manufactured with a Monsanto PVB interlayer. The beams were comprised of two equal thickness, 0.106 in., glass layers. The interlayer was 0.030 in. thick. Each laminated glass beam was 20 in. by 20 in. square. The beams, were simply supported and loaded as shown in Fig. 4-3.

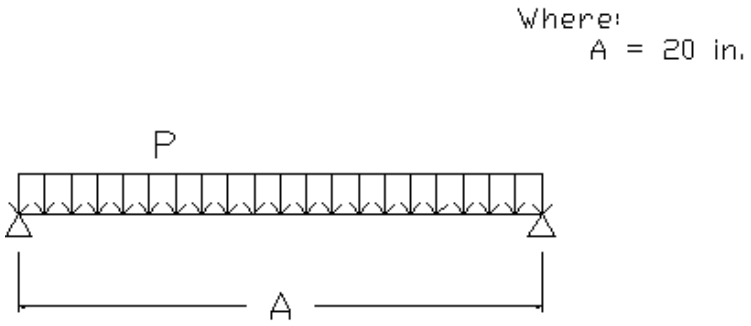

FIG. 4-3. GRTL's Loading Configuration

A uniform pressure load was applied to the beam through the use of a bladder device. The load was slowly applied in 14.5 psf increments from 0 to 58 psf. Each load increment was applied as near linear as possibly over 15 s. Between each increment the load was held for 5 to 7 s. Maximum Strains and deflections were taken after each load increment was applied. This experiment was conducted for three temperatures. A new laminated glass beam was used for each temperature. It is not clear how the specimen's interlayer temperatures were maintained uniformly and constant for the duration of each experiment. Data were provided for 32, 73, and 115 °F. These data were compared to the simplified analytical models and plotted as a function of load. Fig. 4-4 shows the results of these experiments.

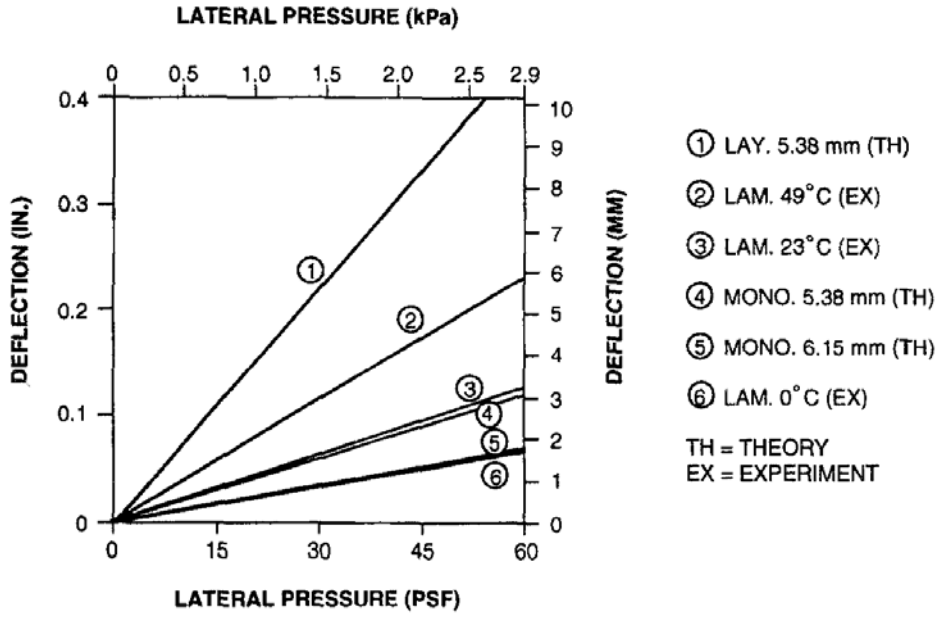

FIG. 4-4. Results of Experiments Conducted by GRTL Source: Behr, Minor, Norville 1993

Further analysis conducted later, on behalf of Edel, found that the GRTL had made an error in calculating the fully monolithic performance model (Edel 1997). Further, Edel found the results of GRTL's experiments closely matched that of Hooper's hard interlayer and not that of the soft interlayer (Edel 1997). The GRTL admittedly states that their results are in sharp contrast to that of Hooper's (Behr, Minor, and Norville 1993). In addition, the GRTL claims that laminated glass behaves like monolithic glass, of an equivalent thickness, for long load durations below 32 °F (Behr, Minor, and Norville 1993). Although the GRTL's definition of equivalent thickness has differed between reports, here it is clearly taken as the thickness of the two glass plates only. Such a loading condition might represent a snow load. Again, both of these claims are in direct contrast to the experiments conducted by Hooper.

From these experiments and others, the GRTL proposes that, for most architectural glazing applications, the design of laminated glass should be based on a monolithic glass of equivalent thickness under short duration loads at or below room temperatures (Behr, Minor, Linden, and Vallabhan 1985; Behr, Minor, and Linden 1986; Behr, Minor, and Norville 1993).

The GRTL stated that for laminated glass to behave similar to an equivalent monolithic glass, the interlayer must be 100 percent effective (Behr, Minor, and Linden 1986). In addition, the GRTL has also stated that, under certain geometry and load conditions, a laminated glass

plate can perform similar to that of a monolithic glass plate of equal thickness even if the interlayer provides no strength (Vallabhan 1987).

EXPERIMENTS CONDUCTED BY STEWART

In 1990, Bob Stewart of PPG Industries ran experiments to quantify the effects of temperature on the bending of laminated glass beams (Stewart 1991). Through informal correspondence, these experiments and their data were collected. The experiments used instrumented laminated glass beams to test their structural behavior as a function of temperature for 60 s load durations.

The beams were 14 in. long by 2 in. wide. The laminated glass beams had two, 0.120 in. thick, glass plates and were manufactured with a PVB interlayer, 0.030 in. thick. The beams were subjected to four point loading as shown in Fig. 4-5. A load of 50 lb was applied.

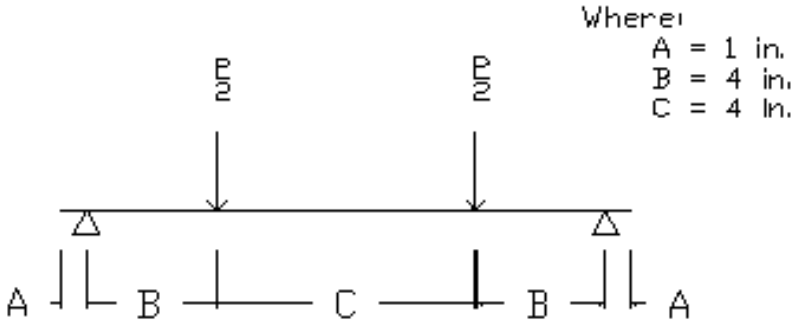

FIG. 4-5. Stewart's Four Point Loading Configuration

Strain gages were used to record the maximum stresses for each glass surface. Interpretation of Stewart's efforts show a transition temperature of the PVB based interlayer to be approximately 77 °F (Edel 1997). Further analysis of Stewart's efforts show, with exception to data collected at 60 °F, the laminated glass beams performed within the limiting boundaries set forth by the fully monolithic performance model as well as the layered performance model (Edel 1997). Ignoring the conflicting data, Stewart's results were consistent with experimental data collected by Hooper for a soft interlayer material (Edel 1997). These data collected are presented in Fig. 4-6.

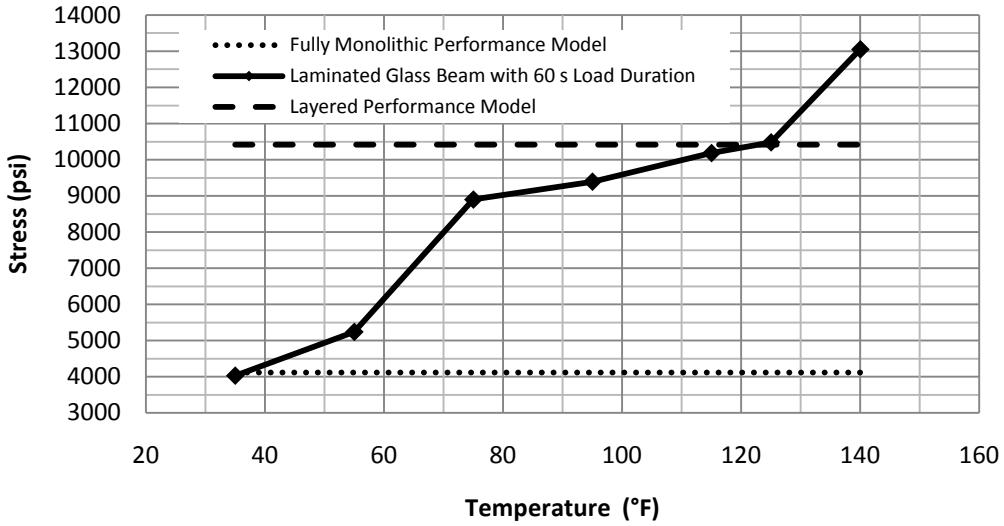

FIG. 4-6. Results of Experiments Conducted by Stewart

EXPERIMENTS CONDUCTED BY EDEL

In 1997, M. T. Edel conducted experiments to quantify the effects of temperature on the bending of laminated glass. Edel's efforts formalized a standard method to determine and describe the effects of temperature on the bending of laminated glass. From this research, Edel produced what is known as the laminated glass temperature transition chart.

The laminated glass temperature transition chart describes the relationship between stress and temperature for laminated glass beams. In addition, the chart compares the actual performance of laminated glass beams to that of the simplified analytical models. An example of this chart is shown in Fig. 4-7.

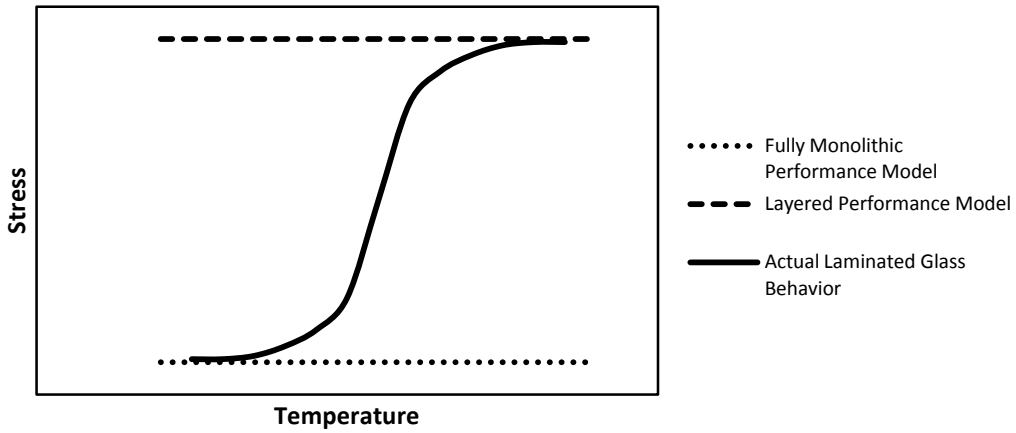

FIG. 4-7. Example of a Typical Laminated Glass Beam Temperature Transition Chart

Edel conducted physical experiments to formalize a standardized procedure for developing the laminated glass temperature transition chart. The experiments quantified the effects of temperature on bending stress for certain laminate glass beams. Experimental data was collected on four laminated glass beams. Each beam was subjected to three point loading as shown in Fig. 4-8. A 20.8 lb load was applied. The beams were 24 in. long by 6 in. wide. The laminated glass beams had equally thick, 0.126 in., glass plates. The PVB interlayer was 0.060 in. thick.

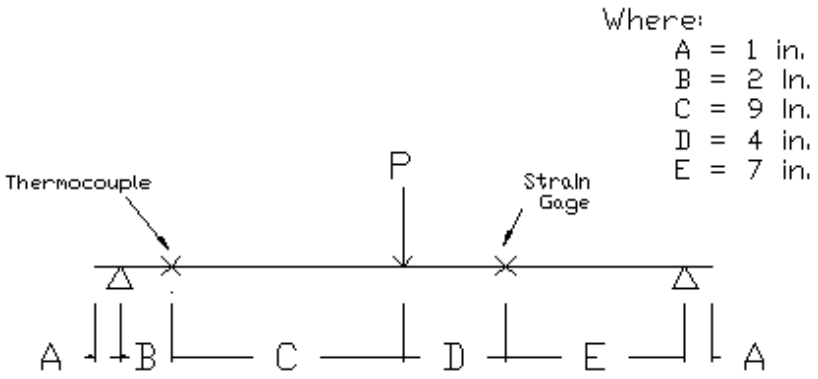

FIG. 4-8. Edel's Three Point Loading Configuration

Each beam was manufactured with commonly used interlayer materials of that time. The interlayer materials were provided by two independent suppliers. These suppliers were Monsanto Company and DuPont Company. Each interlayer material was an architectural grade PVB.

Each beam was instrumented with strain gages located as shown in Fig. 4-8. For a constant load, strain data was collected through a range of temperatures from 20 to 120 °F. Tests were conducted in increments of 10 degrees. Tensile stress in the beam was calculated from the strain readings using the following equation:

$$\sigma = \varepsilon * E_{glass} \tag{4-1}$$

where ε is the strain and E_{glass} is the modulus of elasticity for soda lime glass.

These stress data, for a given laminated glass beam, were plotted as a function of temperature to produce the laminated glass beam temperature transition chart. By averaging the data collected from the four beams at 60 s load durations, a temperature transition chart can be drawn. Fig. 4-9 presents this temperature transition chart for 60 s load durations.

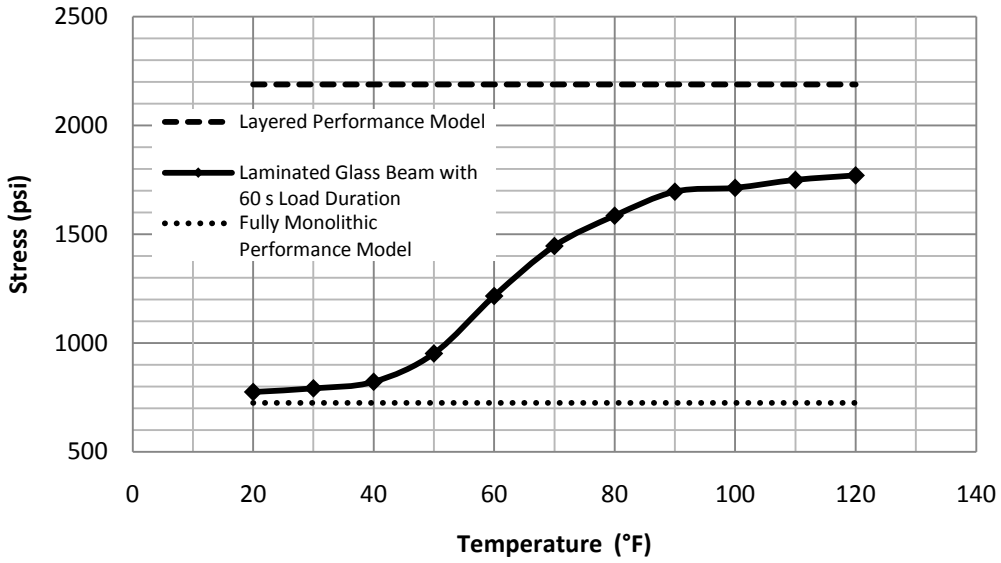

FIG. 4-9. Results of Experiments Conducted by Edel

EXPERIMENTS CONDUCTED BY DUPONT

In the last decade, DuPont Company has released technical bulletins and reports containing engineering values for their primary interlayer materials BUTACITE and SGP. The technic-

al bulletins and reports provide design engineers with mechanical properties for the interlayer materials the company produces.

Most recently, DuPont Company has published a technical report that gives the mechanical properties of SGP for a range of temperatures and load durations. Table 4-1 and Table 4-2 present the modulus of elasticity, *E*, and Poisson's ratio, υ, respectively, for SGP. This report does not contain tabulated engineering values for BUTACITE.

TABLE 4-1. Modulus of Elasticity for DuPont SGP

***E* (psi)**	**Load Duration**						
°F	**1 S**	**3 S**	**1 Min**	**1 Hour**	**1 Day**	**1 Month**	**10 Years**
50	100366.1	98770.7	94419.57	86587.53	80205.87	72373.83	64976.91
68	91083.7	88763.1	82236.4	71503.6	62076.15	47862.45	37129.66
75.2	84266.93	81366.17	73244.06	60335.7	47427.34	31473.19	18709.87
86	64106.68	59900.59	46992.23	25816.72	21465.59	5032.81	2306.1
104	33068.6	27122.06	13285.46	4032.049	1972.513	1430.072	1282.134
122	15664.08	11428.97	4902.276	1827.475	1225.569	948.5468	870.2264
140	5119.832	3553.425	1580.911	739.6925	561.296	469.9223	422.0598
158	1638.926	1273.431	818.0128	365.4951	256.7168	208.8543	195.8009
176	674.4255	574.3494	361.144	139.2362	108.7783	91.37377	78.32038

Source: Bennison, Qin, and Davies 2008

TABLE 4-2. Poisson's Ratio for DuPont SGP

υ	Load Duration						
°F	1 S	3 S	1 Min	1 Hour	1 Day	1 Month	10 Years
50	0.442	0.443	0.446	0.45	0.454	0.458	0.463
68	0.448	0.449	0.453	0.459	0.464	0.473	0.479
75.2	0.452	0.453	0.458	0.465	0.473	0.482	0.489
86	0.463	0.466	0.473	0.485	0.488	0.497	0.499
104	0.481	0.484	0.492	0.498	0.499	0.499	0.499
122	0.491	0.493	0.497	0.499	0.499	0.5	0.5
140	0.497	0.498	0.499	0.5	0.5	0.5	0.5
158	0.499	0.499	0.5	0.5	0.5	0.5	0.5
176	0.5	0.5	0.5	0.5	0.5	0.5	0.5

Source: Bennison, Qin, and Davies 2008

These data may be used to determine the shear modulus for the SGP interlayer using the following equation:

$$G = \frac{E}{2 * (1 + \upsilon)} \tag{4-2}$$

where E and υ are defined previously and G is the shear modulus. Table 4-3 presents the shear modulus for SGP deduce from the previous tables using Equation 4-2.

TABLE 4-3. Shear Modulus for DuPont SGP

G (psi)	Load Duration						
°F	1 S	3 S	1 Min	1 Hour	1 Day	1 Month	10 Years
50	34801.01	34224.08	32648.54	29857.77	27581.11	24819.56	22206.74
68	31451.55	30629.09	28298.83	24504.32	21200.87	16246.59	12552.29
75.2	29017.54	27999.37	25117.99	20592.39	16098.89	10618.48	6282.696
86	21909.32	20429.94	15951.2	8692.497	7212.898	1680.965	769.2128
104	11164.28	9138.159	4452.231	1345.811	657.943	477.0087	427.663
122	5252.876	3827.52	1637.367	609.5649	408.7955	316.1823	290.0755
140	1710.031	1186.056	527.322	246.5642	187.0987	156.6408	140.6866
158	546.6733	424.7603	272.6709	121.8317	85.57227	69.61811	65.26698
176	224.8085	191.4498	120.3813	46.41208	36.25943	30.45792	26.10679

Early data from DuPont presents differing values from those presented above for the shear modulus of SGP interlayer. These earlier data were obtained through informal correspondence through ASTM committee meetings. Within this document, engineering values for the shear modulus and Poisson's ratio are explicitly defined, for both SGP and BUTACITE, as a function of temperature and load duration. Engineering values for the modulus of elasticity were not included in this document. Table 4-4 and 4-5 present these values for SGP and BUTACITE, respectively.

TABLE 4-4. Previously Published Shear Modulus for DuPont SGP

G (psi)	Load Duration					
°F	3 S	1 Min	1 Hour	1 Day	1 Month	>1 Year
68	18129.71	13923.62	6193.11	3132.814	1406.866	942.7451
86	9528.977	5134.335	2117.55	1000.76	449.6169	420.6093
104	3219.837	1682.437	739.6923	420.6093	406.1056	290.0754
122	1029.768	551.1433	420.6093	377.098	290.0754	290.0754

Source: DuPont 2004

TABLE 4-5. Previously Published Shear Modulus for DuPont Butacite (PVB)

G (psi)	Load Duration					
°F	3 S	1 Min	1 Hour	1 Day	1 Month	>1 Year
68	1169.004	237.8618	121.8317	73.67915	53.95402	38.58003
86	140.8316	109.2134	63.96163	40.75559	10.0076	7.54196
104	88.473	65.99215	33.93882	33.93882	7.54196	7.54196
122	63.81659	42.06093	7.54196	7.54196	7.54196	7.54196

Source: DuPont 2004

Engineering values for shear modulus for SGP collected from these data, previous and more current, are compared in Fig. 4-10 for a 60 s load duration. It is clear through examination of Fig. 4-10 that DuPont's assessment of the shear modulus for SGP has changed with time. This presents somewhat of a dilemma for design engineers who must choose between the previous and more current performance estimates. To further complicate the situation, techniques and procedures used to establish these data are not presented by DuPont. Rather, these results are presented apriori. While this is not the most desirable situation from a scientific standpoint, these are the only SGP data available in the open literature at this time.

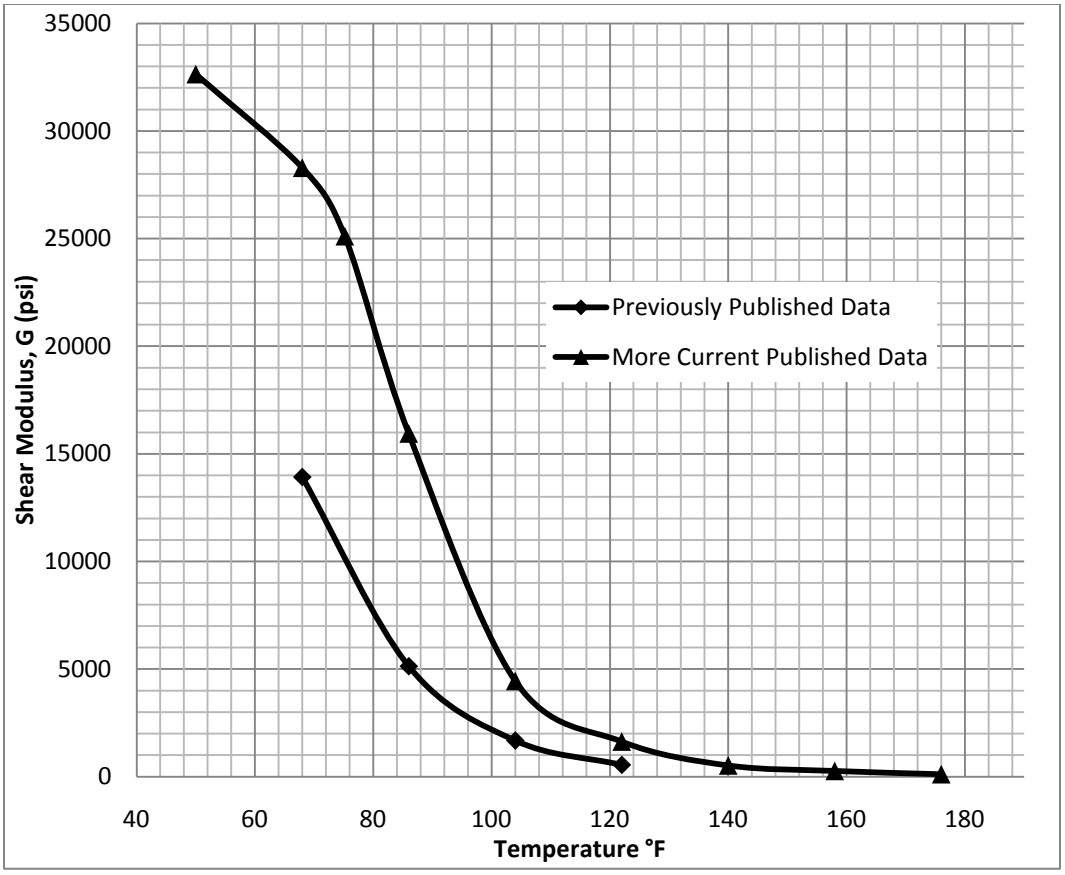

FIG. 4-10. Shear Modulus for SGP as a Function of Temperature for 60 S Load Duration as Provided by DuPont

CHAPTER V

A STANDARD PROCEDURE TO EVALUATE THE SHEAR MODULUS OF LAMINATED GLASS INTERLAYERS

The research discussed in the previous chapter shows that the behavior of laminated glass is directly influenced by the stiffness of the interlayer material. Therefore, the interlayer shear modulus must be clearly defined to understand the behavior of laminated glass. While there have been a few attempts to develop a procedure to estimate the stiffness of laminated glass interlayers, there is no widely accepted technique referenced for use. This chapter presents the development of a standard procedure to estimate the in situ interlayer shear modulus through the use of nondestructive testing and finite element analyses.

The procedure described in this chapter encompasses three separate phases: experimental effort, finite element analyses, and determination of the relationship between shear modulus and temperature. Each of these phases are dependent on one another and are discussed in further detail.

The first phase of the procedure uses straight-forward nondestructive experimental testing to quantify the effects of temperature and load duration on the bending of laminated glass beams. These experiments test the beams to stress levels representative of actual laminated glass installations. The beam's performance (strain and temperature) will be measured as a function of load duration. These data will be used to develop laminated glass beam temperature transition charts, as previously defined, for a given laminated glass beam. The temperature transition chart defines the relationship between stress and temperature for a given laminated glass beam and load duration. These experiments will test laminated glass beams through a temperature range of 30 to 120 °F and load durations from 10 s to 60 min.

The second phase of this procedure employs finite element analyses to quantify the effects of shear modulus on the bending of laminated glass beams. Finite element models will be used to develop a theoretical performance for each beam as a function of shear modulus. Ultimately, these analyses provide a theoretical relationship between stress and shear modulus.

Finally, these data will be used to quantify the variation of the beam's interlayer shear modulus as a function of temperature for a given load duration. Once the performance of a particular type of laminated glass beam has been quantified through experimental testing and finite

element analyses, interpolation techniques can be applied to deduce the interlayer's shear modulus as a function of temperature. More specifically, the data collected from physical experiments can be cross-plotted with data collected through finite element analyses to estimate the interlayer shear modulus as a function of temperature for a given load duration.

These data will ultimately be presented in a convenient tabular and graphical format. These results will provide specific design guidance for laminated glass incorporating the tested interlayer materials. In addition, the standardized procedure lays the framework for future testing to estimate in situ interlayer material properties.

EXPERIMENTAL EFFORT

Freshly manufactured laminated glass beams with an SGP interlayer were purchased from a local glass supplier. As well, freshly manufactured laminated glass beams with a PVB interlayer were purchased from the same glass supplier. Both, the freshly manufactured PVB and SGP beams provided, were 30 in. long by 4 in. wide. The PVB laminated glass beam consisted of two 0.107 in. thick glass plates. The PVB interlayer was 0.030 in. thick. The freshly manufactured SGP beams had two 0.129 in. thick glass plates. The SGP interlayer was 0.090 in. thick. A third set of laminated glass beams, that were manufactured over a decade previously, with a PVB interlayer were also used for experimentation. These older beams have been in a temperature and humidity controlled storage unit. The beams have not been exposed to thermal cycles like that of ordinary laminated glass typically used in architectural glazing applications. Nor have the beams been exposed to direct sunlight for the duration of storage. The decade old PVB laminated glass beams were 24 in. long and 6 in. wide. These laminated glass beam had two 0.129 in. thick glass plates and a 0.060 in. thick interlayer. These dimensions stated, for all three beam types, were measured directly from the beams provided. It is worth noting that a larger interlayer thickness may give a more accurate representation of the interlayer shear stiffness (Hooper 1973). In order to prevent discrepancies or inconsistencies often involved with the cut edge of the laminated glass, a larger length-to-width ratio was selected for the beams.

A direct relationship exists between temperature and load duration to the shear stiffness of laminated glass interlayer. To account for these affects, an environment testing chamber was designed. The environmental testing chamber allows the beams to be tested through a range of temperatures from 30 to 120 °F. In addition, the environmental testing chamber allows for the

beams to be tested for various load durations while maintaining a near uniform ambient temperature. The variations in beam temperature where maintained within, on average, ± 1 °F. Information on the development of the environmental testing chamber can be found in Appendix A. Because the temperature remained constant for each test, a strain gage temperature correction curve to account for the variation of temperature was not used for the experiments conducted herein.

The laminated glass beams were subjected to three point loading as shown in Fig. 5-1 and 5-2 for the freshly manufactured PVB and SGP beams, and the decade old PVB beams, respectively.

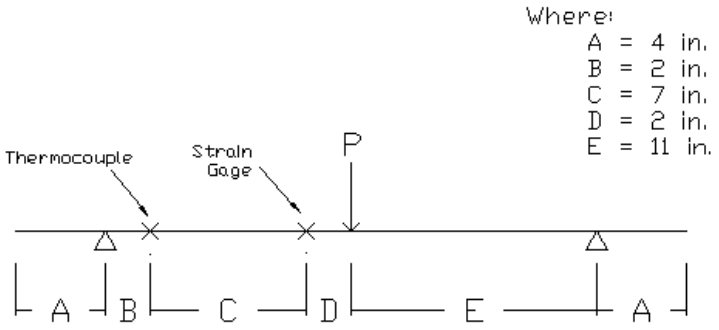

FIG. 5-1. Freshly Manufactured Laminated Glass Beams with PVB and SGP Three Point Loading Configuration

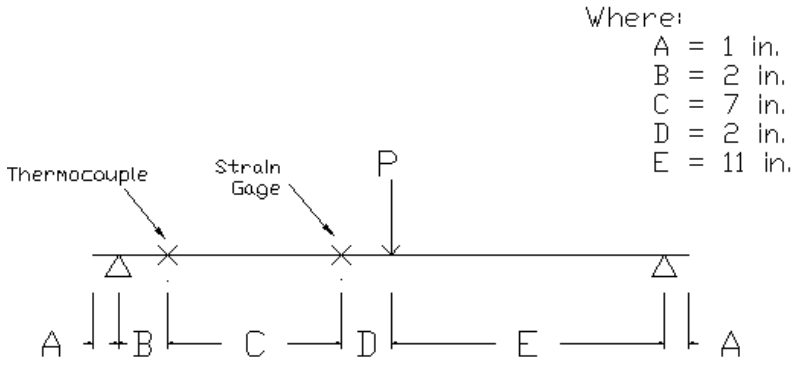

FIG. 5-2. Decade Old Laminated Glass Beams with PVB Three Point Loading Configuration

The three point loading condition shown in Fig. 5-1 and 5-2 were selected to give a constant shear force across the length of the member, a desired advantage in estimating the interlayer shear stiffness. The moment along the beam is a function of the shear. A constant change in

moment allows for the strain at any point along the length of the beams to be easily calculated. A shear and bending moment diagram are shown in Fig. 5-3 and 5-4, respectively.

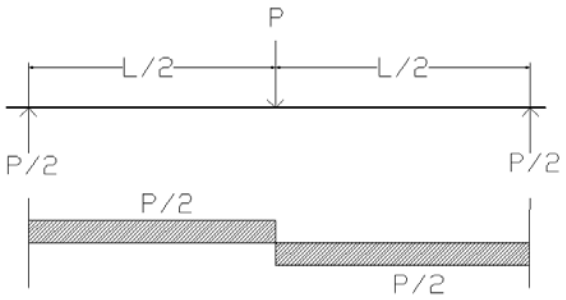

FIG. 5-3. Three Point Loading Shear Diagram

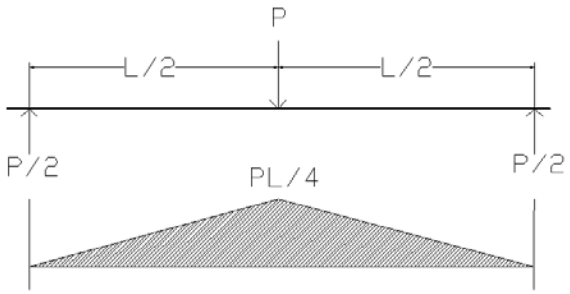

FIG. 5-4. Three Point Loading Moment Diagram

Each laminated glass beam was instrumented, using a quarter Wheatstone bridge circuit, with 350 ohm strain gages. The strain gages were used to measure tensile strains on the outer most face of the glass plates. Further, the strain gage measured strains in the longitudinal direction of each beam. For the loading condition shown in Fig. 5-1 and 5-2, the maximum tensile strain occurs on the bottom most face for each beam. The quarter Wheatstone bridge circuit is shown in Fig. 5-5.

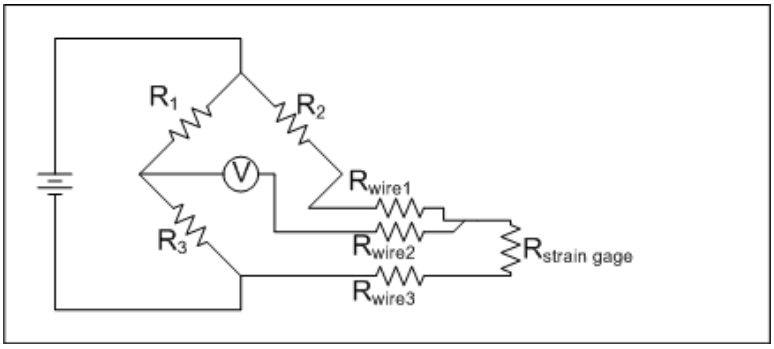

FIG. 5-5. Quarter Wheatstone Bridge Circuit

CEA-06-500UW-350 strain gages were used to measure the performance of each beam tested. Each strain gage was 350 Ohms ± 0.3% at 24 °C with a gage factor of 2.080 ±0.5% at 24 °C. Prior to laying each strain gage, the glass surface was cleaned and prepared with a PH neutralizing solution and secured with an adhesive bonding agent. After the strain gages were attached to each beam, the strain gages were generously coated with a silicone protective layer. The silicone layer served to protect the strain gage from slight impacts and provided a cover of insulation from the extreme temperatures. In addition, the insulation cover helped to reduce the risk of condensation forming on the strain gage. Condensation could accumulate as an affect from the extreme temperature differentials the beams experience while loading and unloading in the environmental testing chamber. A 3-conductor wire, flux, and solder were used to connect between the strain gages and strain indicator. Fig. 5-1 and 5-2 show the position of the strain gauges for each laminated glass beam. These positions take advantage of Saint-Venant's Principle. Thus, the strain gages are located away from the point of load application. Saint-Venant's Principle states that a statistically equivalent force distribution can be used to represent an actual force distribution and that the stress and strain in the body are altered only at regions nearest the point of load application (Ugural and Fenster 2008).

To measure the beam's interlayer temperature, type K thermocouples were embedded into the interlayer, between the glass plates. If embedment was not possible, such as in cases where the interlayer material is to thin or hard, the beam's temperature was measured on the outer surface of the glass. Embedment was not possible for the freshly manufactured PVB and SGP beams. The thermocouples were positioned as shown in Fig. 5-1 and 5-2. The beams were stored in the environmental testing chamber for an appropriate amount of time, prior to testing,

to allow the beam's temperature to stabilize at the correct testing temperature. Fig. 5-6 and 5-7 show an instrumented beam with strain gages and thermocouples, respectively.

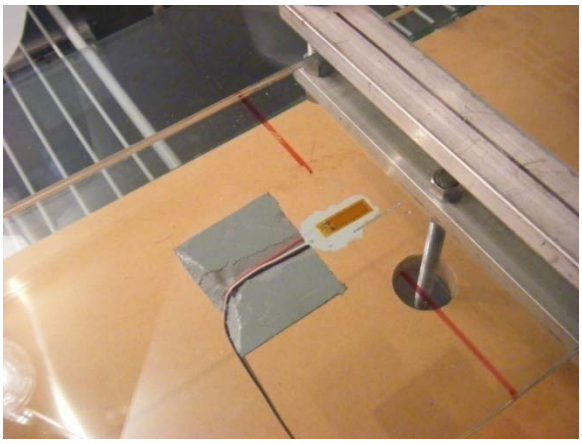

FIG. 5-6. Laminated Glass Beam Instrumented with 350 Ohm Strain Gage

FIG. 5-7. Laminated Glass Beam Instrumented with, Interlayer Embedded, Type K Thermocouple

Strain data was collected using a digital strain indicator. Temperature readings were taken using a digital thermocouple indicator. The predetermined time interval at which both the strain and temperature data were collected was determined using a simple stopwatch.

Each experiment was documented using a video recorder. An LED indicator was placed next to the strain indicator to specify the exact time the load was applied. The manner in which the load is applied near instantaneously is discussed later in this chapter. Video recording allows for further data analysis and/or verification of the data collected. A frame by frame analysis is

possible using the recorded video for more accurate results. The instrumentation setup and video recorder are shown in Fig. 5-8 and 5-9, respectively.

FIG. 5-8. Strain Indicator, Thermocouple Indicator, and Timer Setup

FIG. 5-9. Video Recording and Instrumentation Setup

It is important to test each beam specimen to stress levels that appropriately represent wind loads on architectural glazing installations. A loading assembly was developed to safely and accurately load the beams. The loading assembly loads the beams to a determined stress level while maintaining deflections within desired tolerances. The loading assembly consists of various components working together to provide a controlled three point loading condition. This assembly includes: the loading platform, load spreading bar, pneumatic cylinder assembly, and weight basket. These items will be discussed further.

The loading platform provides simply supported reaction points for the beams to be subjected to three point loading. The base of the loading platform is made from ¾ in. medium density fiberboard (mdf) and is cut to dimensions. The base is 32 in. long by 11 ½ in. wide. A 1 ¼ in. hole drilled directly in the center allows for the load spreading bar to penetrate. Two 7 in., 2x4 in., southern pine timbers were placed 11 in. on center from the base's centerline in each direction. Centered atop these is another timber cut into an approximate equilateral triangle. These triangular pieces create a loading point for the beams and will be referred to as loading points. To prevent crushing under load, the loading points were fabricated with hard, dense wooden materials. Red oak was used for the experiments conducted herein. Each loading point was 7 in. long with approximately ¾ in. sides. A single tip of the loading point was shaved slightly to create a 1/16 in. wide surface for the beams to rest on. Then, double sided taped was used to attached the two components, the loading point to the bottom timber. This gave a simple support system for the beams, 22 in. on center span length. The loading platform is shown in Fig. 5-10.

FIG. 5-10. Loading Platform

The second component of the loading assembly is the load spreading bar. The load spreading bar serves to distribute the load, to be applied, across the width of the beams. The

load spreading bar is configured such that all its components are in tension or bending. This configuration increases stability and stiffness, while eliminating buckling issues that occur when members are in compression. Aluminum materials were selected to minimize the weight of the load spreading bar. This device is shown in Fig. 5-11.

FIG. 5-11. Load Spreading Bar

The load spreading bar is made from two, 8 in. long, aluminum bars. Each bar is coupled together with 5/16 in. all thread rods at each end. The bars are 3/8 in. thick and ¾ in. wide. The upper face of the bottom bar is spaced 1 ¼ in. from the bottom face of the upper bar. This allows the laminated glass beams to pass through. The upper bar transfers load to the beam specimen through a ¼ in. by ¼ in. rubber strip. The rubber strip is attached to the aluminum bar using double sided tape. The bottom bar attaches to a 5/16 in. all thread rod, in the center. The all thread rod is 24 in. long and serves to attach the load spreading bar to the pneumatic cylinder assembly. A closer view of this configuration is shown in Fig. 5-12. Fig. 5-13 depicts how the three point loading condition is achieved when the load spreading bar is coupled with the loading platform.

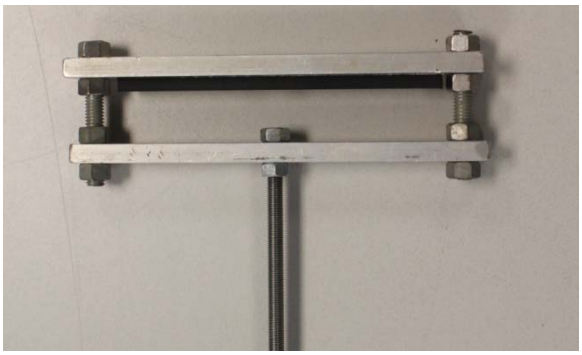

FIG. 5-12. Load Spreading Bar Head Assembly

FIG. 5-13. Load Spreading Bar Coupled with Loading Platform

It is important to allow each beam's ambient temperature to stabilize at the desired testing temperature, prior to each experiment. Once the beam temperature has reached equilibrium the environmental testing chamber cannot be opened without the risk of disturbing the state of thermal equilibrium. This situation restricts access to the beam for applying load. For this reason, a pneumatic cylinder assembly was developed and used to near instantaneously load the beam. Using the pneumatic cylinder assembly, load could be applied to the beam without disturbing the environmental testing chamber's temperature. Further, this prevented the beam temperature's state of equilibrium from being disturbed.

A front nose mount, double action pneumatic cylinder, shown in Fig. 5-14, was used for the experiments conducted herein. The pneumatic cylinder had a 3.0 in. stroke and 1-1/16 in. diameter bore. It had the capability of 250 psi, maximum pressure, at temperatures of -20 to 200

°F. At working pressures of 100 psi the pneumatic cylinder is capable of extending 90 lb and retracting 82.3 lb. These specifications exceed those required for loading the laminated glass beams. The cylinder weighed 0.5 lb.

FIG. 5-14. Pneumatic Cylinder

The pneumatic cylinder served to link the weight basket to the load spreading bar and allow the beam specimens to be loaded without disturbing the environmental testing chamber's temperature. Once pressure has been engaged, the pneumatic cylinder retracts from an extended position, prior to loading, to lift the weight basket off its supports and transfer the load into the load spreading bar. As seen in Fig. 5-15, the shaft of the cylinder connects to the 5/16 in. all thread rod of the load spreading bar with a 5/16 in. coupling nut. A locking nut tightens atop the coupling nut to prevent loosening during experiments.

FIG. 5-15. Pneumatic Cylinder Assembly Attachment to Load Spreading Bar through a Coupling Nut

A soft spring and damping device, placed on the shaft of the pneumatic cylinder, act in tandem to counter the dynamic effects that occur when the pneumatic cylinder is engaged. These devices act to change the rate at which the pneumatic cylinder accelerates to a stop once the pneumatic cylinder has been engaged and load has been transferred to the beams. For damping, a ¼ in. diameter, thick walled, o-ring, fitting tightly around the pneumatic cylinder's shaft, was used. The o-ring was placed above the spring as shown in Fig. 5-16 below. A 5/16 in. washer was placed between each component to prevent them from overlapping. The spring stiffness and length was selected by experimentation.

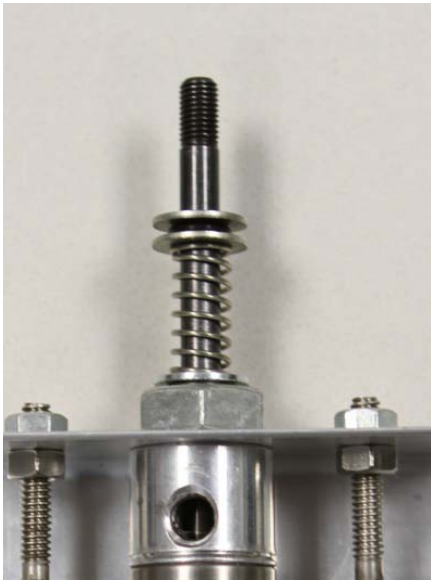

FIG. 5-16. Pneumatic Cylinder Shaft with Spring and O-ring

A 1-1/2 x 1-1/2 x 1/8 in. piece of aluminum angle, 4 in. long, was adapted to attach the weight basket to the pneumatic cylinder nose mount. The attachment bracket is shown in Fig. 5-17. The pneumatic cylinder mounts in a 5/8 in. hole drilled directly in the center of the bracket. Two ¼ in. eye bolts are mounted 1 in. from the center of the bracket, in each direction.

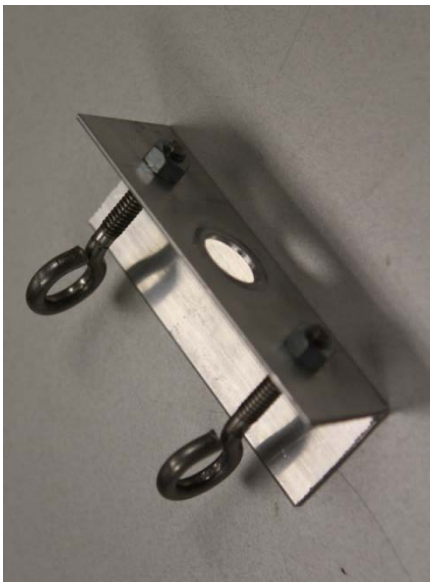

FIG. 5-17. Pneumatic Cylinder Aluminum Mounting Bracket

Basic 1/8 in. chain and chain links where used between the four mounting eyes of the weight basket and the eye bolts. Each link had a 220 lb load capacity. These components and their configuration are shown in Fig. 5-18. Fig. 5-19 shows the light weight wire basket selected to carry the load. The weight basket is 11 ½ in. long, 9 in. wide, and 6 in. deep with four mounting eyes. Fig. 5-20 and 5-21 are front and side views, respectively, of the pneumatic cylinder and weight basket assembly.

FIG. 5-18. Pneumatic Cylinder Assembly with Aluminum Bracket Attachment

FIG. 5-19. Weight Basket

FIG. 5-20. Pneumatic Cylinder Assembly Attached to Weight Basket (Front View)

FIG. 5-21. Pneumatic Cylinder Assembly Attached to Weight Basket (Side View)

The loading assembly was ergonomically placed inside the environmental testing chamber to allow for easy loading and unloading of the laminated glass beams. The loading assembly was also placed such that the beams were in the visibility of the environmental testing chamber's viewing window. The loading platform was supported by a steel wire frame shelf mounted inside the environmental testing chamber. This setup is shown in Fig. 5-22. The load spreading bar passed through the wire frame shelf to attach to the pneumatic cylinder assembly below.

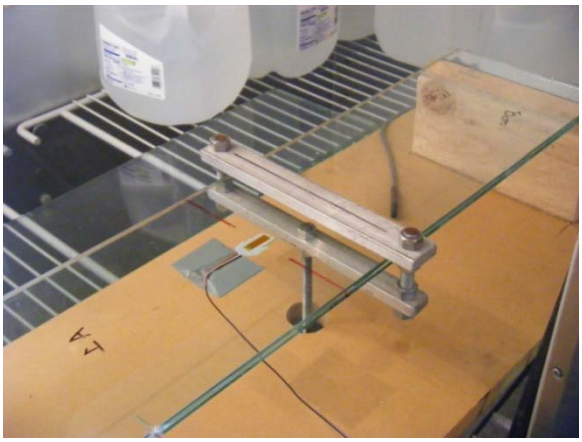

FIG. 5-22. Loading Platform Mounted on Environmental Testing Chamber Shelf

Prior to engaging the pneumatic cylinder, the weight basket rested on two rubber support pads. Fig. 5-23 shows the supports, placed on the floor of the environmental testing chamber. Once the pneumatic cylinder is pressurized the weight basket is lifted off the rubber support pads.

FIG. 5-23. Pneumatic Cylinder Assembly and Weight Basket on Rubber Supports in Environmental Testing Chamber

A complete schematic diagram of the loading assembly, setup inside the environmental testing chamber is shown in Fig. 5-24.

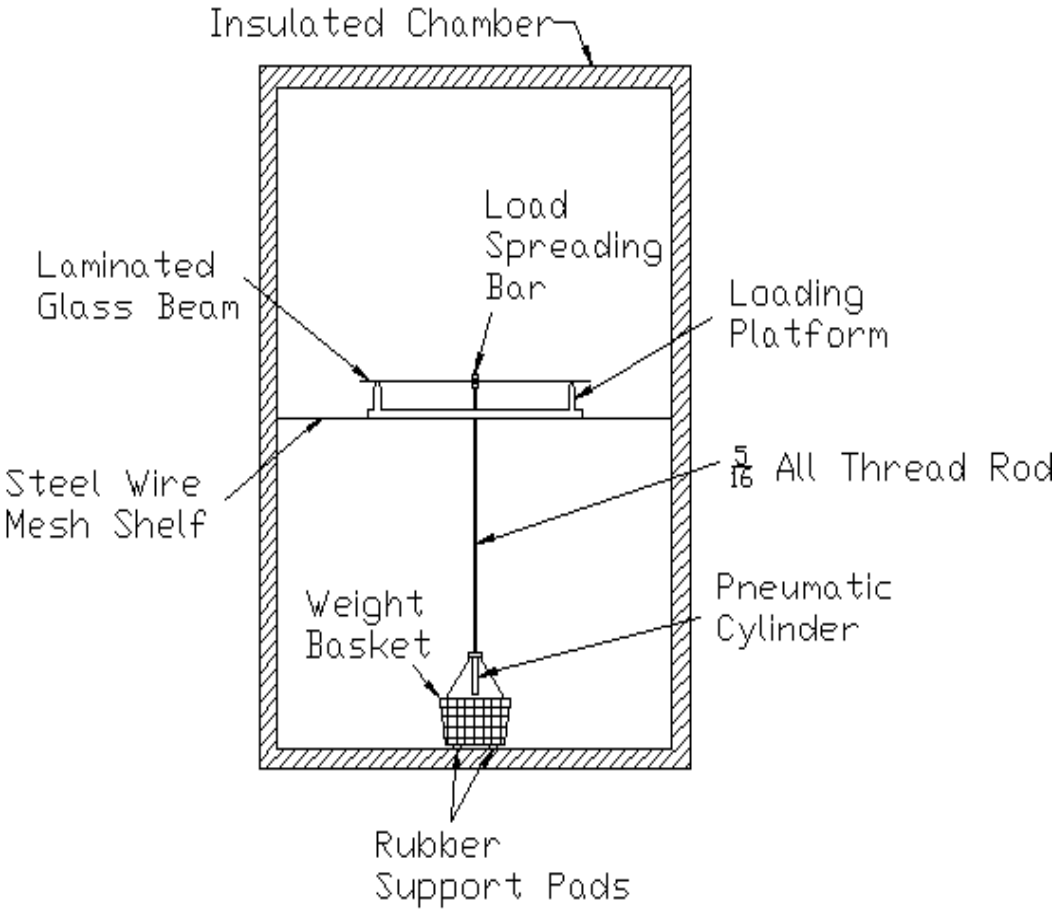

FIG. 5-24. Loading Assembly Schematic Diagram

A closed loop, high pressure pneumatic system was developed to control the pneumatic cylinder. For experiments conducted herein, a high volume of air flow, in cubic feet per min (cfm), can be neglected. Here, air pressure is important for engaging the pneumatic cylinder. An industrial air compressor provided clean, pressurized air at 125 psi.

For each beam, strains and temperatures were recorded at predetermined time intervals. This required precise timing for the load to be applied. To achieve this, a 24 volt electric valve injects pressurized air into the pneumatic cylinder near instantaneously. The air injection valve was engaged with the push of a button. The air injection engagement switch is shown in Fig. 5-25 below.

FIG. 5-25. Pneumatic Cylinder Air Injection Engagement Switch

Once the electronic valve is engaged, the air pressure is regulated using a basic air pressure regulator. The air pressure regulator was set to a predetermined pressure. The preset pressure was determined by experimentation and just slightly lifted the weight basket from its supports. Further, this was done with as little dynamic implications on the laminated glass beams as possible. A preset pressure of approximately 70 psi was used for all experiments conducted herein.

To protect the pneumatic system and its components, an air filter-dryer system was installed. The filter was used to remove debris from the air source to prevent damage to the pneumatic cylinder walls. Due to the extreme temperatures within the environmental testing chamber, a dryer was used to remove moisture from the air source to prevent frosting in the lines. The pneumatic system's control components are shown in Fig. 5-26.

FIG. 5-26. Pneumatic System Controls

All of the pneumatic system's components transfer air through ¼ in. NPT ports. Several devices are interconnected with quick links. An 8 foot, 3/8 in., rubber hose provides a link between the pneumatic controls and pneumatic cylinder connections inside the environmental testing chamber. The hose is made of EPDM rubber, reinforced with synthetic fiber, and provides a working pressure rating of 200 psi at all temperature ranges. The rubber layer provides insulation between the pneumatic system and the environmental testing chamber's extreme temperatures. Trial experiments were conducted with a 5/16 in. OD, 3/16 in. ID polyvinyl chloride (vinyl) tubing. However, the vinyl tubing was not able to withstand temperatures above 100 °F at the needed pressures.

Due to the weight and stiffness of the rubber supply hose, it could not be directly connected to the pneumatic cylinder. Connecting the rubber hose directly to the pneumatic cylinder would cause variation in the load applied to the beams. Fig. 5-27 shows a ¼ in. nylon recoil hose that connects between the rubber air supply hose and pneumatic cylinder to prevent such load variations. Nylon material was selected for a 200 psi working pressure and temperature ratings of up to 200 °F.

FIG. 5-27. Pneumatic Cylinder Assembly with Nylon Recoil Hose

The nylon recoil hose attached direct to the pneumatic cylinder. Brass connectors were used to adapt the hose's ¼ in. NPT male connection, to the pneumatic cylinder's 1/8 in. female NPT port. Opposite the pneumatic cylinder connection, the recoil hose connected to the rubber air supply hose with quick link connectors. Inside the environmental testing chamber, the recoil hose was supported in a horizontal position by the pneumatic cylinder on one side and a 24 in. elastic strap on the opposite side of the pneumatic cylinder. The strap was fixed to the environmental testing chamber's steel wire frame shelf. Placing the recoil hose in a horizontal position reduces the change in angle as the pneumatic cylinder moves up and down. A change in angle of the recoil hose causes a slight variation in force imposed on the laminated glass beams. This change in force will be quantified and described later in this chapter. Fig. 5-28 show the setup described above.

FIG. 5-28. Pneumatic Cylinder Assembly with Nylon Recoil Hose in Environmental Testing Chamber

In building the components of the load assembly, it is important to maintain as light of weight as possible. The weight of the loading assembly should be minimal as compared to the load to be applied to the laminated glass beams. This will minimize the effects of the loading assembly on the structural response of the beams. The load spreading bar and pneumatic cylinder assembly weighed 2.08 lb. However, to neglect the weight of the loading device and pneumatic cylinder, the strain gages were zeroed once the loading device was in contact with the laminated glass beams. This zeroed strain does not include the strain caused by the weight basket, partial chain links, and effects from the nylon recoil hose.

Machined steel bricks of exact dimensions were used as weights to load the beams to a precise predetermined load. The bricks were available in three sizes. This makes it possible to achieve the desired load within reasonable tolerances. Designated large, medium, and small, the bricks weighed 4.5 lb, 1.76 lb, and 0.56 lb, respectively. The brick's weight were determined by a calibrated scale and verified by direct measurements of the bricks dimensions. The volume of the known material can be multiplied by its density to calculate the bricks exact weight. Fig. 5-29, from left to right, shows the small, medium, and large bricks used to load the beam specimens to a predetermined load.

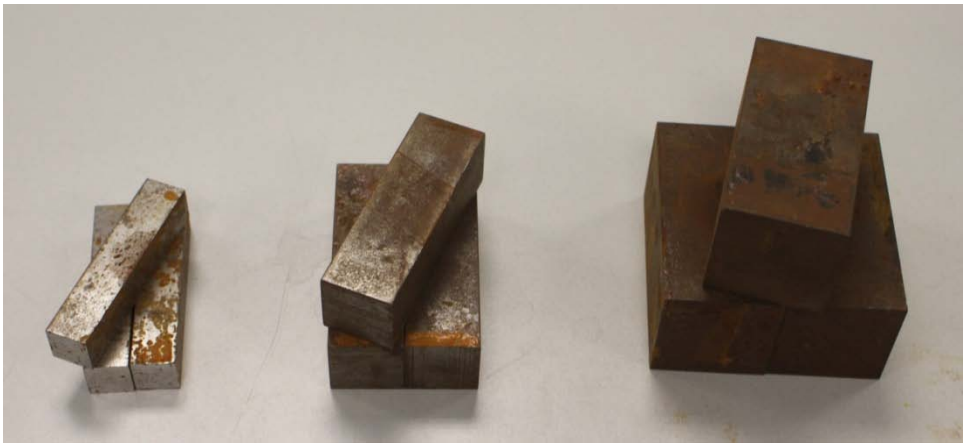

FIG. 5-29. Metal Bricks Used to Load the Laminated Glass Beams

The load applied by the use of machined bricks was adjusted to include the additional load applied by the weight basket, partial chain links, and the nylon recoil hose. The weight of the loading basket is 1.49 lb. This weight was measured using a calibrated scale. Further, this measured weight does not account for the load contributions from the nylon recoil hose and the partial lengths of chains that are engaged when the pneumatic cylinder is pressurized and lifts the weight basket off of its supports. These contributions were determined using an instrumented 1/4 in. monolithic glass beam. The monolithic glass beam had dimensions, 30 in. by 4 in. and an exact thickness of 0.225 in. The monolithic glass beam was placed in the loading assembly and its strain gage zeroed prior to the pneumatic cylinder being engaged. For this experiment, the weight basket was empty. Then, the pneumatic cylinder was pressurized lifting the empty weight basket off its supports. The load applied to the glass beam can be back calculated using the recorded strain of 19.5 με. The applied load was calculated to be 1.521 lb. These calculations can be found in Appendix B. Engineering judgment would suggest this is a reasonable approach to determine the contributions, from the weight basket, partial chain links, and nylon recoil hose, to the load applied on the beam specimen. This experiment determined that the nylon recoil hose and partial chain links add an additional 0.031 lb to the 1.49 lb basket weight. A load of 1.521 lb must be added to the load from bricks for all experiments conducted.

Each beam was tested to enforce stress levels that are representative of load conditions and load durations meaningful to glass plates under wind load pressures. The maximum stress level for each beam was determined for the worst experimental case. A benchmark load was determined for the laminated glass beams at 120 °F to yield an approximate target tensile stress.

A target stress of 3000 psi was selected to determine a load for the decade old PVB beams and the freshly manufactured SGP beams. The load selected for the freshly manufactured PVB beams was determined to give a 2000 psi target tensile stress. Both the freshly manufactured SGP and decade old PVB specimens were heat strengthened and tempered, respectively. This allows for higher stresses to be comfortably achieved without the risk of fracture. Table 5-1 encompasses the load applied to each beam to reach the target stress at 120 °F. The load in Table 5-1 includes the contributions of the weight basket in addition to the machined bricks. Table 5-2 shows the brick count used to achieve the desired load for each beam. Note, that Table 5-2 does not account for the additional load from the weight basket.

TABLE 5-1. Required Load to Achieve Target Stress Level at 120 °F

Specimen	Applied Load	Target Stress
Decade Old PVB	25.76 lb	3000 psi @ 120 °F
Freshly Manufactured PVB	9.681 lb	2000 psi @ 120 °F
Freshly Manufactured SGP	37.49 lb	3000 psi @ 120 °F

TABLE 5-2. Brick Count to Achieve Desired Load for the Laminated Glass Beams

Specimen	Brick Count		
	Large	Medium	Small
Decade Old PVB	5	1	0
Freshly Manufactured PVB	0	4	2
Freshly Manufactured SGP	8	0	0

The same ¼ in. monolithic glass beam discussed previously was used to validate the accuracy of the strain gage instrumentation and loading assembly setup. Plane sections remain plane in the bending of a monolithic glass beam, thus elementary bending theory can be applied to calculate the expected stresses induced for a given load. A single large brick, weighing 4.49618 lb, was used to load the beam as shown in Fig. 5-1. Using elementary bending theory

the expected tensile strain induced from the load, at the position of the strain gage, was calculated to be 57.64 με. During the field experiment the strain was recorded to be 57.5 με. Calculations for this experiment can be found in Appendix B.

The laminated glass beams were subjected to bending stresses by a three point loading condition as shown in Fig. 5-1 and 5-2. This induced either tensile or compressive stresses along the longitudinal axis of the extreme fibers of the beams. The induced stresses can be calculated using Hooke's law given by the following equation:

$$\sigma = \epsilon * E_{glass} \tag{5-1}$$

where ϵ is the strain and E_{glass} is the modulus of elasticity for soda lime glass.

The environmental testing chamber was developed to measure the response of laminated glass beams through a range of temperatures: 30, 40, 60, 80, 100, and 120 °F. The interlayer temperature was stabilized over several minutes prior to conducting each experiment. Strain measurements and ambient temperature were taken at predetermined time intervals of 3, 5,10, and 60 s, 5, 10, 20, 40, and 60 min.

Post test analysis revealed a slight trace of dynamic loading for load durations below 5 s. Frame by frame video analysis showed that the force approached a static load after approximately 5 s. For this reason, data collected for load durations below 10 s are not included. Averaging data through the use of numerical methods could possibly be used to produce temperature transition charts for load durations below 10 s. However, these methods were not considered for the research in this thesis.

The beams were allowed ample time to relax between each test temperature. This period of relaxation allowed the interlayer material to relieve stresses induced during the previous test. For temperatures below 80 °F, stresses were locked into the interlayer material. To relieve these stresses, the beams were allowed to relax over night in a stress relief heating chamber. The stress relief heating chamber allowed the laminated glass beams to lie flat, while maintaining their ambient temperature above 100 °F. Four 150 watt heat lamps were used to heat the laminated glass beams to approximately 110 °F. A rheostat was used to control the output of the heat lamps. Fig. 5-30 shows the stress relief heating chamber.

FIG. 5-30. Stress Relief Heating Chamber

Data sheets were used to collect the laminated glass beam's applied load, strain, load duration, and temperature for each experiment. Once the experiments were conducted these data were digitized for further analysis.

To obtain the induced stress, Equation 5-1 was applied to the strain data for each experiment. The modulus of elasticity, E_{glass}, is taken to be $10.4*10^6$ psi for soda lime glass (McLellan and Shand 1984). These data were then plotted as a function of temperature to produce the laminated glass beam temperature transition charts. In addition, these data were compared to the layered performance model and fully monolithic performance model for each corresponding experiment. The laminated glass beam temperature transition charts for the decade old PVB, freshly manufactured PVB, and freshly manufactured SGP are shown in Fig. 5-31 through 5-37, 5-39 through 5-45, and 5-47 through 5-53, respectively. Fig. 5-38, 5-46, and 5-54 summarize the laminated glass temperature transition charts for the decade old PVB, freshly manufactured PVB, and freshly manufactured SGP, respectively. Tabulated experimental datasheets are presented in Appendix C. In addition, calculations used to determine the performance models can be found in appendix B.

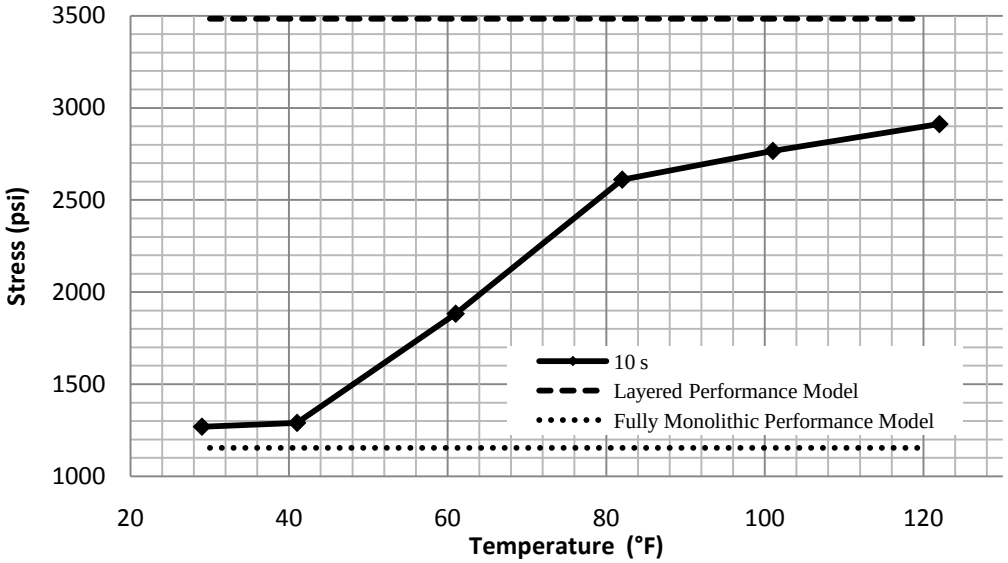

FIG. 5-31. Decade Old PVB Laminated Glass Beam Temperature Transition Chart – 10 S Load Duration

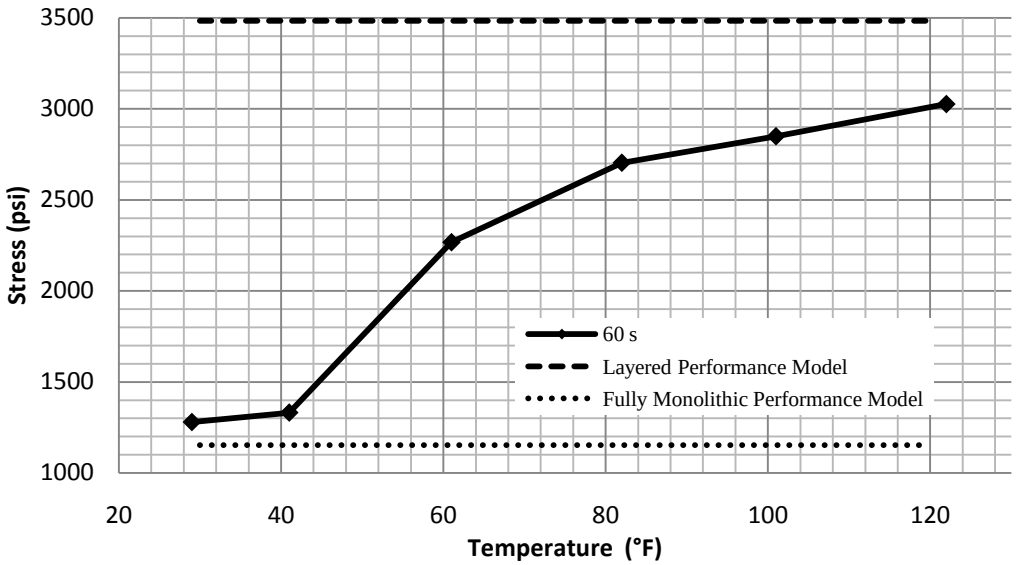

FIG. 5-32. Decade Old PVB Laminated Glass Beam Temperature Transition Chart – 60 S Load Duration

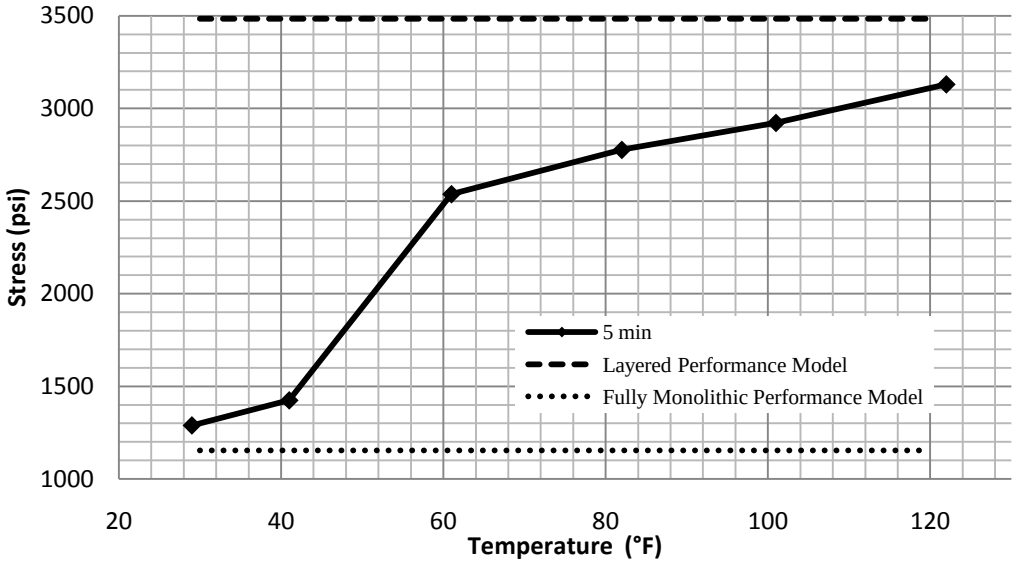

FIG. 5-33. Decade Old PVB Laminated Glass Beam Temperature Transition Chart – 5 Min Load Duration

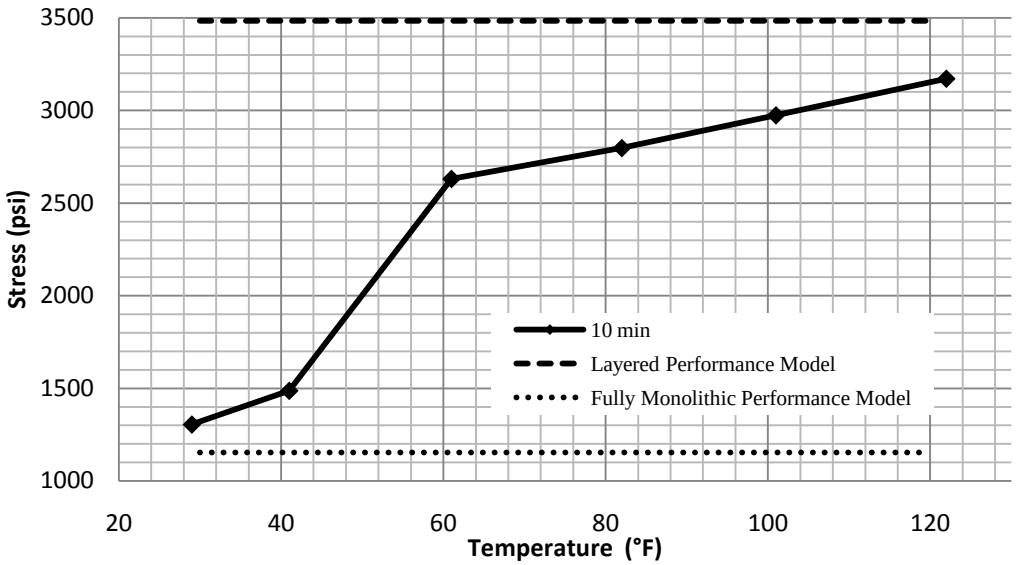

FIG. 5-34. Decade Old PVB Laminated Glass Beam Temperature Transition Chart – 10 Min Load Duration

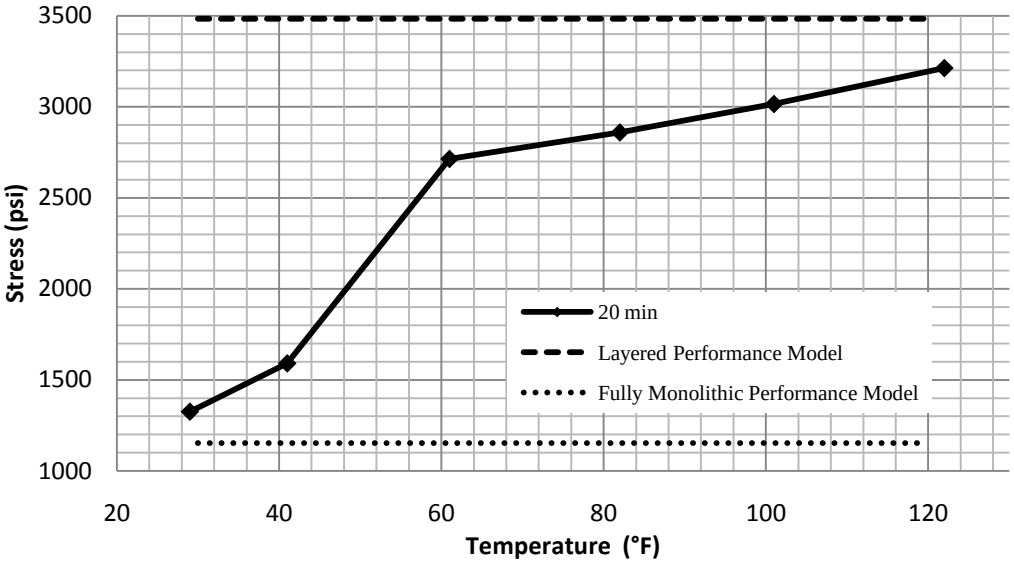

FIG. 5-35. Decade Old PVB Laminated Glass Beam Temperature Transition Chart – 20 Min Load Duration

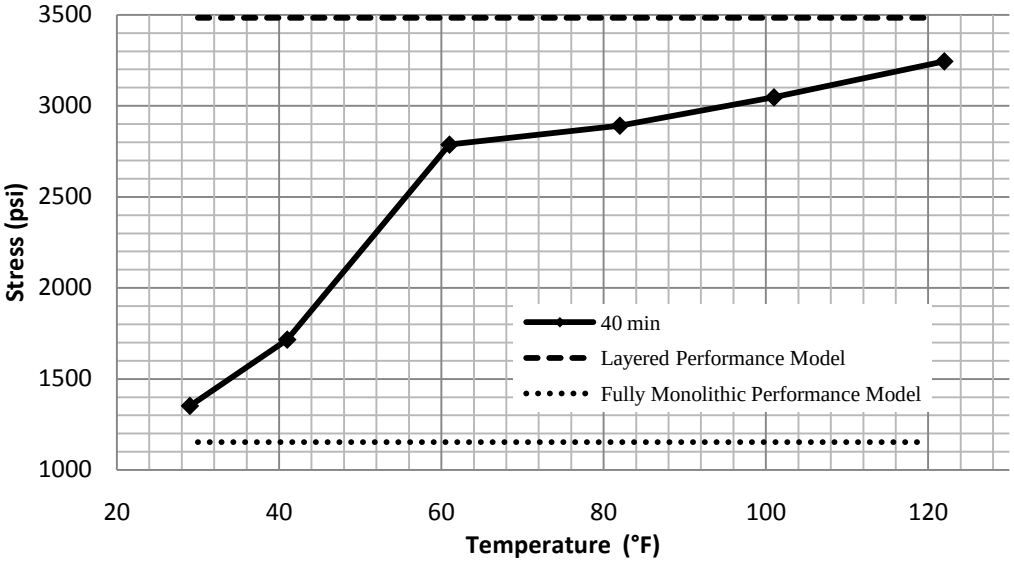

FIG. 5-36. Decade Old PVB Laminated Glass Beam Temperature Transition Chart – 40 Min Load Duration

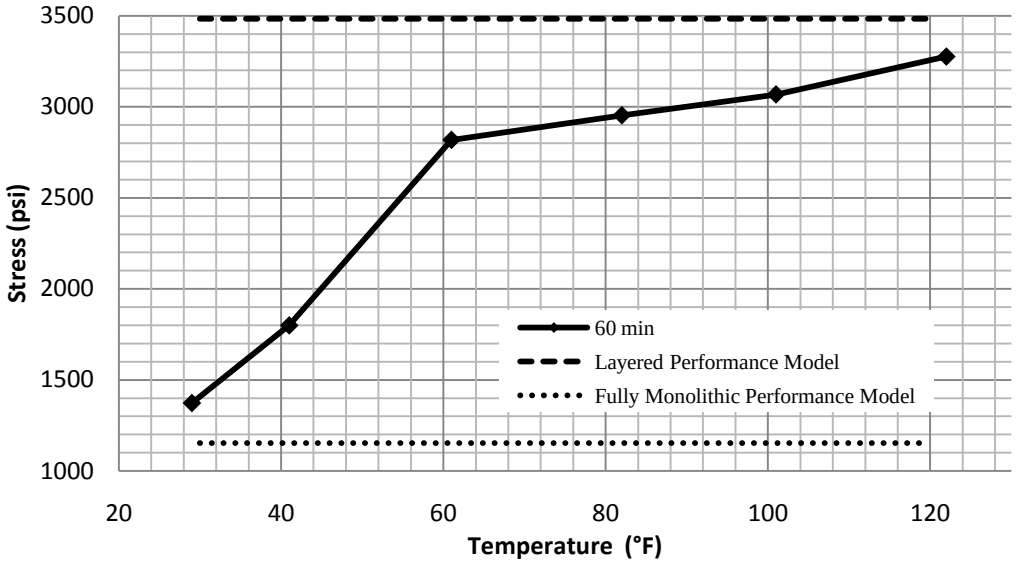

FIG. 5-37. Decade Old PVB Laminated Glass Beam Temperature Transition Chart – 60 Min Load Duration

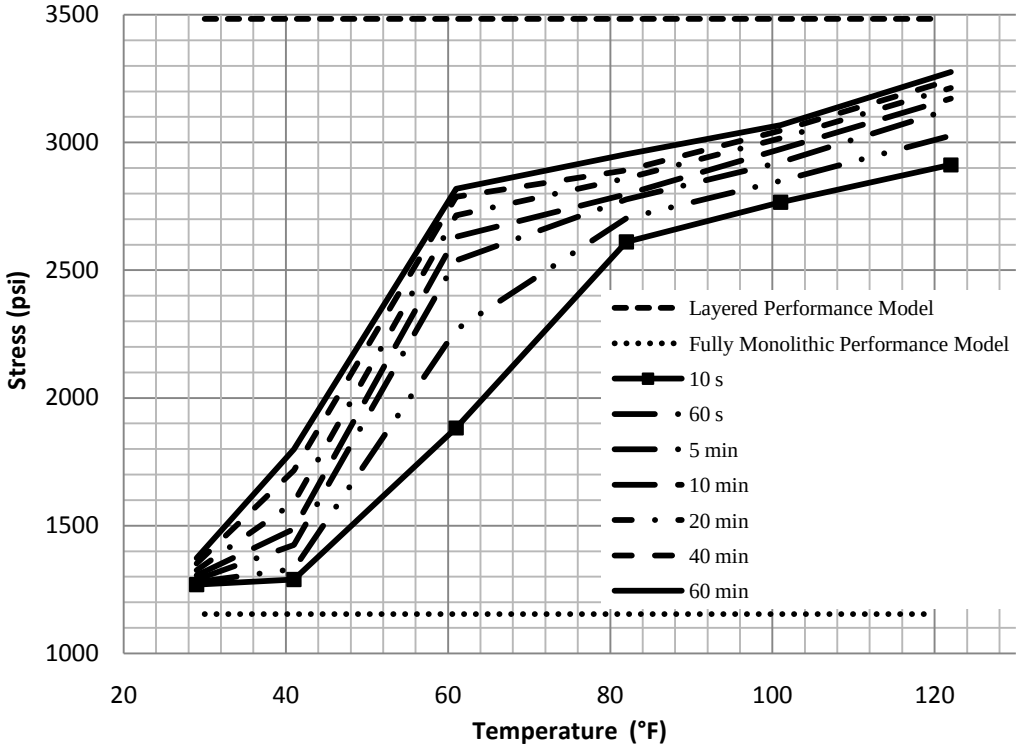

FIG. 5-38. Decade Old PVB Laminated Glass Beam Temperature Transition Chart

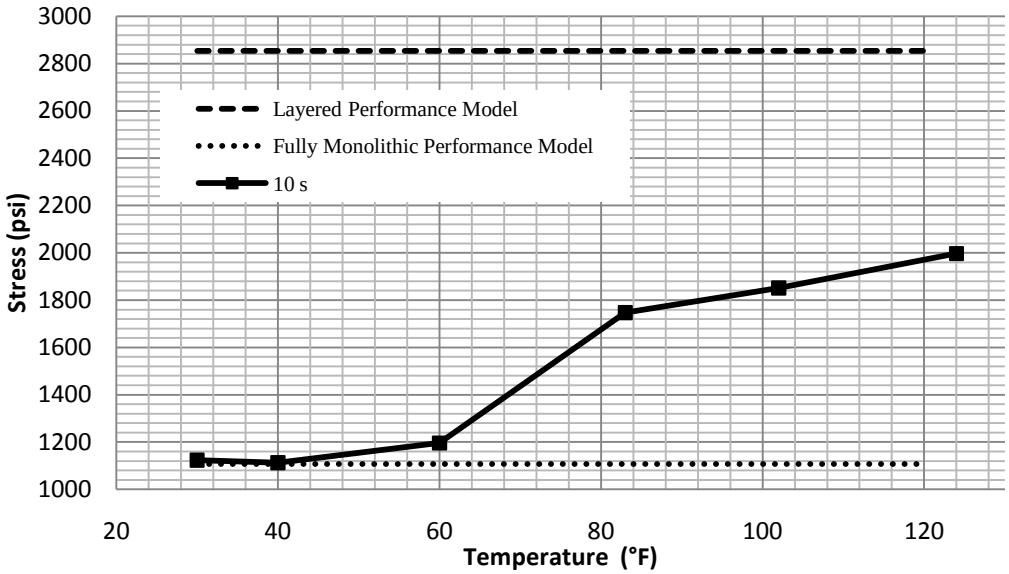

FIG. 5-39. Freshly Manufactured PVB Laminated Glass Beam Temperature Transition Chart – 10 S Load Duration

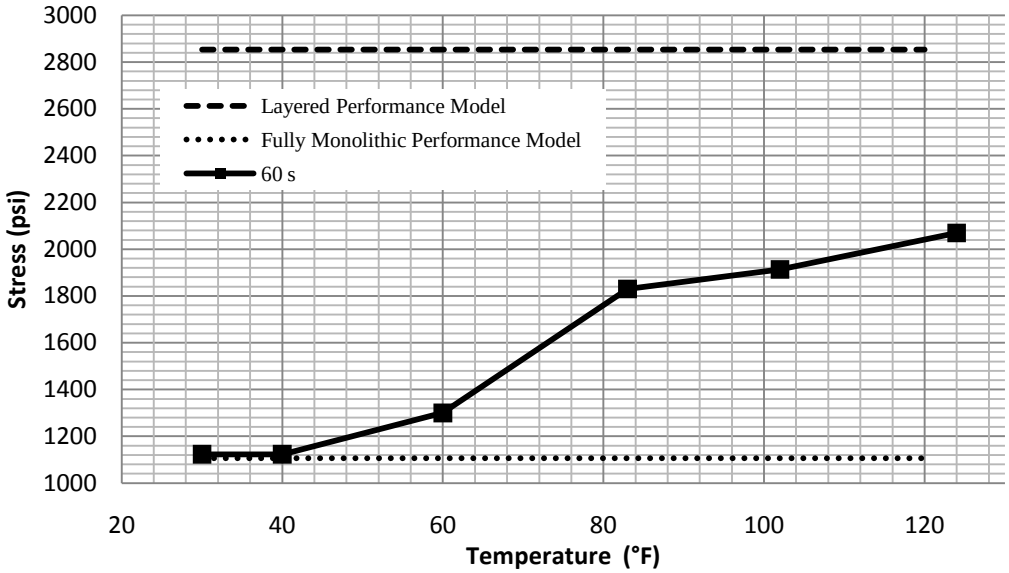

FIG. 5-40. Freshly Manufactured PVB Laminated Glass Beam Temperature Transition Chart – 60 S Load Duration

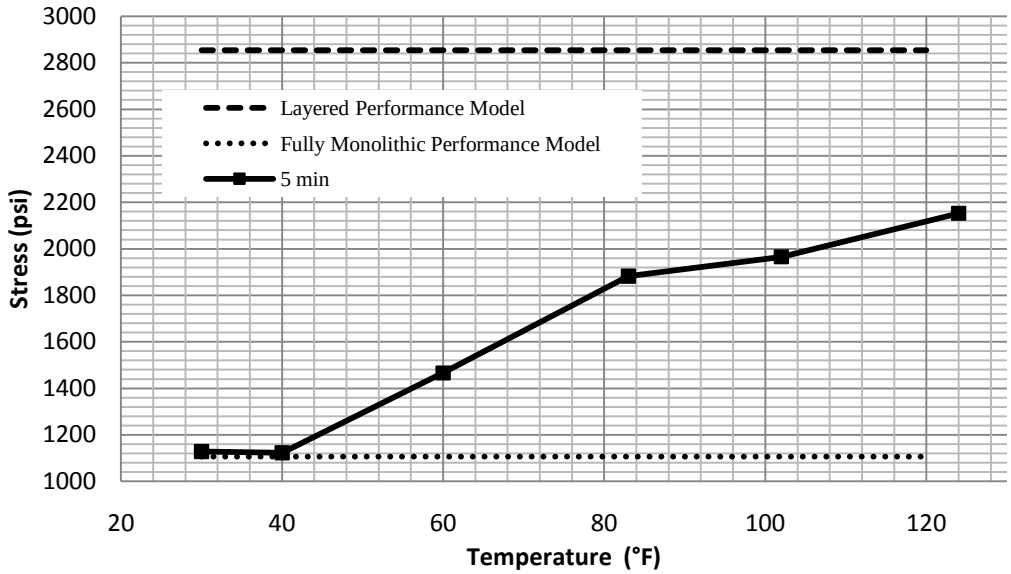

FIG. 5-41. Freshly Manufactured PVB Laminated Glass Beam Temperature Transition Chart – 5 Min Load Duration

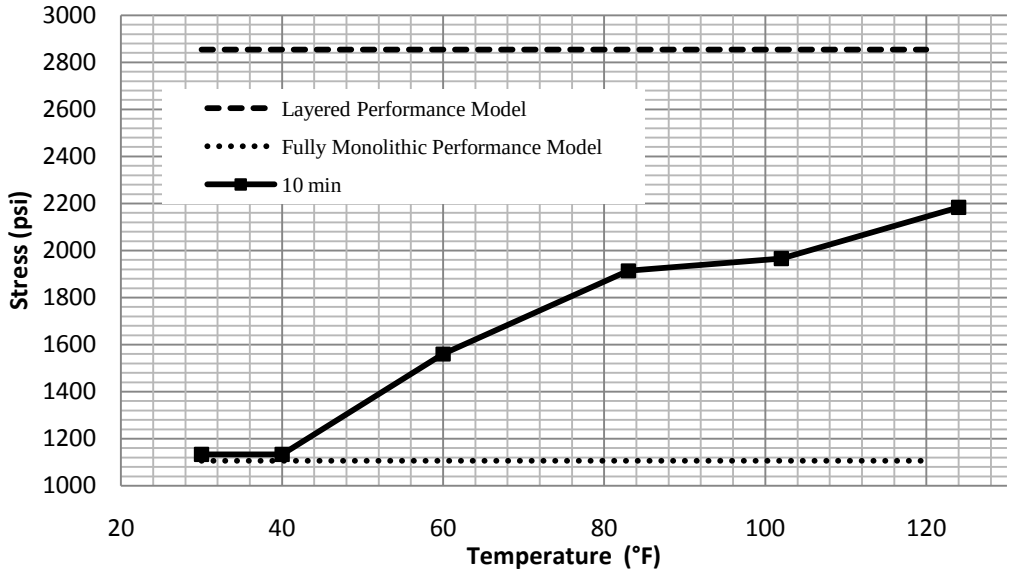

FIG. 5-42. Freshly Manufactured PVB Laminated Glass Beam Temperature Transition Chart – 10 Min Load Duration

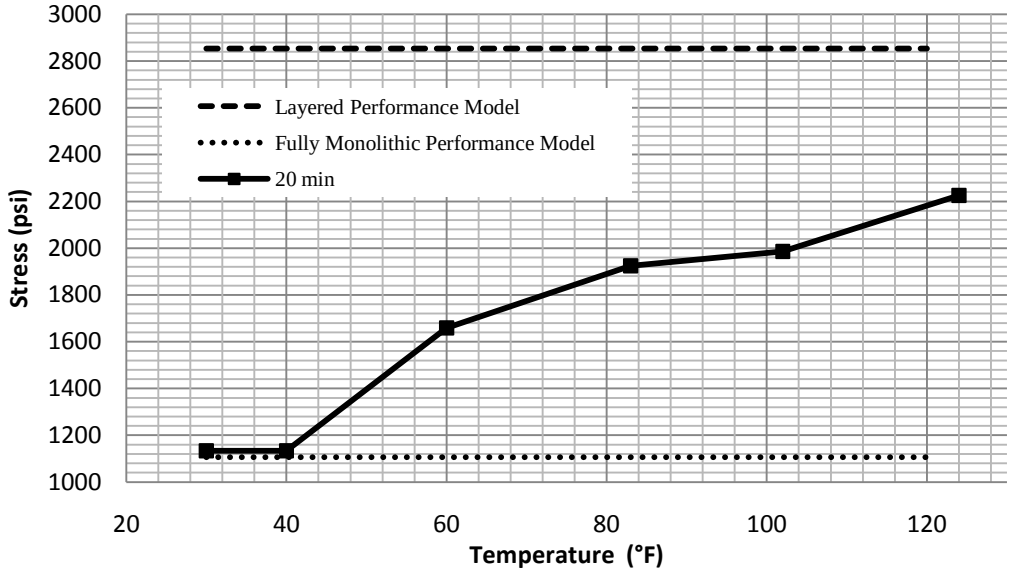

FIG. 5-43. Freshly Manufactured PVB Laminated Glass Beam Temperature Transition Chart – 20 Min Load Duration

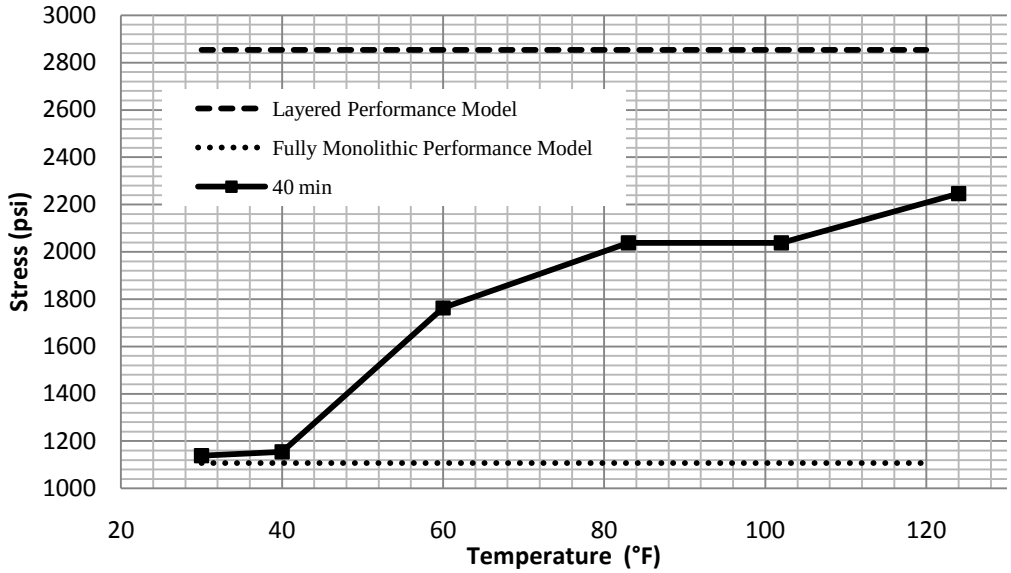

FIG. 5-44. Freshly Manufactured PVB Laminated Glass Beam Temperature Transition Chart – 40 Min Load Duration

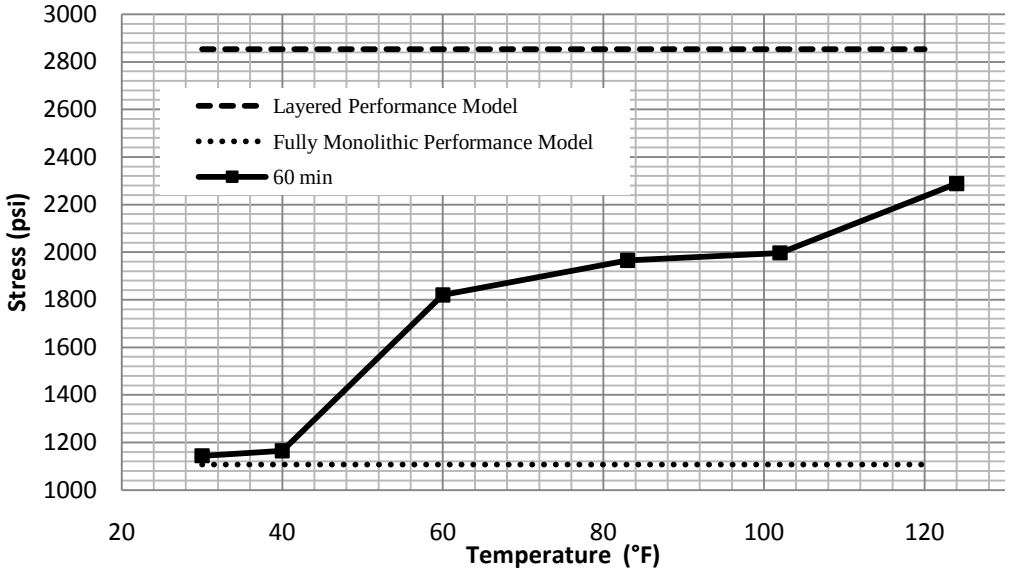

FIG. 5-45. Freshly Manufactured PVB Laminated Glass Beam Temperature Transition Chart – 60 Min Load Duration

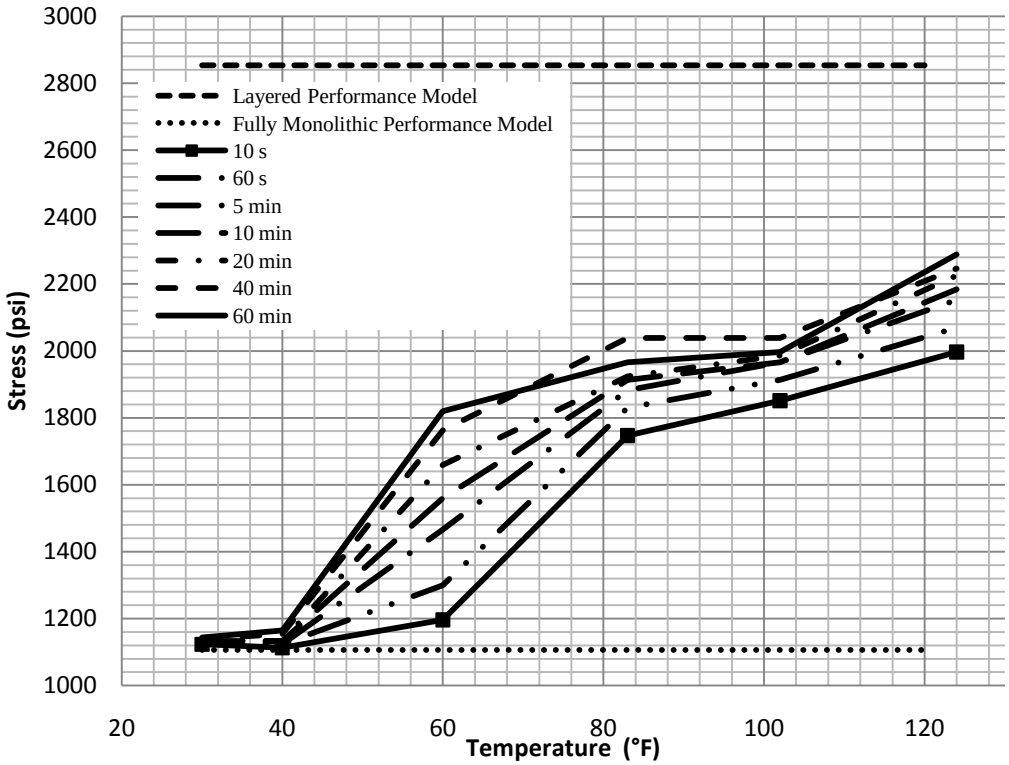

FIG. 5-46. Freshly Manufactured PVB Laminated Glass Beam Temperature Transition Chart

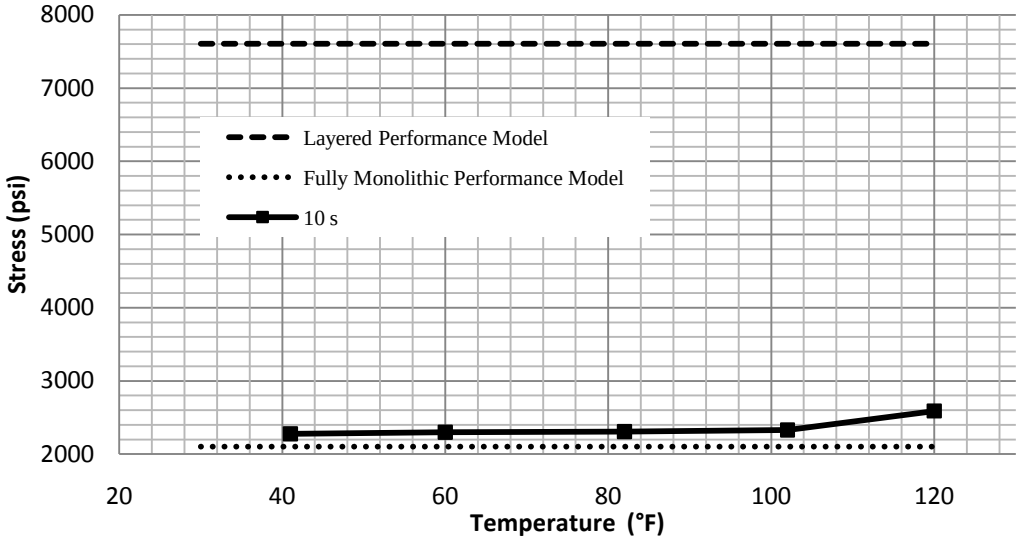

FIG. 5-47. Freshly Manufactured SGP Laminated Glass Beam Temperature Transition Chart – 10 S Load Duration

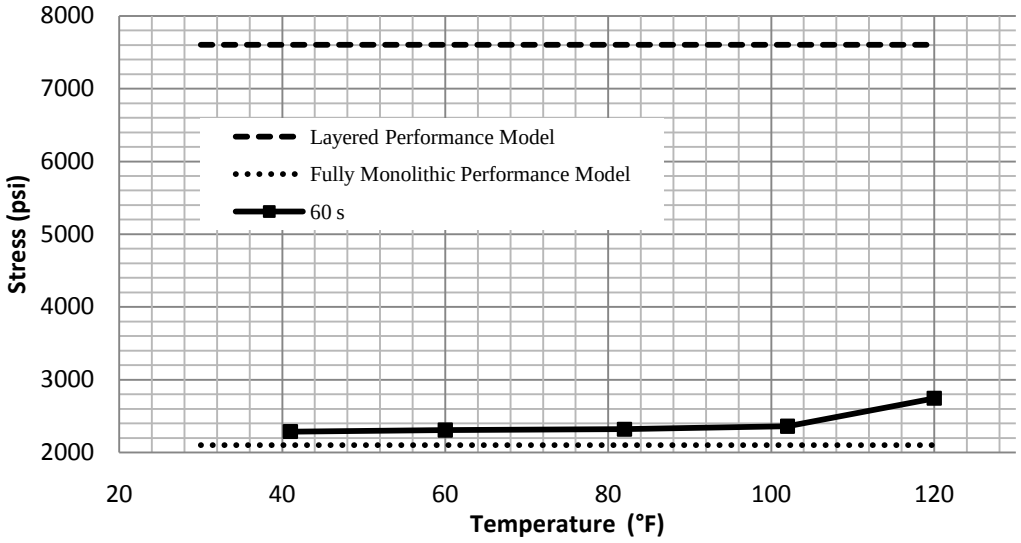

FIG. 5-48. Freshly Manufactured SGP Laminated Glass Beam Temperature Transition Chart – 60 S Load Duration

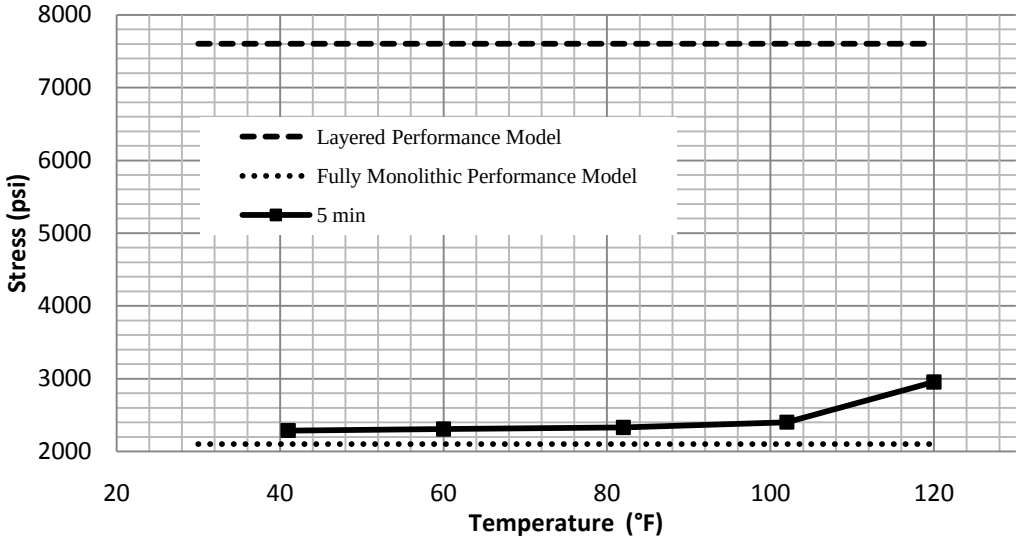

FIG. 5-49. Freshly Manufactured SGP Laminated Glass Beam Temperature Transition Chart – 5 Min Load Duration

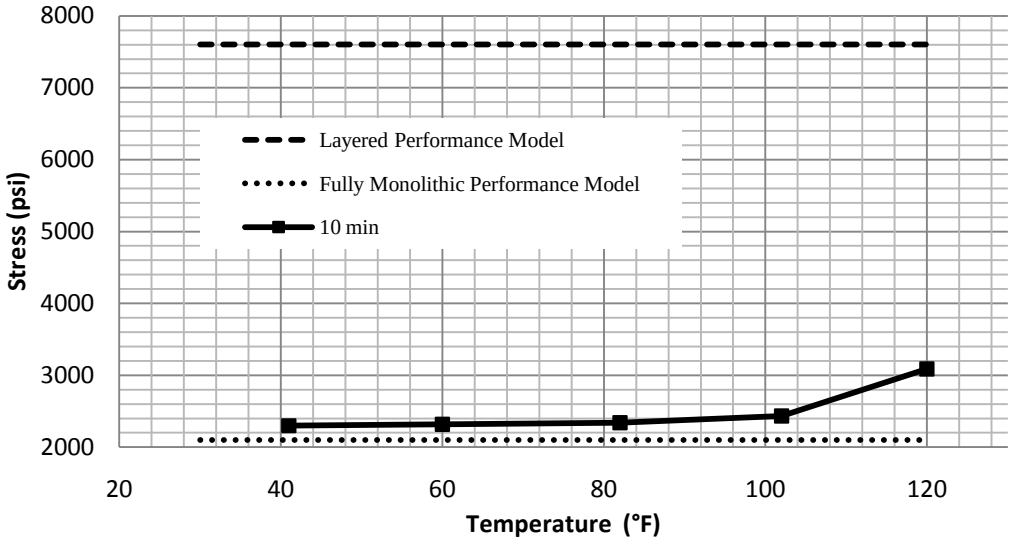

FIG. 5-50. Freshly Manufactured SGP Laminated Glass Beam Temperature Transition Chart – 10 Min Load Duration

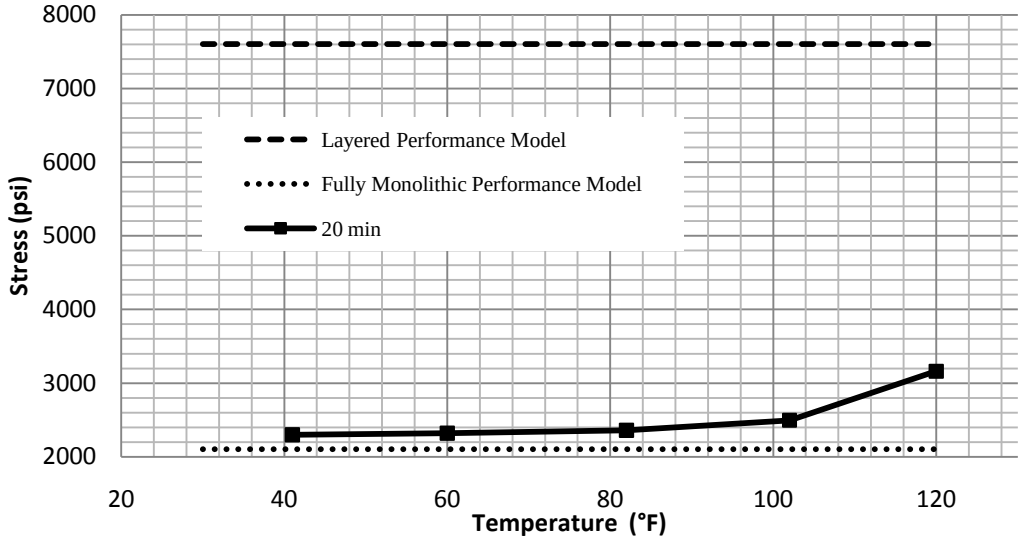

FIG. 5-51. Freshly Manufactured SGP Laminated Glass Beam Temperature Transition Chart – 20 Min Load Duration

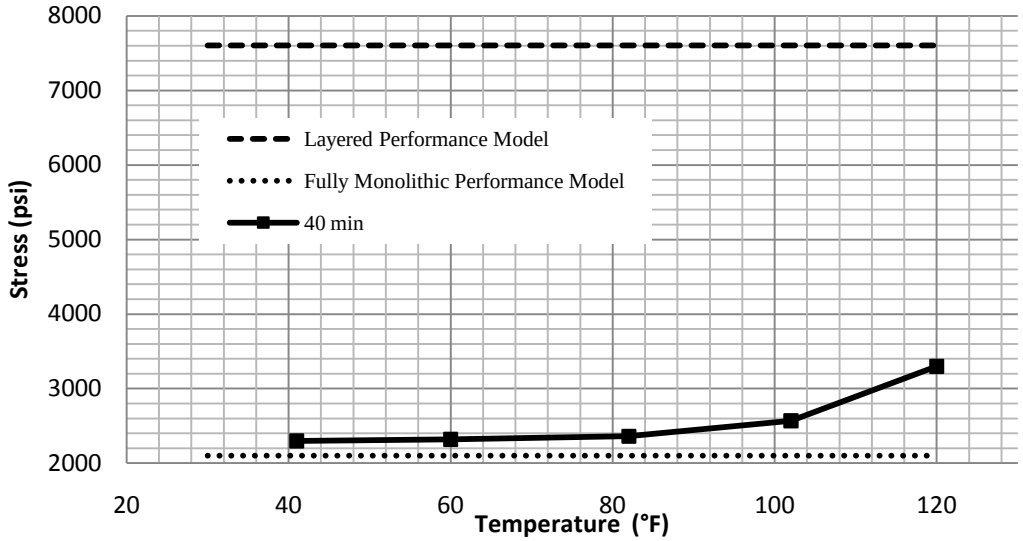

FIG. 5-52. Freshly Manufactured SGP Laminated Glass Beam Temperature Transition Chart – 40 Min Load Duration

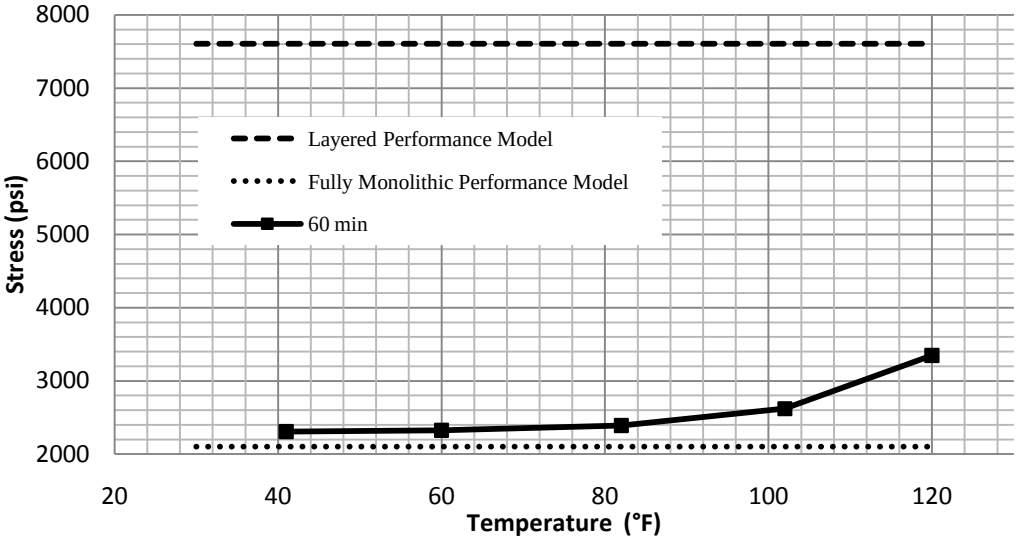

FIG. 5-53. Freshly Manufactured SGP Laminated Glass Beam Temperature Transition Chart – 60 Min Load Duration

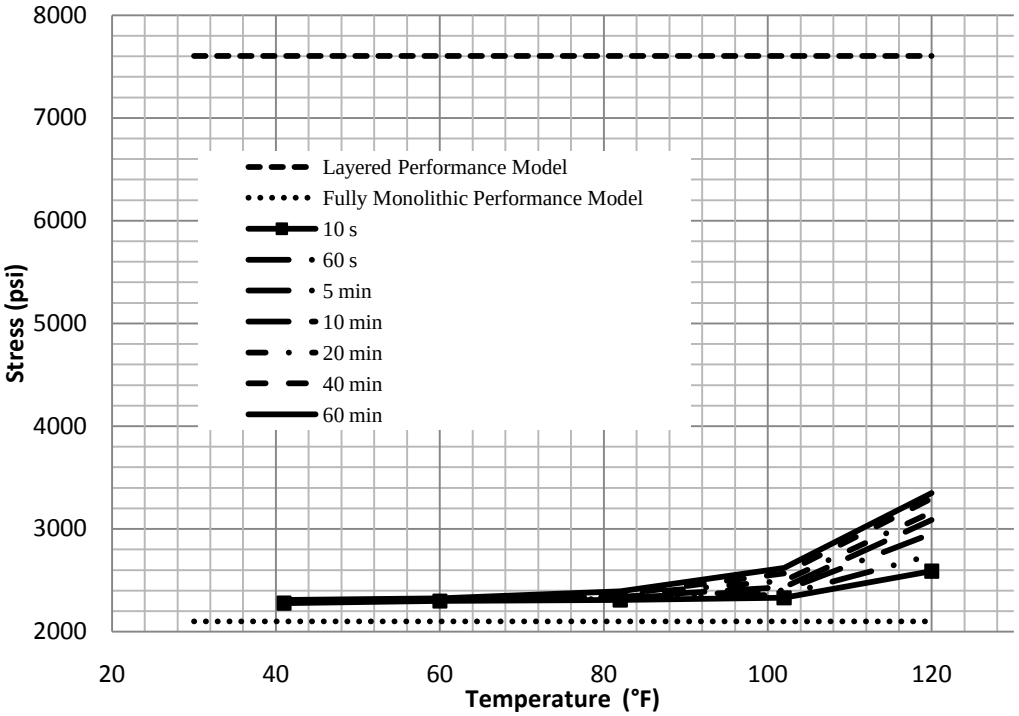

FIG. 5-54. Freshly Manufactured SGP Laminated Glass Beam Temperature Transition Chart

FINITE ELEMENT ANALYSIS

It is well known that the elastic properties of glass remain stable over the range of temperatures through which the experimental effort was conducted (Beason 1980, McLellan & Shand 1984). Therefore, all variations in the structural behavior of the laminated glass beams are the result of variation in the interlayer stiffness. Several attempts have been made to develop closed form theoretical formulations for laminated glass. While these attempts have met with some success, they are limited to specific cases and geometries. Numerical methods provide a more flexible approach to the problem. Specifically, theoretical structural response models can be easily developed for laminated glass loaded and supported under a wide range of conditions using finite element analysis.

The aforementioned laminated glass beam experiments quantified the structural performance of three particular types of laminated glass beams as a function of temperature and load duration. The specimens used during the experimental effort were then modeled using finite element analyses. These analyses provide a theoretical relationship between stress and shear modulus for each laminated glass beam. The finite element models were generated using Superdraw III version 20.00-WIN and analyzed with ALGOR version 20.00.01.0021. Each laminated glass beam specimen was modeled according to its exact dimensions measured during the experimental effort. The calculated output from the finite element analyses included stresses and deflections.

Element Selection

Various types of elements are widely available for use in finite element analyses. ALGOR has three common types of elements that were considered for the analysis herein. These element types included: plate, 8-noded brick, and 20-noded brick elements. Fig. 5-55, 5-56, and 5-57 show the typical plate, 8-noded brick, and 20-noded brick elements, respectively, used in finite element analysis.

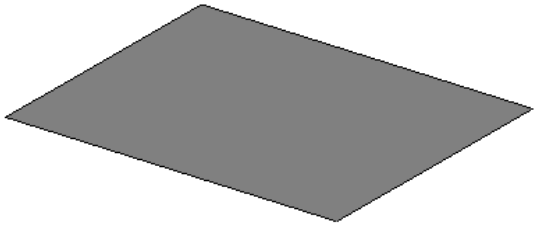

FIG. 5-55. Plate Element

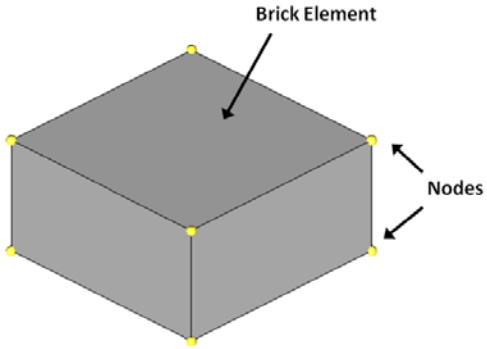

FIG. 5-56. 8-noded Brick Element

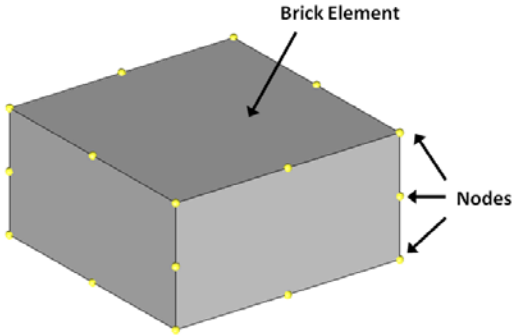

FIG. 5-57. 20-noded Brick Element

A model of laminated glass using plate elements is shown in Fig. 5-58. Constructing a finite element model using plate elements, the elements must be defined at the center of the layer being modeled. The plate element thickness, as defined by its section property, extends half of the thickness in each direction from this original plane. This makes modeling the connectivity

between the layers of laminated glass very difficult to achieve. If plate elements are to be used, it is necessary to derive functional relationships that couple the plate elements and their nodes for each layer. These function relationships must define the interaction behavior between layers of laminated glass units where, as previously stated, plane sections do not remain plane. Ultimately, plate elements provide an ineffective approach for the modeling of laminated glass.

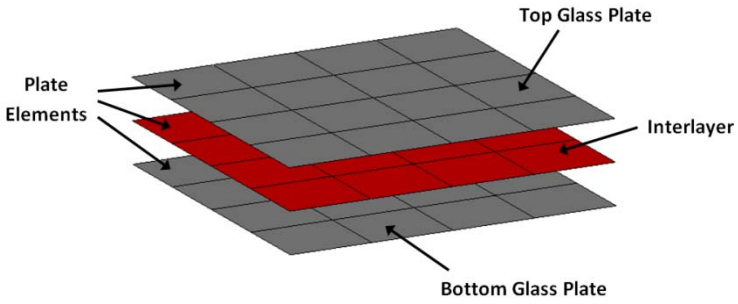

FIG. 5-58. Laminated Glass Model Using Plate Elements

The use of brick elements relieve the issues that arise from nodal connectivity with the use of plate elements. Brick elements allow for direct nodal connectivity between laminated glass layers as the two different materials share common nodes. Fig. 5-59, shows the use of brick elements stacked on top of one another to model laminated glass.

Stresses in brick elements are calculated at each node. In some cases, higher order elements that incorporate additional nodes can give more accurate stress approximations with fewer elements. However, for the analysis conducted herein, 8-noded bricks were selected because the 8-noded bricks enforce Kirchoff's assumption through each layer individually. This is important to capture the true behavior of the layered plate.

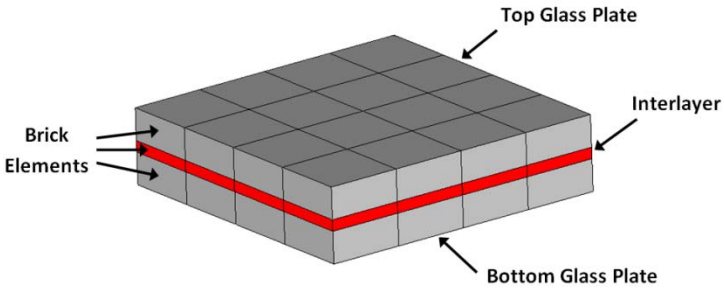

FIG. 5-59. Laminated Glass Model Using Brick Elements

Modeling Using Quarter-Plate-Models

Three dimensional finite element models were made for each laminated glass beam geometry using 8-noded brick elements. Models for the decade old PVB, freshly manufactured PVB, freshly manufactured SGP, and a ¼ in. monolithic plate control specimen were built. The finite element models take advantage of double symmetry, so that each beam is modeled with a quarter-plate-model. Fig. 5-60 shows an isometric view of a typical quarter-plate-model.

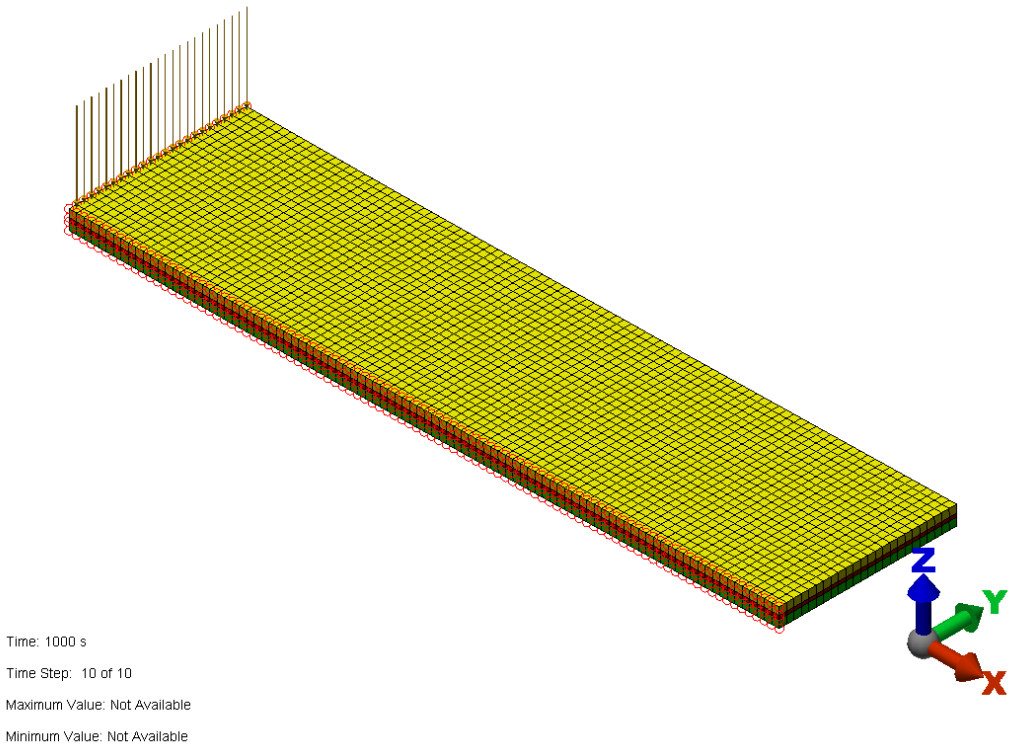

FIG. 5-60. Isometric View of Typical Laminated Glass Beam Quarter-Plate-Model

Boundary conditions were used to enforce the physical bending behavior of the model and symmetry conditions. The displacement of the left edge of the quarter-plate-model is locked in the X-direction through the thickness and the bottom edge of the quarter-plate-model is locked in the Y-direction through the thickness. These boundary conditions enforce symmetry and assure that plane sections remain plane through the thickness at these edges. The laminated glass beams were simply supported with a span of 22 in. Since the finite element models are quarter-

plate-models, this means that the line of support is 11 in. from the left edge of the quarter-plate-model. The bottom most nodes along this line were locked in the Z-direction. Loads were applied to each of the quarter-plate-models using surface pressure loads to simulate the load applied during the experimental effort. The area over which the surface pressure load was applied corresponded to the area of the neoprene strip mounted on the load spreading bar. This is shown using arrows in Fig. 5-60.

Verification of Finite Element Analysis

Verification of the finite element analyses were conducted in two ways. First, a convergence study was conducted with varying element geometries to assure the stability of the numerical modeling procedures. Second, tests were conducted on a fully monolithic glass beam. Because the monolithic beam was simply supported and subjected to a standard three point loading, it is possible to calculate reasonable estimates of the stresses and deflections of the beam using basic mechanics. In this verification, the monolithic beam was loaded and the strains were measured and compared to strains determined through the finite element methods, basic mechanics methods, and field experiments. Both of these verification procedures are described below.

Convergence Study

A convergence study was conducted to ensure the stability of the finite element models. Using the decade old PVB specimen, three three-dimensional finite element models were developed to analyze the effects of mesh size and element aspect ratios. The model is comprised of a 0.060 in. thick PVB interlayer sandwiched between two glass layers, each 0.129 in. thick. The overall dimensions of the quarter-plate-models were 3 in. by 12 in. A Saflex PVB interlayer was used for the interlayer material. The mechanical properties for the interlayer were taken at 120 °F and a 60 s load duration. Its modulus of elasticity was 191.43 psi and Poisson's ratio 0.49999. The mesh density was the only variable between the 3 convergence models.

The first of these models had a coarse mesh, ¼ in. density, shown in Fig. 5-61. The model has 48 elements along the length, 12 elements along the width, and 1 element for each layer of the cross-section. The glass layers have a 2-1 aspect ratio, whereas the interlayer has a

4-1 aspect ratio. A segment pressure load of 8.08 psi was applied to the first row of elements of the top glass plate surface.

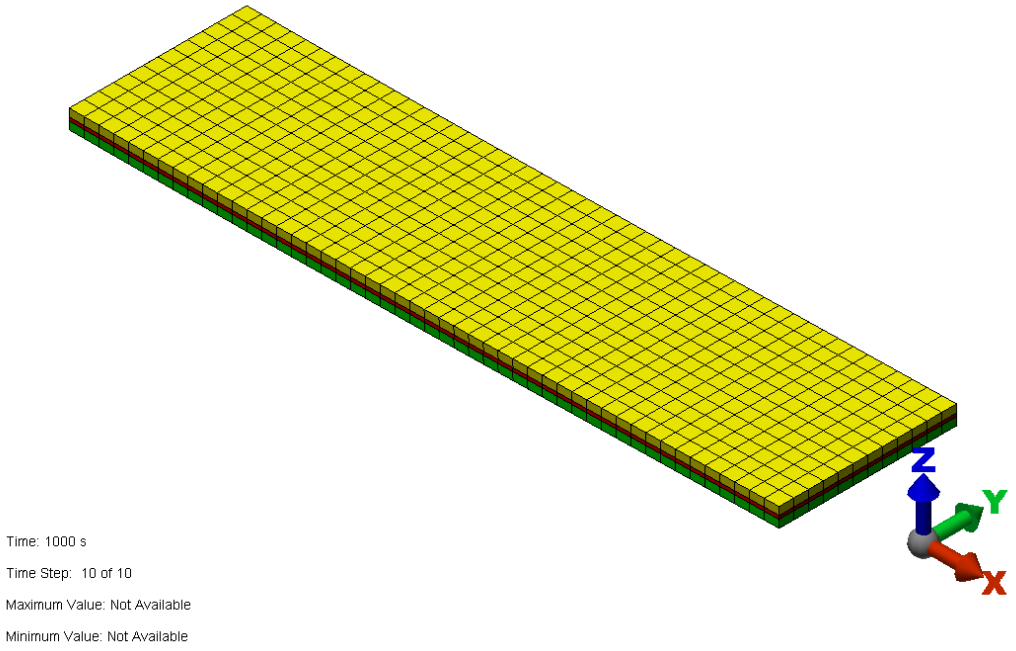

FIG. 5-61. Convergence Study Model with ¼ in. Mesh Density

The second model had a finer mesh, 1/8 in. density, shown in Fig. 5-62. This model has 96 elements along the length, 24 elements along the width, and 1 element for each layer of the cross-section. The glass layers have a 1-1 aspect ratio, whereas the interlayer has a 2-1 aspect ratio. A segment pressure load of 16.16 psi was applied to the first row of elements of the top glass plate surface. This pressure is twice that of the first model. This is to account for the smaller area in which the load is applied.

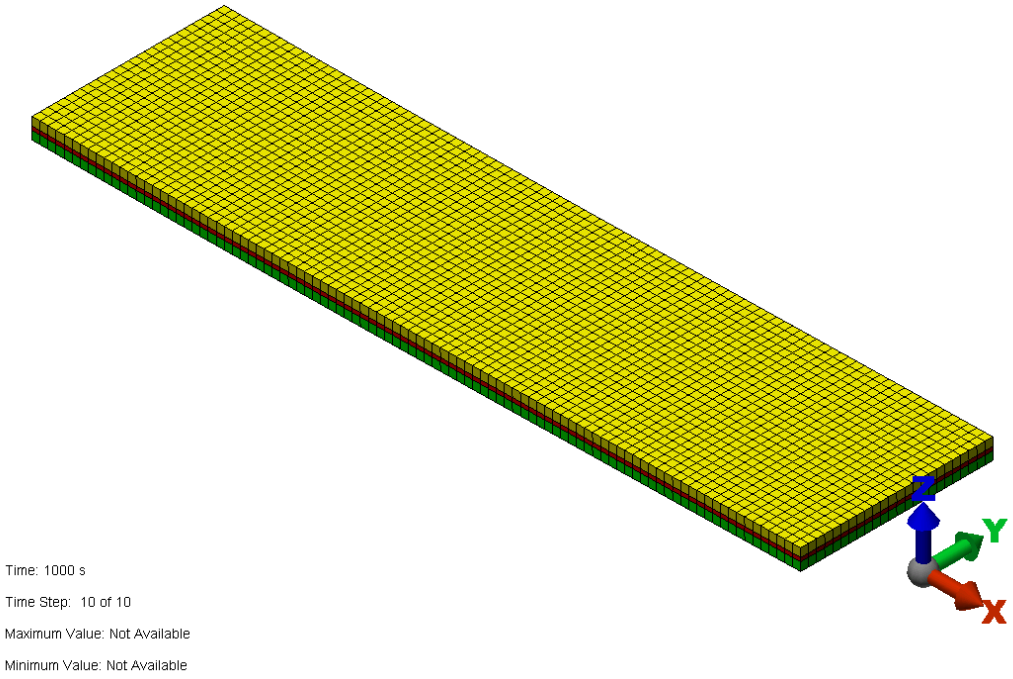

FIG. 5-62. Convergence Study Model with 1/8 in. Mesh Density

The third model had the finest mesh. This model, 1/16 in. mesh density, is shown in Fig. 5-63. This model has 192 elements along the length, 48 elements along the width. Across the cross-section, each glass layer has 2 elements and the interlayer, 1 element. Both the glass layers and interlayer have an approximate 1-1 aspect ratio. A segment pressure load of 16.16 psi was applied to the first two rows of 1/16 in. elements of the top glass plate surface.

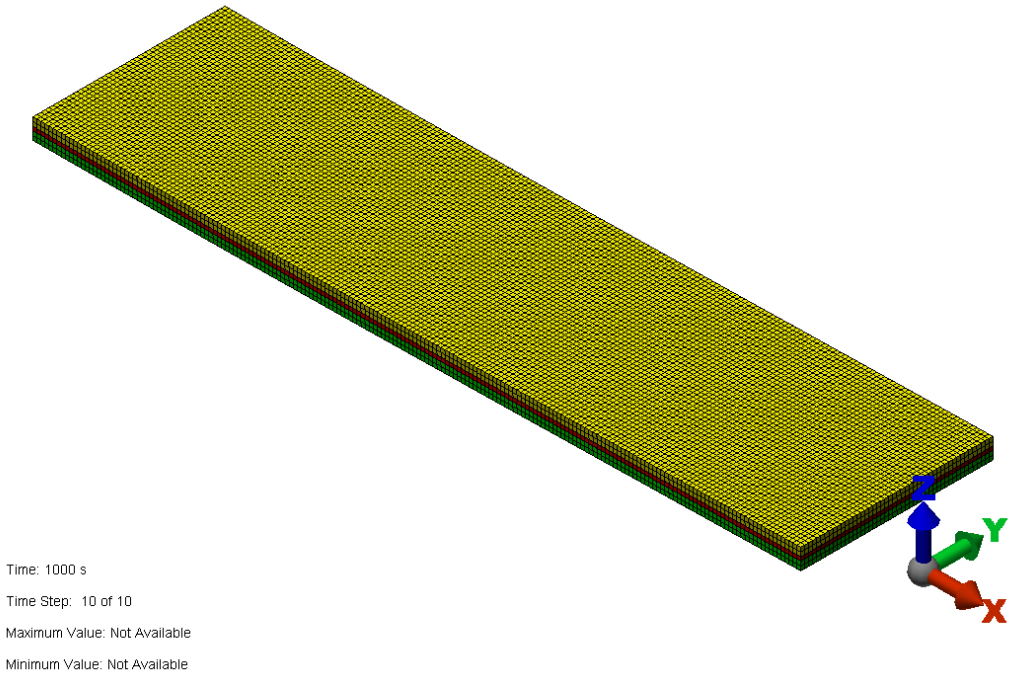

FIG. 5-63. Convergence Study Model with 1/16 in. Mesh Density

Displacements in the Z-direction, taken positive downward, were measured at the point of maximum deflection, located at lower, left corner of the model. In addition, the maximum principal stress was recorded at this location. The displacement and stress data recorded are given in Table 5-3 and 5-4, respectively. The 1/16 in. mesh density was used as a datum to calculate the percent difference in these tables.

TABLE 5-3. Convergence Study Z-Displacements for Various Mesh Densities

Mesh Density	Z-Displacement	% Difference
1/4	0.156708	0.046
1/8	0.156773	0.0045
1/16	0.15678	0

TABLE 5-4. Convergence Study Model Stresses for Various Mesh Densities

Specimen	Stress	% Difference
1/4	3032.42	1.0539
1/8	3059.061	0.179
1/16	3064.546	0

These data are plotted in Fig. 5-64 and 5-65 for Z-displacements and stresses, respectively.

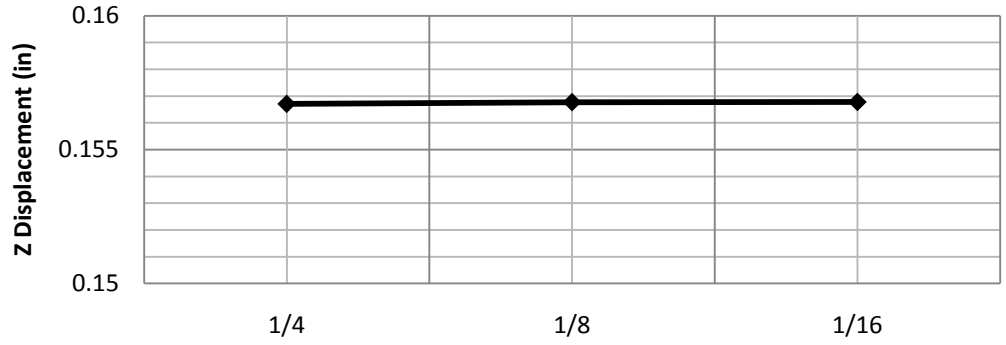

FIG. 5-64. Convergence Study Z-displacements for Various Mesh Densities

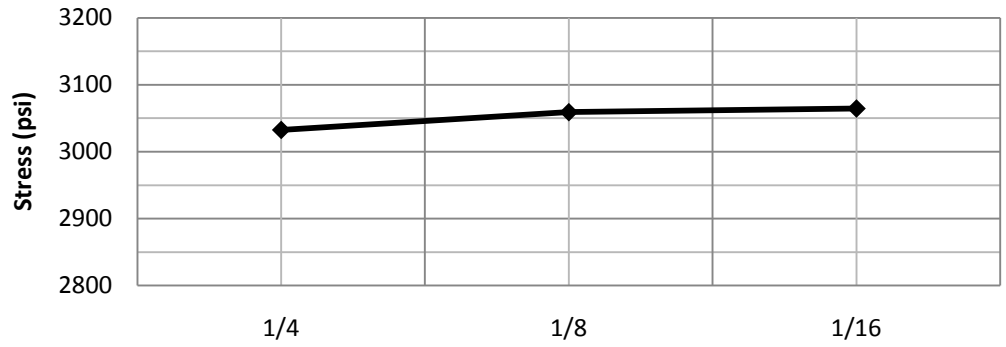

FIG. 5-65. Convergence Study Stresses for Various Mesh Densities

From these data presented, a 1/8 in. mesh density showed reliable results while maintaining a desired simulation runtime. A 1/8 in. mesh density was appropriately used for all further analysis herein.

Monolithic Glass Beam Validation

The ¼ in. monolithic glass plate finite element model was used to validate the finite element analysis to field calculated results, and theoretical approximations, both discussed previously in this chapter. The stress in a monolithic glass plate can be calculated using elementary bending theory and is independent of load duration and ambient temperature.

The ¼ in. monolithic glass plate quarter-plate-model was 2 in. wide by 15 in. long and 0.225 in. thick. It is modeled using 120 elements along the length, 16 along the width, and 2 elements for the cross-section.

During the experimental effort, a 0.225 in. monolithic glass beam specimen, 4 in. wide by 30 in. long, was loaded using single large brick weighing 4.49618 lb. The beam was supported as shown in Fig. 5-1. For this load, a strain of 57.5 με was measured. Elementary beam theory was then applied and approximated that the monolithic glass beam experiences 57.64 με. These results were then used to validate the finite element model. A finite element analysis of the monolithic glass beam with the same loading condition, approximated that the glass beam would experience 57.3 με. These values are conveniently tabulated in Table 5-5. In addition, the percentage error is within reason of experimental error. Calculations for this experiment can be found in Appendix B.

TABLE 5-5. Monolithic Glass Beam Validation

	Strain	**Error**
	με	%
Elementary Bending Theory	57.64	0
Experimental Results	57.5	0.243
Finite Element Analysis	57.3	0.590

DETERMINING A RELATIONSHIP BETWEEN STRESS AND SHEAR MODULUS USING FINITE ELEMENT ANALYSES

Finite element analyses were used to quantify the effects of interlayer shear modulus on the bending of laminated glass beams. These analyses were conducted using the geometries of the various laminated glass beams described previously in the experimental effort. These geometries included the decade old PVB, freshly manufactured PVB, and freshly manufactured SGP laminated glass beams. In addition, these beams were modeled with support conditions and loads representative of those in the experimental effort.

For all finite element analyses, the glass plates were modeled using a soda lime glass material. Soda lime glass is assumed to be perfectly elastic to the point of failure. The modulus of elasticity, *E*, for soda lime glass is taken to be $10.4*10^6$ psi and Poisson's ratio is 0.21 (McLellan and Shand 1984). To determine a relationship between interlayer shear modulus and stress for these laminated glass beams, a matrix of simulations was developed where the interlayer's shear modulus was allowed to vary with each simulation.

As a homogenous isotropic material, the elastic interlayer material can be defined using three parameters. These parameters include the modulus of elasticity, *E*, the shear modulus, *G*, and Poisson's ratio, υ. For an elastic material, these parameters, *E*, *G*, and υ, are not independent of one another and are related by the following equation:

$$G = \frac{E}{2 * (1 + \upsilon)} \tag{5-2}$$

where all variables are as previously defined.

For most elastic material models used in finite element analysis, two of these material parameters are required to fully define the behavior of a homogeneous isotropic material. ALGOR requires that Poisson's ratio, υ, and the modulus of elasticity, E, be defined.

Based on results presented by DuPont and others, it seems reasonable to estimate Poisson's ratio for a polymer, such as PVB or SGP, to be close to 0.5 (Edel 1997; DuPont 2004; Bennison, Qin, and Davies 2008). For all simulations discussed in this section, a Poisson's ratio of 0.4999 was used. Further, minor variations of this value will not affect the outcome of the simulation.

Multiple simulations were conducted to quantify the effects of shear modulus on the bending of laminated glass beams. For each simulation, the modulus of elasticity, *E*, varied. The modulus of elasticity used for each simulation was determined using Equation 5-2 for a desired shear modulus, *G*. The values of *E* and its corresponding value of *G* used for the matrix of simulations are shown in Table 5-6.

TABLE 5-6. Matrix of Simulations as a Function of Shear Modulus

Simulation	G (psi)	E (psi)
1	5	14.999
2	10	29.998
3	15	44.997
4	50	149.99
5	100	299.98
6	200	599.96
7	300	899.94
8	400	1199.92
9	500	1499.9
10	700	2099.86
11	1000	2999.8
12	1500	4499.7
13	3000	8999.4
14	10000	29998
15	100000	299980
16	1000000	2999800

The decade old PVB model had a 0.060 in. thick PVB interlayer between two glass layers, each 0.129 in. thick. The overall dimensions of the quarter-plate-models were 3 in. by 12 in. The model had 96 elements along the length, 24 elements along the width, and 1 element for each layer of the cross-section. A segment pressure load of 17.1746 psi was applied to the first row of 1/8 in. elements along the top surface of the top glass plate. The second model, freshly manufactured PVB, had a 0.030 in. thick interlayer and two 0.107 in. thick glass layers. The

overall dimensions of the quarter-plate-models were 2 in. by 15 in. The model had 120 elements along the length, 16 elements along the width, and 1 element for each layer of the cross-section. A segment pressure load of 9.691 psi was applied in the same manner as the decade old PVB model. Third, the freshly manufactured SGP model had a 0.090 in. thick interlayer and two 0.129 in. thick glass layers. The model had the same overall dimensions and mesh as that of the freshly manufactured PVB model. A segment pressure load of 37.49044 psi was applied to this model. Table 5-7 shows the area and loads used to determine the segment pressure load to be applied to each model.

TABLE 5-7. Finite Element Model Applied Loads

	Load Applied (from Experimental Effort)	**Area**	**Pressure**
	lb	in^2	psi
Decade Old PVB	25.76	1.5	17.175
Freshly Manufactured PVB	9.68	1	9.69
Freshly Manufactured SGP	37.49	1	37.49

In all simulations, the tensor stress in the longitudinal direction was recorded at the location of the strain gages, shown in Fig. 5-1. These data collected for each simulation were then used to define the variation of normal stress as a function of shear modulus. These stress data were plotted versus the shear modulus, *G*. These calculated stresses must be bounded by the fully monolithic performance model and the layered performance model. The relationship between stress and shear modulus for the decade old PVB, freshly manufactured PVB, and freshly manufactured SGP, are shown in Fig. 5-66, 5-67, and 5-68, respectively. It can be seen from the figures, that this relationship may be represented with two straight lines and a curved transition zone. There is a loss in sensitivity for stresses near the fully monolithic performance model. As expected the data asymptotically reach the fully monolithic performance model. Values near the fully monolithic performance model are not shown in the graphical presentation so as to preserve the curvature of the relationship in the critical transition zone below a shear modulus around 1500 psi. The complete data are tabulated in Table 5-8.

TABLE 5-8. Laminated Glass Beam Response as a Function of Shear Modulus

	Stress (psi)		
G (psi)	Decade Old PVB	Freshly Manufactured PVB	Freshly Manufactured SGP
5	3303.703	2626.354	7153.327
10	3210.131	2478.963	6903.764
15	3124.815	2362.112	6681.465
50	2689.977	1929.494	5621.422
100	2334.918	1687.25	4827.933
200	1976.830	1486.938	4062.7
300	1792.874	1391.641	3668.694
400	1678.852	1333.737	3418.724
500	1600.315	1294.273	3242.187
700	1497.800	1243.493	3004.606
1000	1408.546	1200.480	2789.923
1500	1328.638	1163.705	2591.087
3000	1236.092	1124.864	2353.344
10000	1166.182	1101.140	2168.510
100000	1148.387	1096.829	2121.987

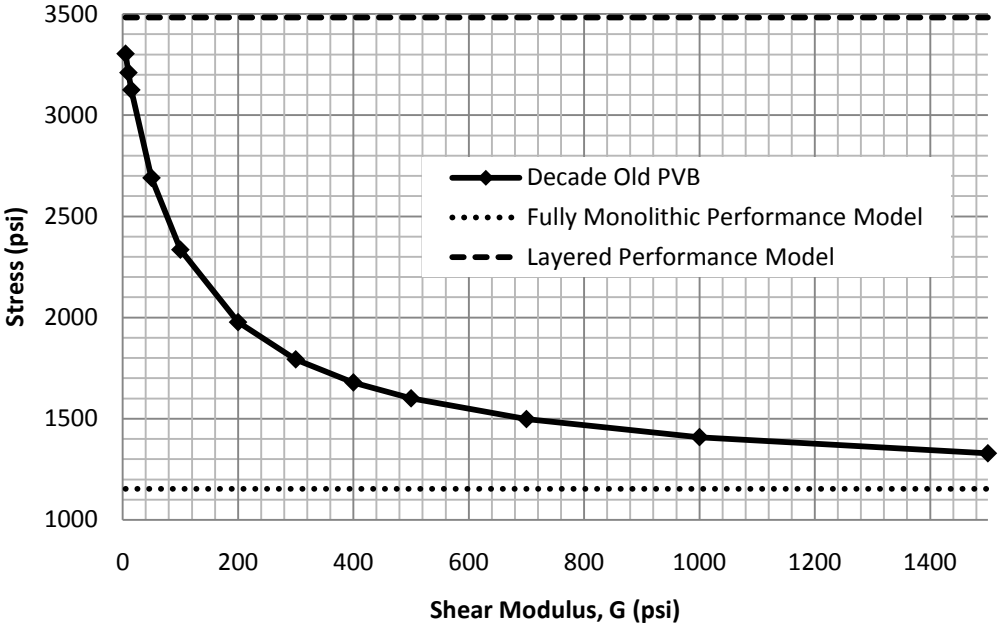

FIG. 5-66. Decade Old PVB Laminated Glass Beam Response as a Function of Shear Modulus

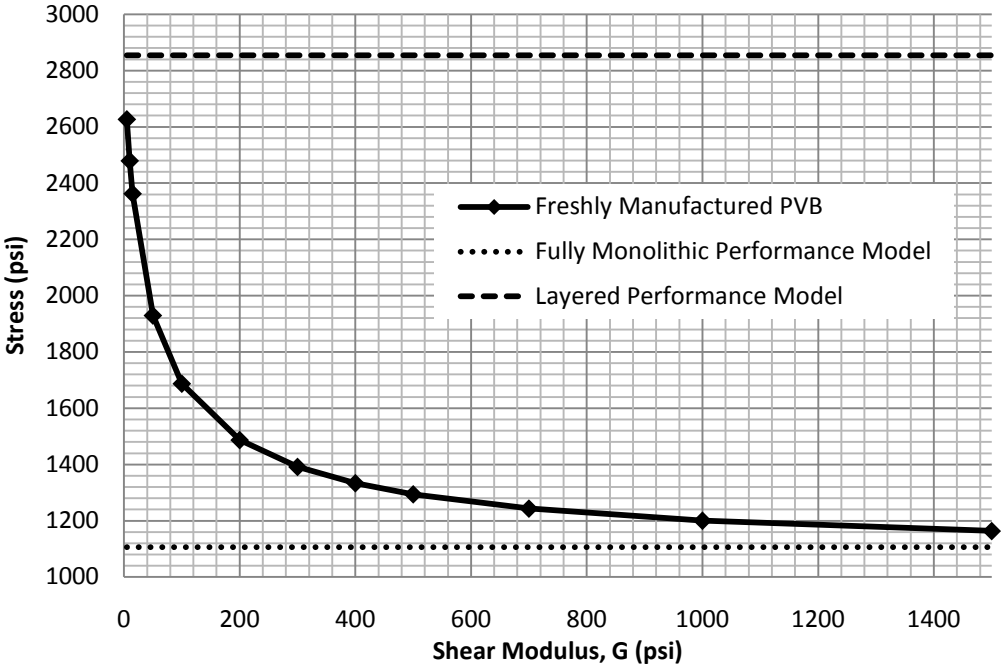

FIG. 5-67. Freshly Manufactured PVB Laminated Glass Beam Response as a Function of Shear Modulus

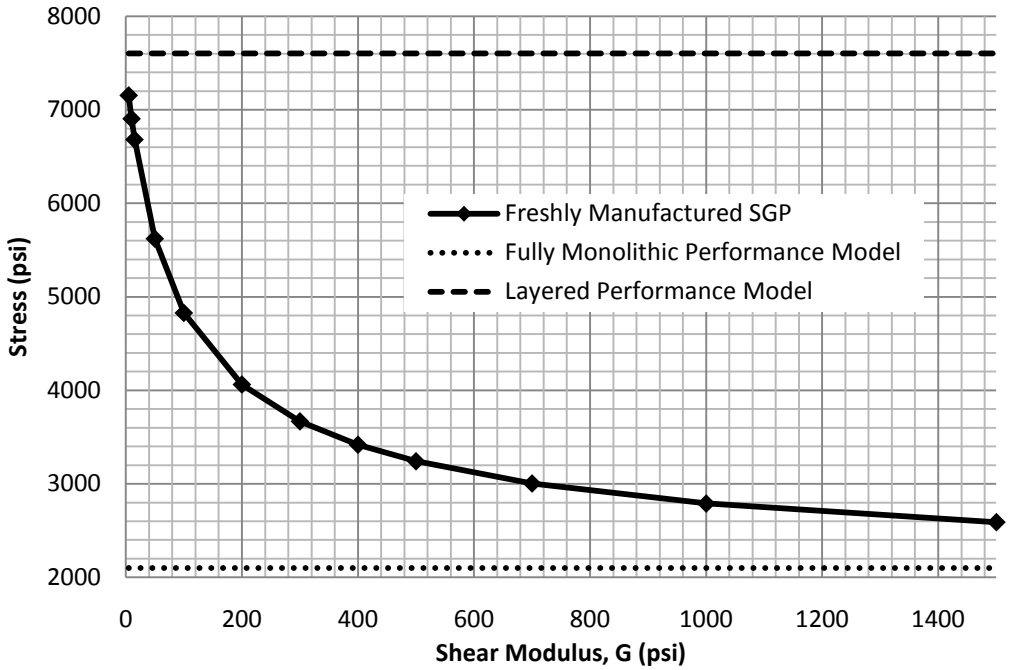

FIG. 5-68. Freshly Manufactured SGP Laminated Glass Beam Response as a Function of Shear Modulus

DETERMINATION OF A RELATIONSHIP BETWEEN SHEAR MODULUS AND TEMPERATURE

The primary result of the experimental effort was the measurement of the variation of longitudinal beam stress at a selected point as a function of temperature and load duration. These data were used to develop laminated glass beam temperature transition charts defined previously. These charts present a relationship between stress and temperature for selected load durations.

Finite element analyses were then used to quantify the effects of variations in shear modulus on the bending stress of laminated glass beams. These data were used to define a theoretical relationship between interlayer shear modulus and stress for laminated glass beams.

Next, the variation of interlayer shear modulus was quantified as a function of temperature and load duration using the data collected from the experimental effort and finite element analyses. Cross-plots, using simple linear interpolation techniques, between these data can be used to develop these relationships. An example of this technique is described for a single point below. Data collected for the freshly manufactured PVB beam were used.

Using the laminated glass beam temperature transition chart, a stress value can be estimated for a given temperature. As shown in red (Fig. 5-69), for 60 °F a stress value of 1196 psi is estimated.

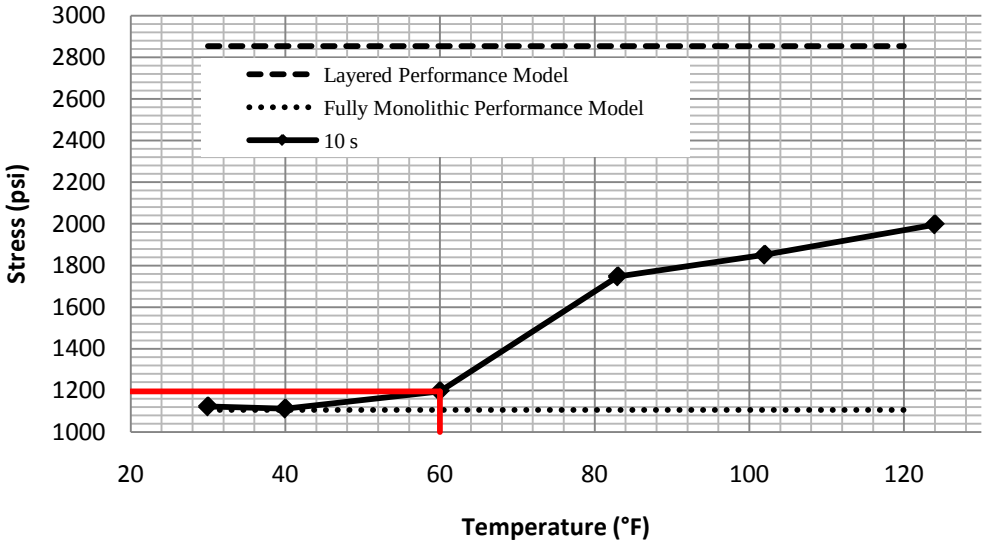

FIG. 5-69. Freshly Manufactured PVB Stress for a Given Temperature

The stress from the temperature transition chart, 1196 psi, can then be mapped to a shear modulus using the theoretical relationship between stress and shear modulus (Fig. 5-70). This relationship was produced using finite element analyses. As seen in Fig. 5-70, for a stress of 1196 psi, the shear modulus is taken to be 1061 psi. Therefore, for a temperature of 60 °F the shear modulus, for this particular interlayer, is taken to be 1061 psi. This method is repeated for each data point collected and load duration. These data are used to produce Fig. 5-71. Fig. 5-71 defines a relationship between shear modulus and temperature for a given load duration of 10 s for laminated glass employing a fresh PVB interlayer.

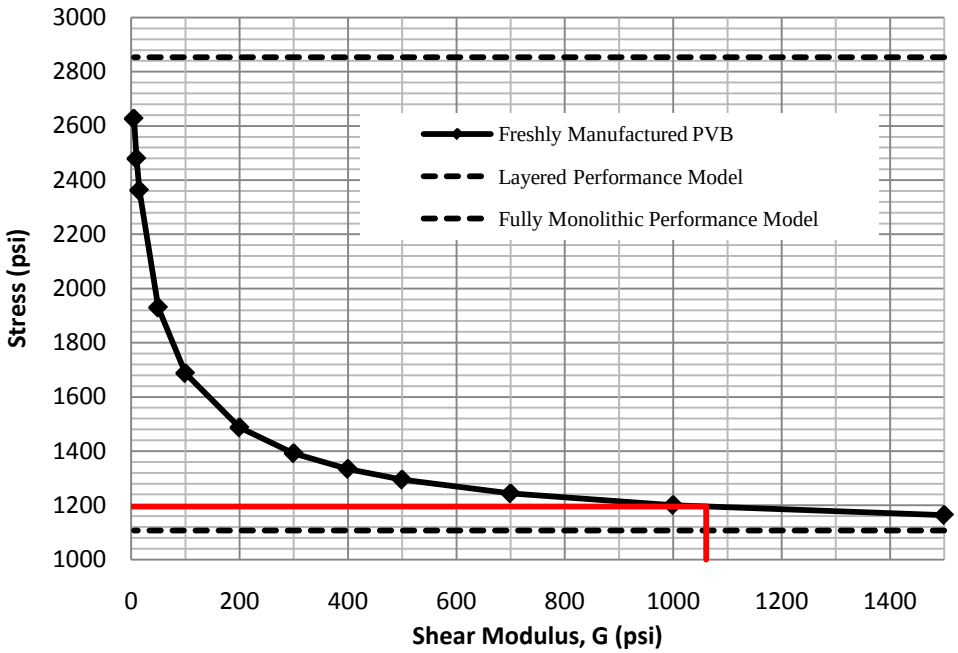

FIG. 5-70. Freshly Manufactured PVB Stress for a Given Shear Modulus

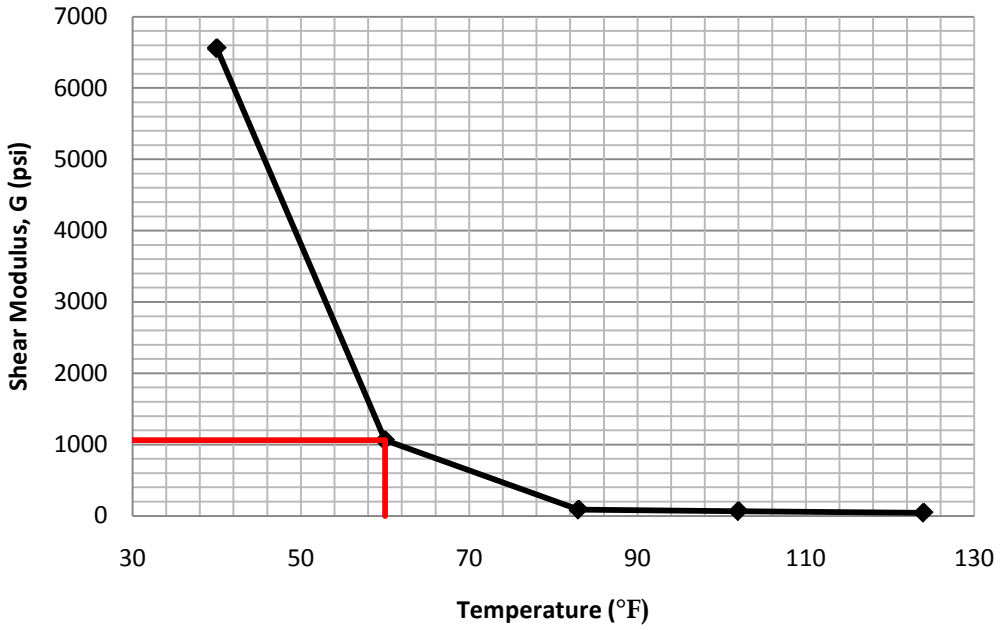

FIG. 5-71. Freshly Manufactured PVB Shear Modulus for a Given Temperature

The shear modulus results for the decade old PVB, freshly manufactured PVB, and freshly manufactured SGP are presented in Fig. 5-72 through 5-78, 5-80 through 5-86, and 5-88 through 5-94, respectively. Fig. 5-79, 5-77, and 5-95 summarize these data for each type of interlayer.

It should be noted that, the procedure lost sensitivity as the behavior of the laminated glass beams approached the fully monolithic model. However, the procedure is very sensitive as the behavior of the laminated glass approaches the layered model. In most cases, it is the near layered response that controls the design of laminated glass beams. This is the case because as the beam approaches the monolithic performance it takes a large change in shear modulus to cause a small change in beam response. Further, the loss of sensitivity seems to occur below the interlayer's glass transition temperature. This is consistent with conclusions drawn by Edel. Edel showed that the rate of change in the interlayer material properties occur very rapidly for temperatures below the glass transition temperature. In addition, Edel showed that the rate of change in interlayer material properties, above the transition temperature, where gradual. These findings are consistent with data presented herein. (Edel 1997)

The data presented in the Fig 5-72 through 5-95 is tabulated below in Table 5-9 through 5-11. These results provide specific design guidance for laminated glass that incorporates these interlayer materials.

TABLE 5-9. Decade Old PVB Laminated Glass Beam Shear Modulus as a Function of Temperature

	G (psi)						
T (°F)	***10 S***	***60 S***	***5 Min***	***10 Min***	***20 Min***	***40 Min***	***60 Min***
29	2469.868	2301.304	2132.740	1879.893	1542.765	1353.822	1223.671
41	2132.740	1483.972	945.368	735.629	517.782	367.420	296.561
61	251.333	118.911	71.458	58.277	48.034	42.175	39.663
82	61.206	48.871	43.012	41.337	36.315	33.804	28.781
101	43.849	37.152	31.292	27.107	23.758	21.247	19.573
122	32.129	22.921	14.673	12.235	9.815	8.147	6.480

TABLE 5-10. Freshly Manufactured PVB Laminated Glass Beam Shear Modulus as a Function of Temperature

	G (psi)						
T (°F)	***10 S***	***60 S***	***5 Min***	***10 Min***	***20 Min***	***40 Min***	***60 Min***
40	6559.617	3490.892	3490.892	2662.616	2662.616	1859.352	1485.115
60	1060.917	485.489	221.551	163.526	114.203	84.406	72.600
83	87.626	70.453	59.720	53.281	51.134	41.189	47.079
102	66.160	53.281	47.079	47.079	45.396	41.189	44.555
124	44.555	38.665	31.934	29.410	26.044	24.361	20.996

TABLE 5-11.Freshly Manufactured SGP Laminated Glass Beam Shear Modulus as a Function of Temperature

	G (psi)						
T (°F)	***10 S***	***60 S***	***5 Min***	***10 Min***	***20 Min***	***40 Min***	***60 Min***
41	5868.580	5474.713	5474.713	5080.846	5080.846	5080.846	4686.980
60	5080.846	4686.980	4686.980	4293.113	4293.113	4293.113	4096.180
82	4686.980	4293.113	3899.246	3505.380	2952.961	2952.961	2756.109
102	3899.246	2952.961	2690.491	2493.640	2099.936	1640.615	1425.282
120	1509.381	1111.457	771.277	629.124	567.840	469.064	439.609

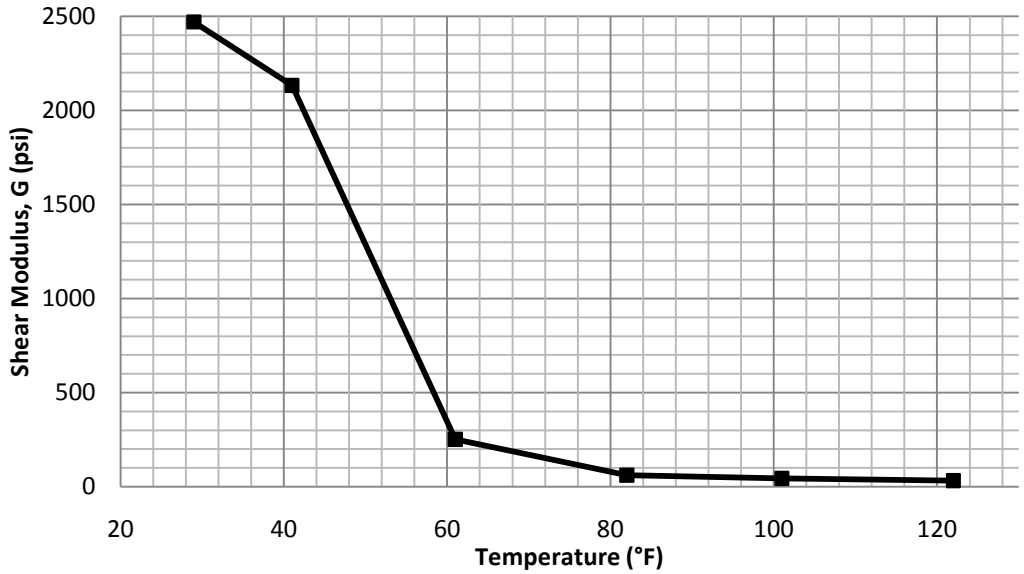

FIG. 5-72. Decade Old PVB Laminated Glass Beam Shear Modulus as a Function of Temperature – 10 S Load Duration

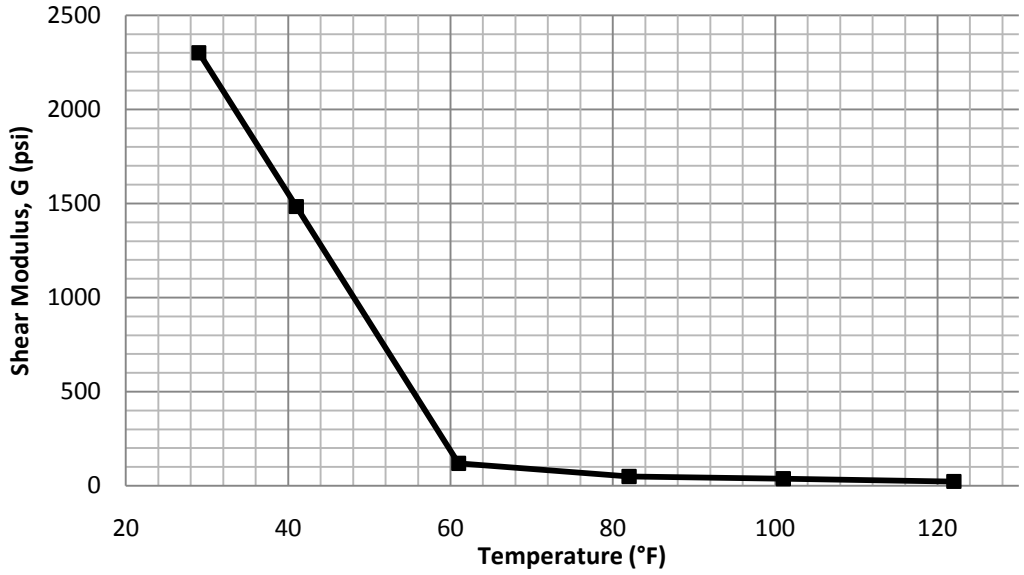

FIG. 5-73. Decade Old PVB Laminated Glass Beam Shear Modulus as a Function of Temperature – 60 S Load Duration

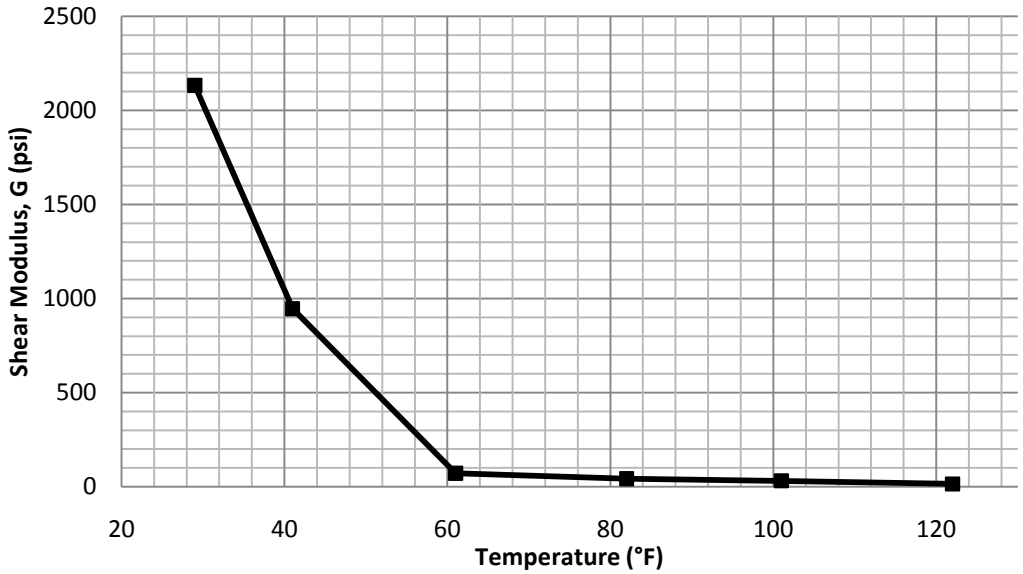

FIG. 5-74. Decade Old PVB Laminated Glass Beam Shear Modulus as a Function of Temperature – 5 Min Load Duration

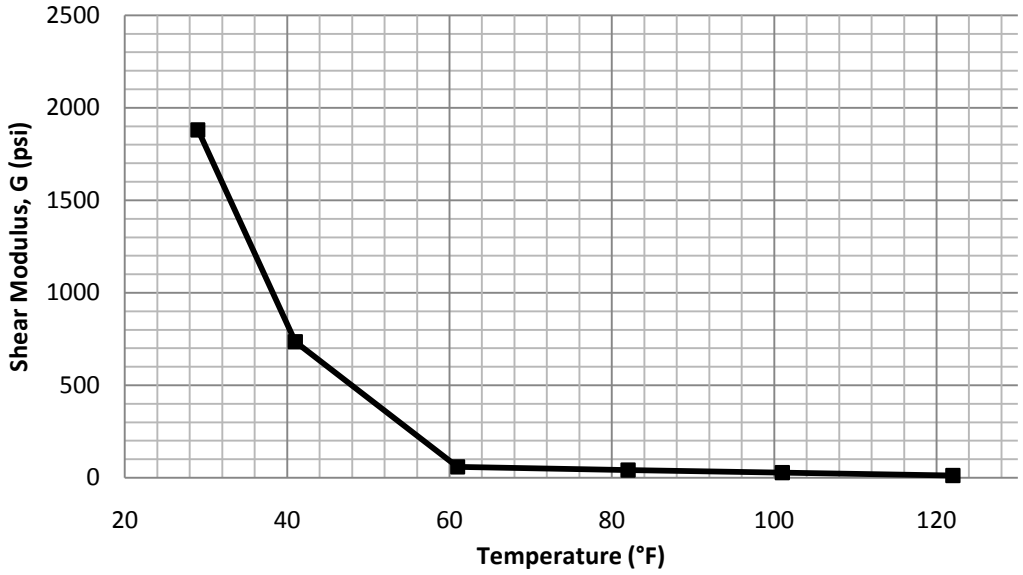

FIG. 5-75. Decade Old PVB Laminated Glass Beam Shear Modulus as a Function of Temperature – 10 Min Load Duration

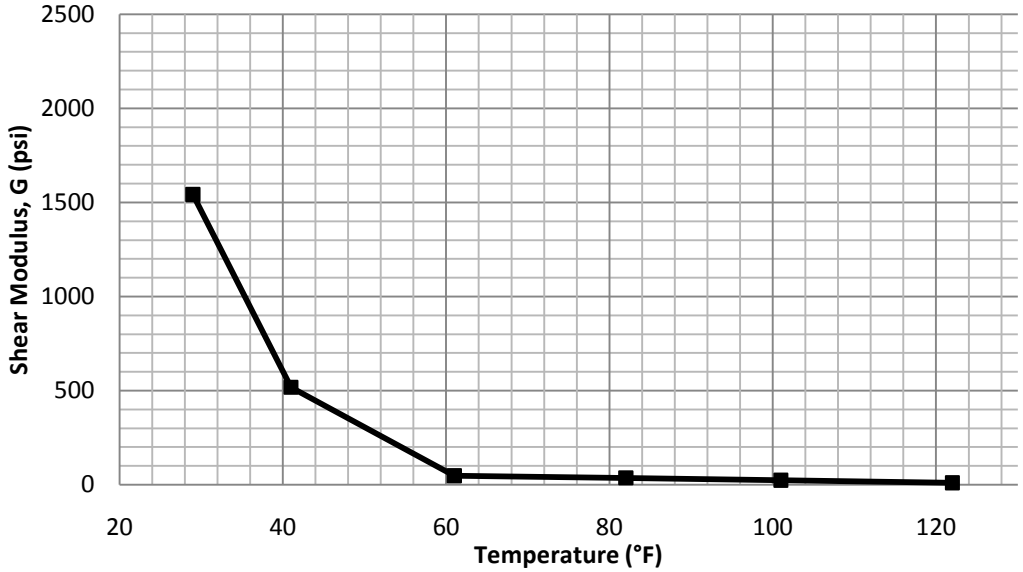

FIG. 5-76. Decade Old PVB Laminated Glass Beam Shear Modulus as a Function of Temperature – 20 Min Load Duration

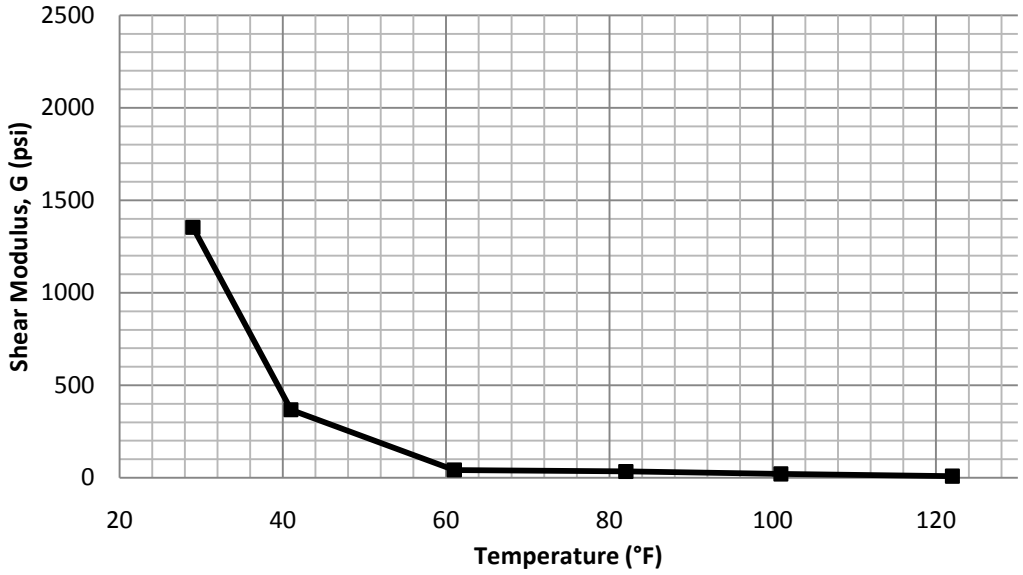

FIG. 5-77. Decade Old PVB Laminated Glass Beam Shear Modulus as a Function of Temperature – 40 Min Load Duration

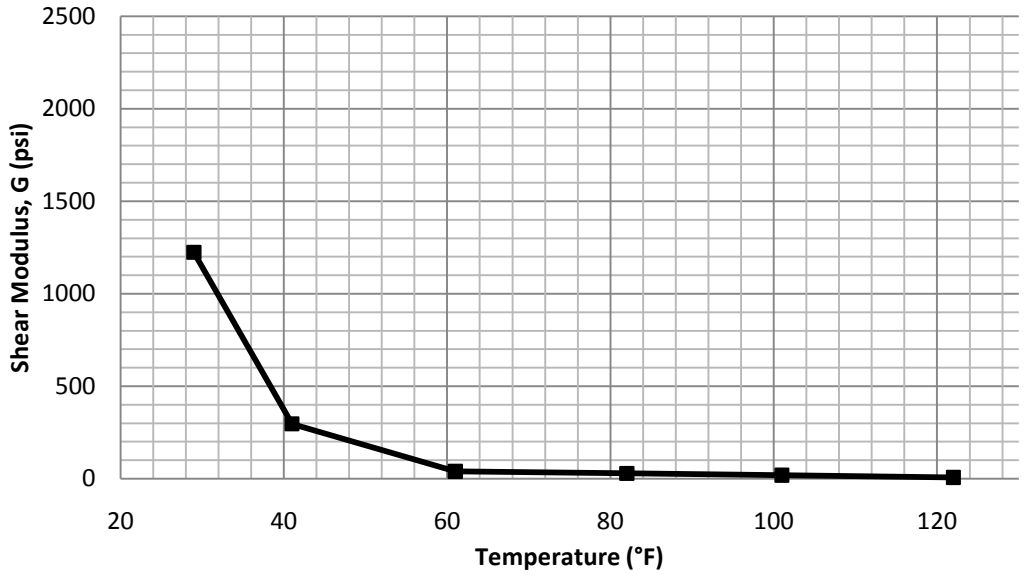

FIG. 5-78. Decade Old PVB Laminated Glass Beam Shear Modulus as a Function of Temperature – 60 Min Load Duration

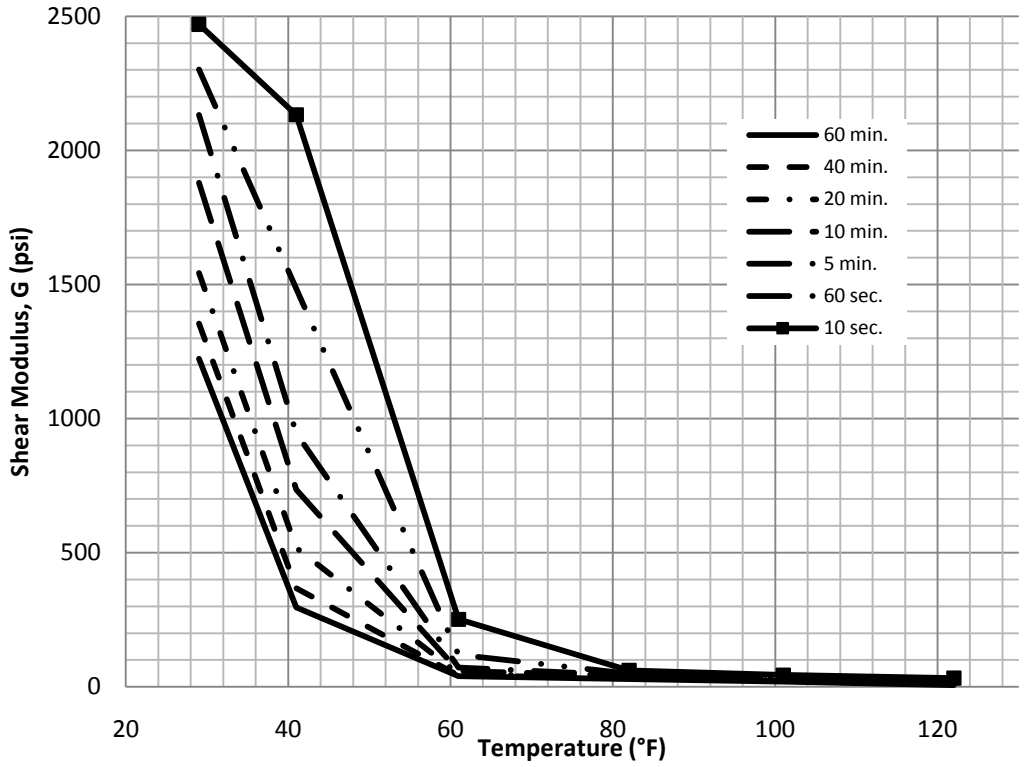

FIG. 5-79. Decade Old PVB Laminated Glass Beam Shear Modulus as a Function of Temperature

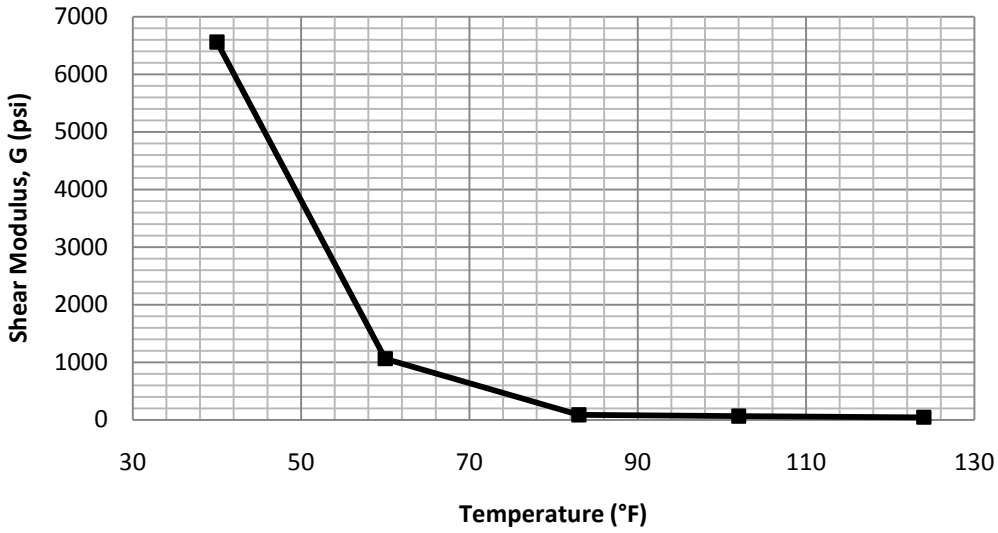

FIG. 5-80. Freshly Manufactured PVB Laminated Glass Beam Shear Modulus as a Function of Temperature – 10 S Load Duration

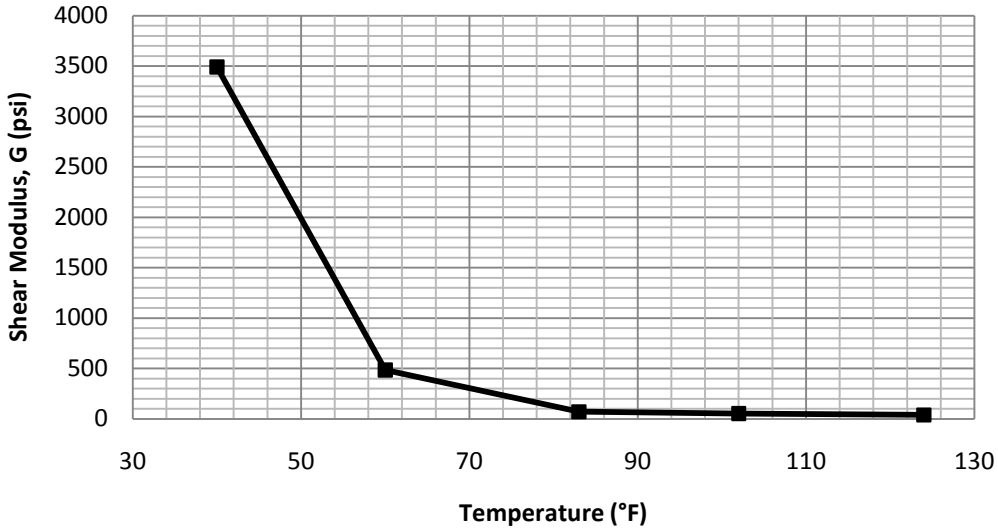

FIG. 5-81. Freshly Manufactured PVB Laminated Glass Beam Shear Modulus as a Function of Temperature – 60 S Load Duration

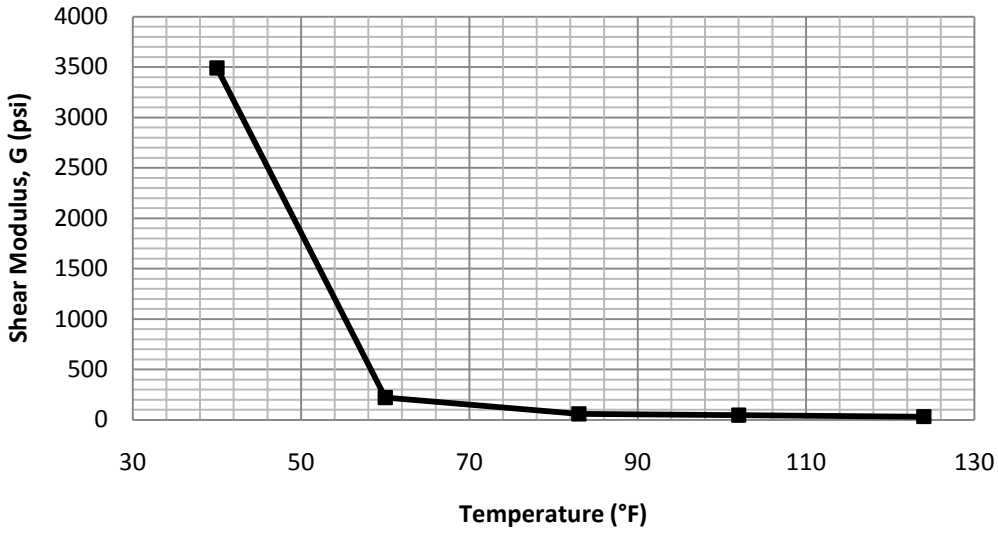

FIG. 5-82. Freshly Manufactured PVB Laminated Glass Beam Shear Modulus as a Function of Temperature – 5 Min Load Duration

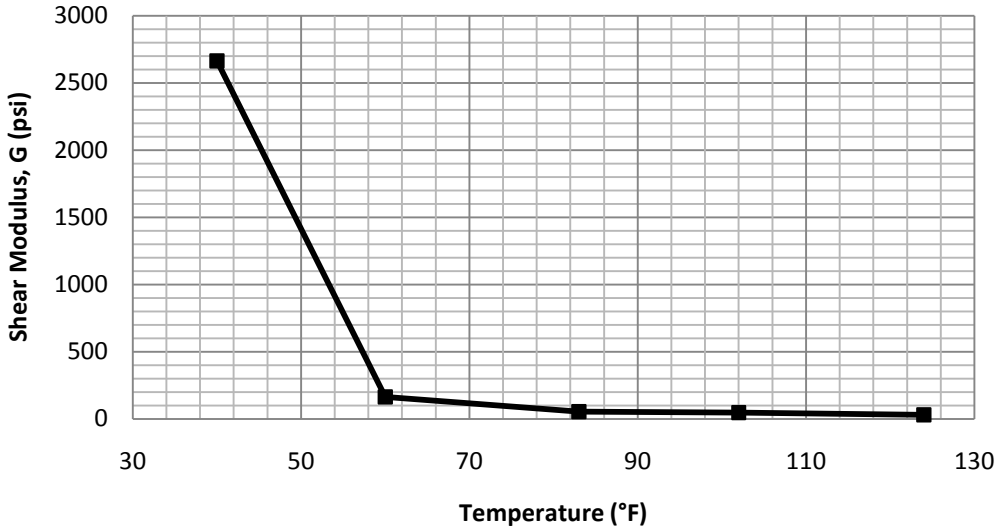

FIG. 5-83. Freshly Manufactured PVB Laminated Glass Beam Shear Modulus as a Function of Temperature – 10 Min Load Duration

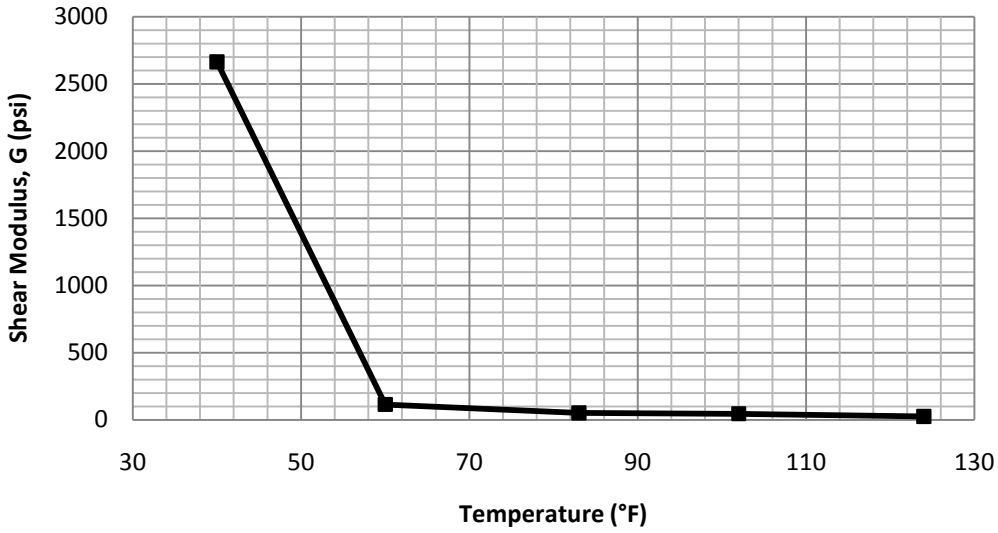

FIG. 5-84. Freshly Manufactured PVB Laminated Glass Beam Shear Modulus as a Function of Temperature – 20 Min Load Duration

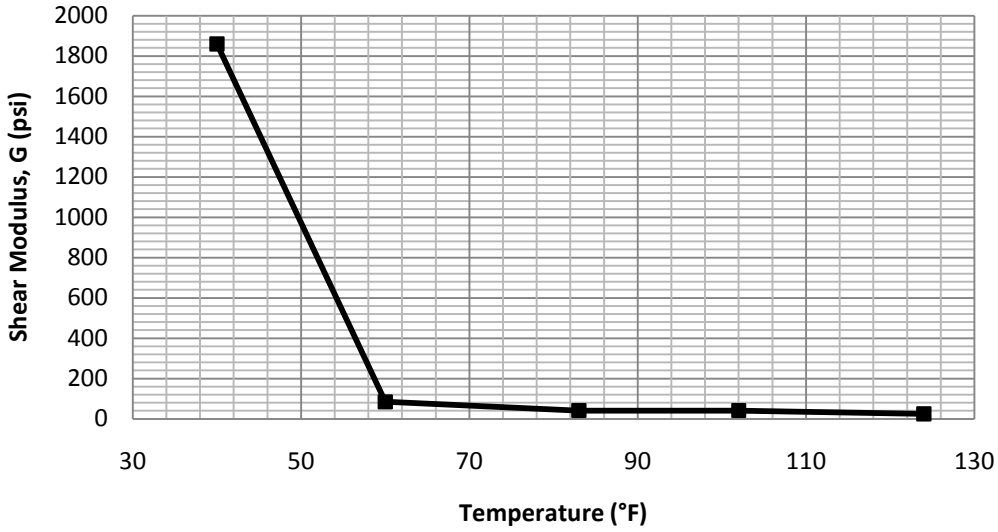

FIG. 5-85. Freshly Manufactured PVB Laminated Glass Beam Shear Modulus as a Function of Temperature – 40 Min Load Duration

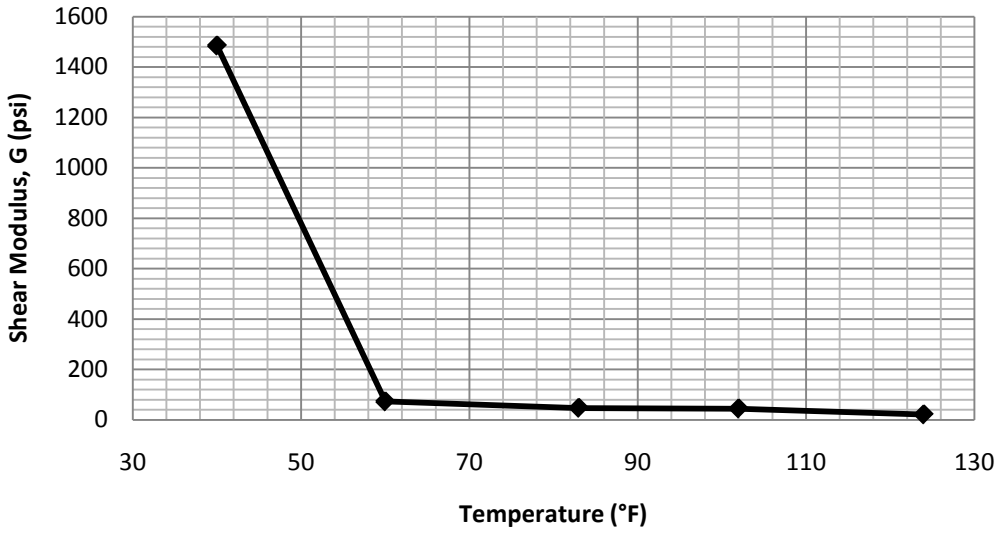

FIG. 5-86. Freshly Manufactured PVB Laminated Glass Beam Shear Modulus as a Function of Temperature – 60 Min Load Duration

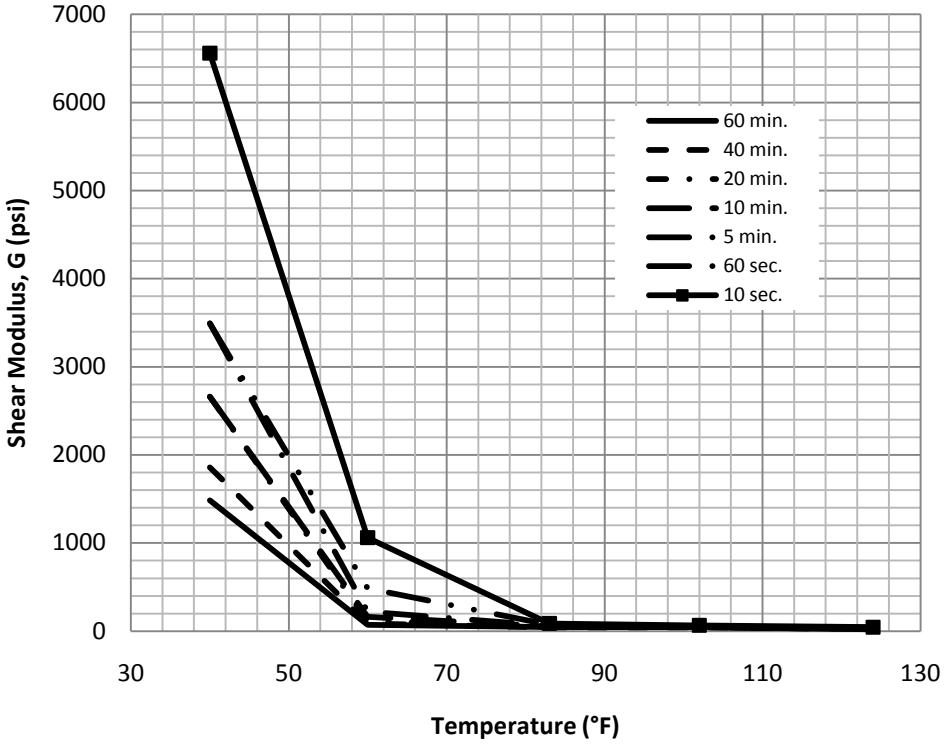

FIG. 5-87. Freshly Manufactured PVB Laminated Glass Beam Shear Modulus as a Function of Temperature

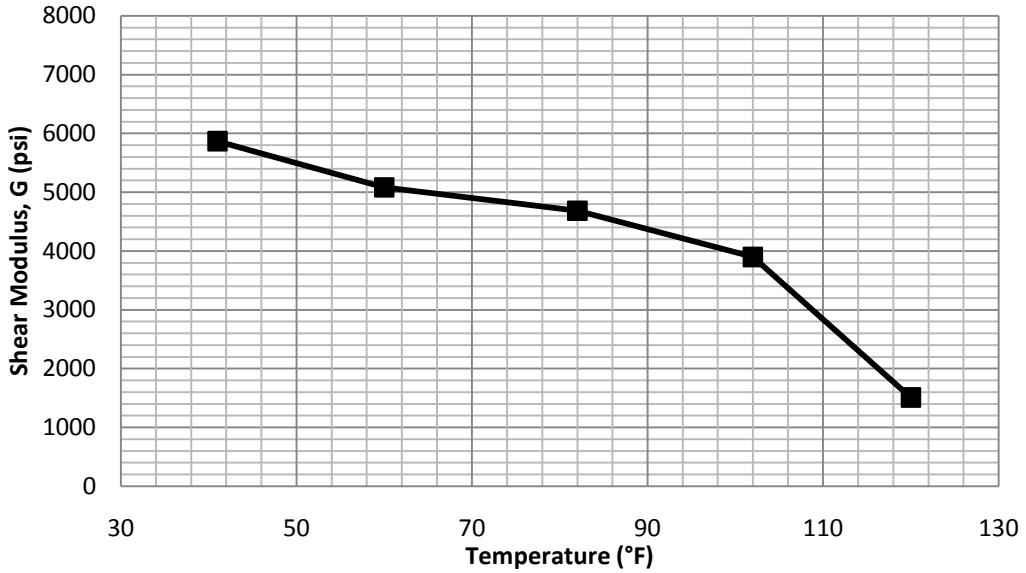

FIG. 5-88. Freshly Manufactured SGP Laminated Glass Beam Shear Modulus as a Function of Temperature – 10 S Load Duration

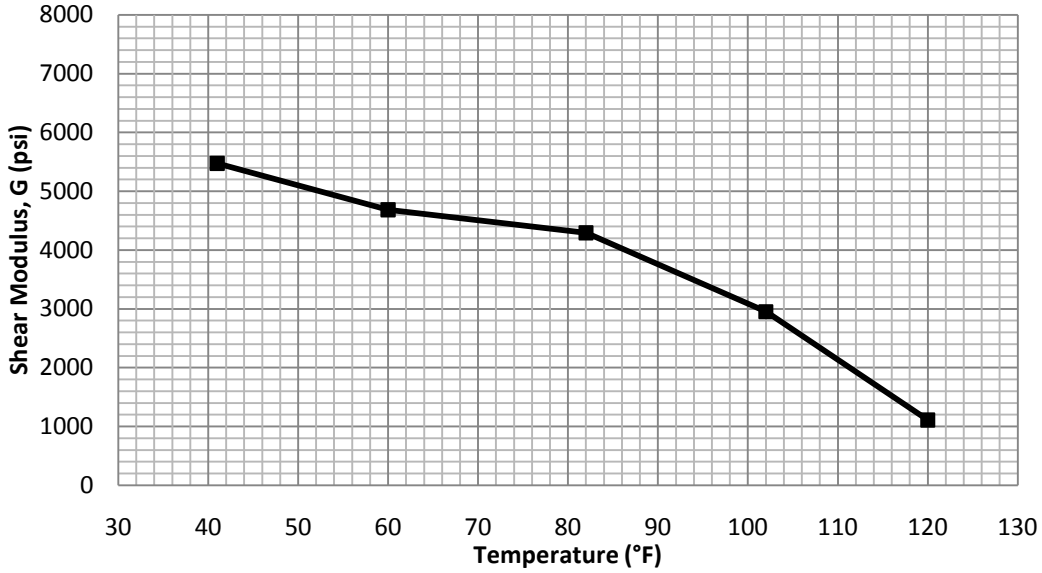

FIG. 5-89. Freshly Manufactured SGP Laminated Glass Beam Shear Modulus as a Function of Temperature – 60 S Load Duration

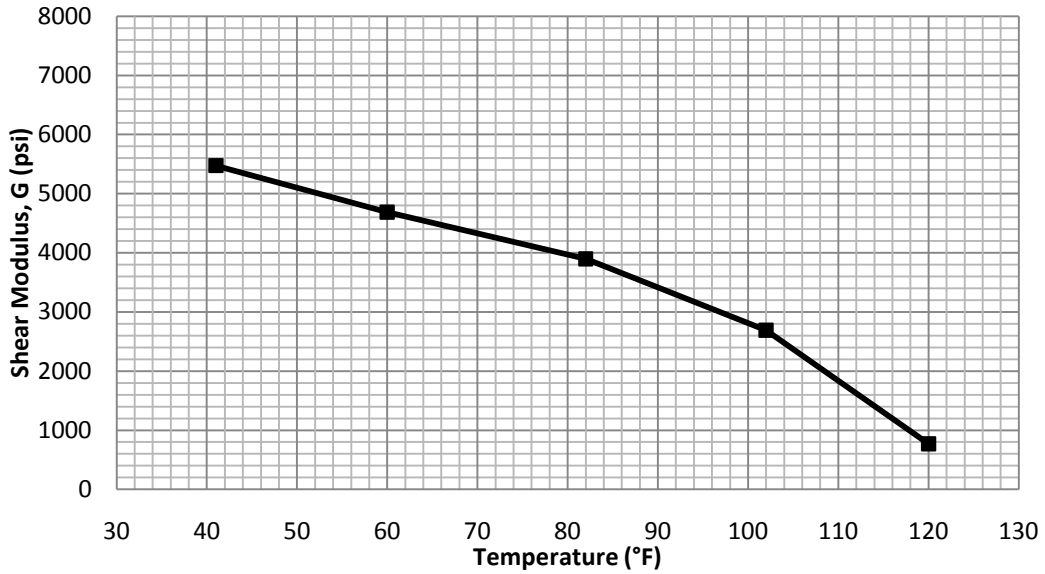

FIG. 5-90. Freshly Manufactured SGP Laminated Glass Beam Shear Modulus as a Function of Temperature – 5 Min Load Duration

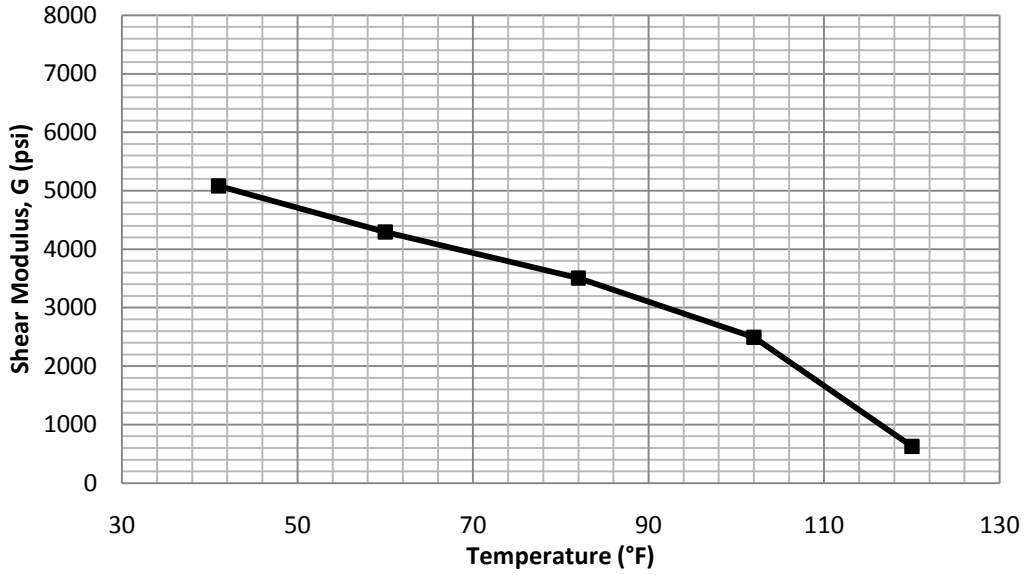

FIG. 5-91. Freshly Manufactured SGP Laminated Glass Beam Shear Modulus as a Function of Temperature – 10 Min Load Duration

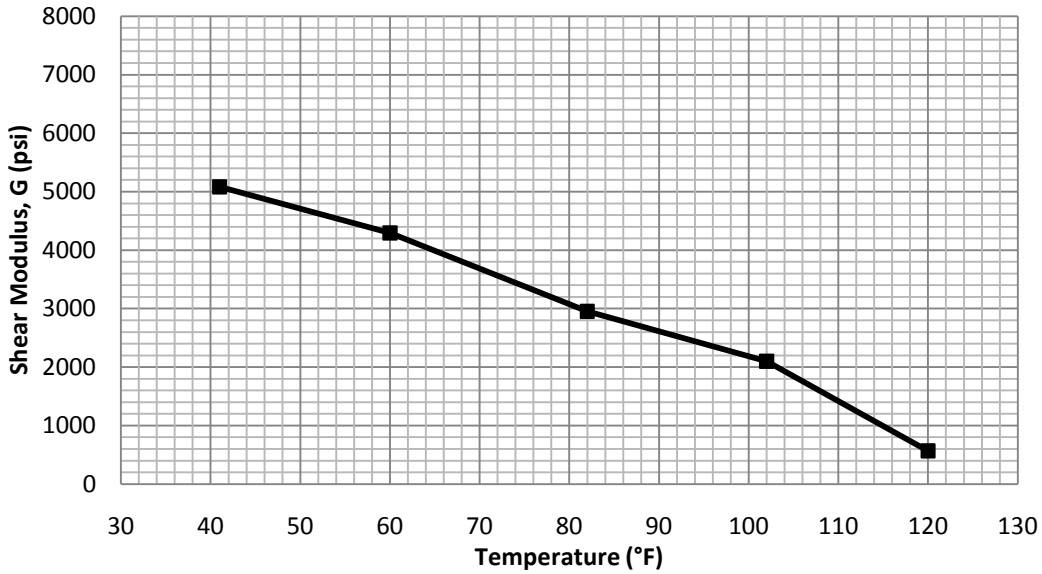

FIG. 5-92. Freshly Manufactured SGP Laminated Glass Beam Shear Modulus as a Function of Temperature – 20 Min Load Duration

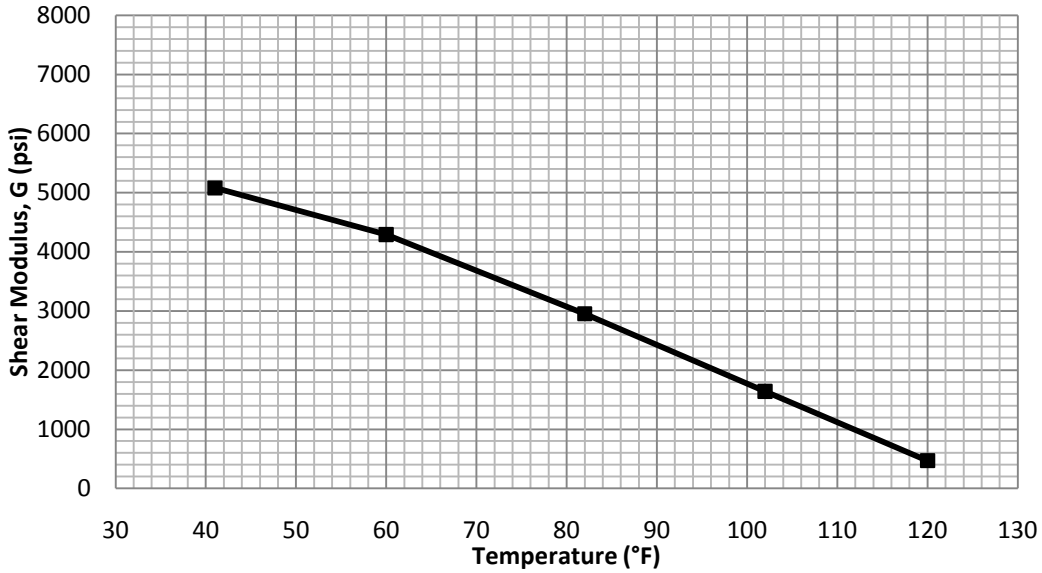

FIG. 5-93. Freshly Manufactured SGP Laminated Glass Beam Shear Modulus as a Function of Temperature – 40 Min Load Duration

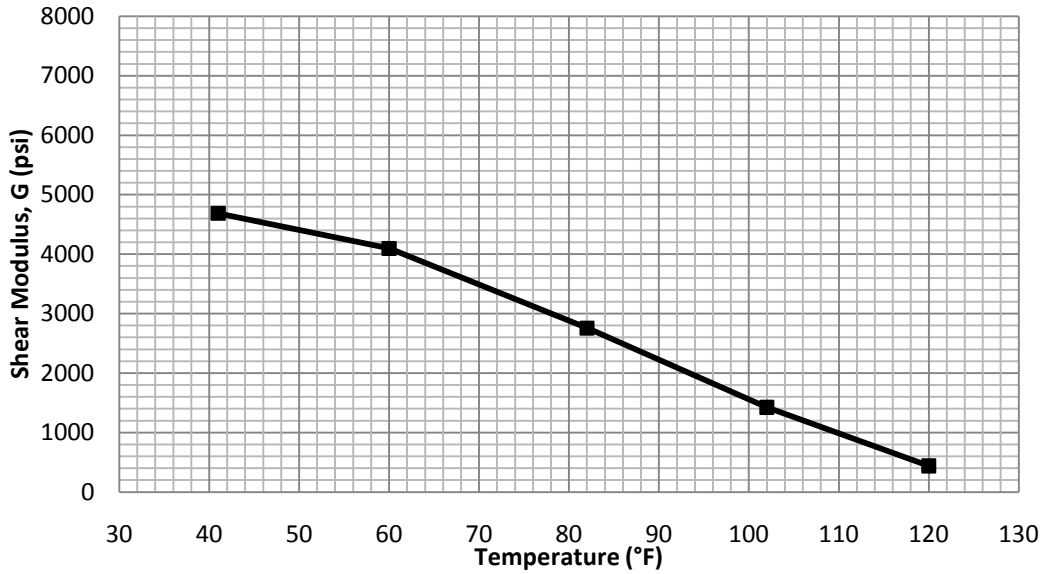

FIG. 5-94. Freshly Manufactured SGP Laminated Glass Beam Shear Modulus as a Function of Temperature – 60 Min Load Duration

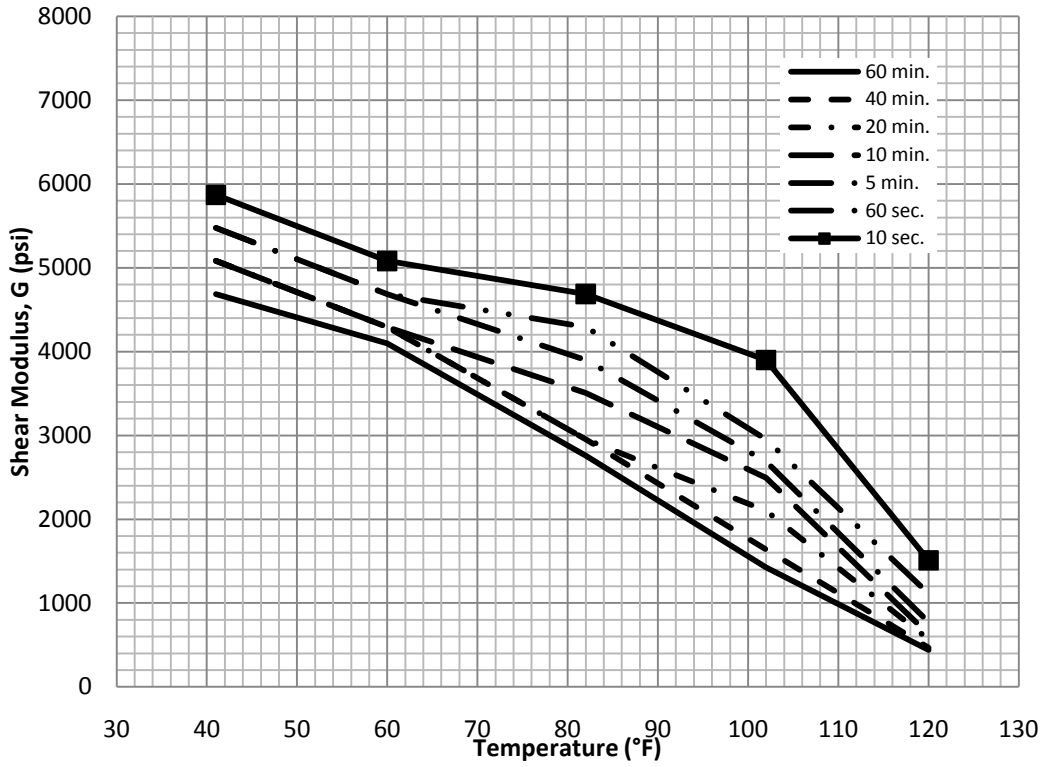

FIG. 5-95. Freshly Manufactured SGP Laminated Glass Beam Shear Modulus as a Function of Temperature

Fig. 5-96 compares the shear modulus values determined from the research conducted herein to those given by DuPont Company for the SGP interlayer. The data presented in Fig. 5-96 were discussed in detail, previously in Chapter IV. It appears that the latest data presented by DuPont represent a substantially stiffer interlayer than that tested by the writer. Based on this limited observation, it is recommended that the original SGP dataset presented by DuPont be used in lieu of the more recent data.

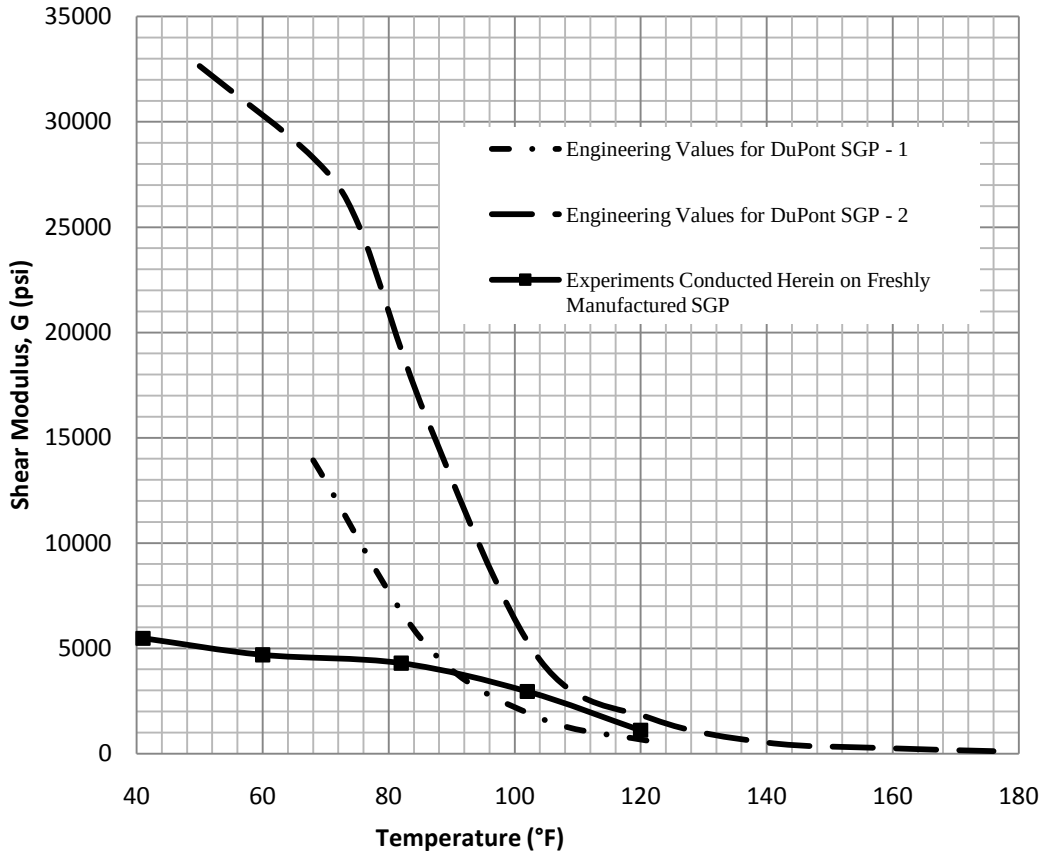

FIG. 5-96. SGP Laminated Glass Shear Modulus as a Function of Temperature

CHAPTER VI

THE APPLICATION OF THE STANDARD PROCEDURE TO PREVIOUS RESEARCH

While research has previously been conducted on the structural performance of laminated glass, not all research goes so far as to determine a relationship between interlayer shear modulus and temperature for a given load duration. In addition, previous research that does give this estimation for the shear modulus of laminated glass interlayers, may not outline the method in which these values were derived.

Chapter V presented a standard procedure to evaluate the shear modulus of laminated glass interlayers. This procedure may be applied to data presented previously by various researchers to estimate the shear modulus of the given interlayer material. In particular, this chapter discusses the application of the procedure to experimental data presented by the GRTL, Stewart, and Edel. These data are presented and then, if applicable, they were compared to the research conducted herein.

Previous research conducted by the GRTL, Stewart, and Edel examined the effects of temperature on the bending of laminated glass beams. While these experiments may not be representative of actual laminated glass installations or implied wind loads, these data can be used to produce laminated glass beam temperature transition charts. These data give a relationship between stress and temperature for the given laminated glass beam and load duration. These data have been presented in Chapter IV.

Using the geometry and loading conditions for the three previous research experiments, as described in Chapter IV, finite element analyses were employed to develop a theoretical stress response as a function of interlayer shear modulus. The process for applying finite element analyses to such data is discussed in Chapter V. Table 6-1 shows the relationship between shear modulus and laminated glass performance for experiments conducted by the GRTL, Stewart, and Edel. These values were derived through the use of the finite element analyses, described previously. Then, these data were used to develop shear modulus performance charts for the three different beams and loadings. As discussed previously, there is a loss in sensitivity for stresses near the fully monolithic performance model. In the graphical presentation, data were truncated at 1500 psi shear modulus so as to preserve the curvature of the relationship in the critical transi-

tion zone. As is apparent in these figures, these curves can be represented with two straight lines and a curved transition zone. Fig. 6-1, 6-2 and 6-3 present these data graphically.

TABLE 6-1. Laminated Glass Beam Response as a Function of Shear Modulus

	Stress (psi)		
G (psi)	Experiments by GRTL	Experiments by Stewart	Experiments by Edel
5	-	-	10265.470
10	-	2009.734	10095.676
15	5007.975	1948.046	9935.365
50	4136.917	1637.831	9017.5
100	3517.792	1388.895	8117.584
200	2972.286	1145.38	7046.06
300	2724.216	1026.201	6426.136
400	2582.98	955.795	6019.628
500	2492.141	909.501	5731.233
700	2382.635	852.727	5347.226
1000	2296.861	807.802	5009.497
1500	2228.525	772.436	4708.856
3000	2159.796	739.74	4373.1
10000	2113.062	-	4153.986
100000	2097.416	-	4121.294

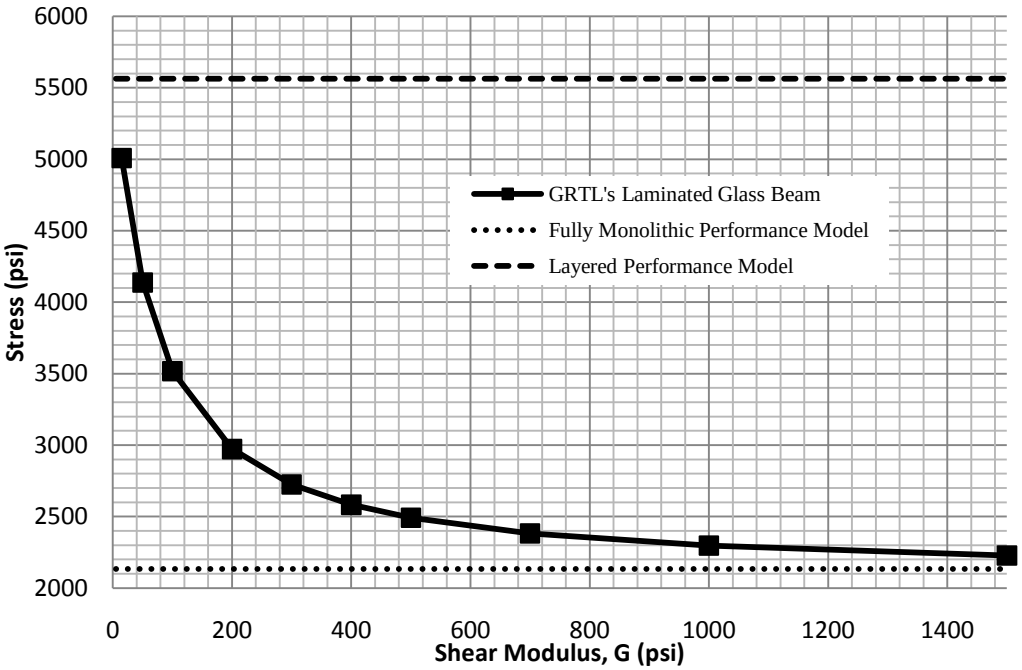

FIG. 6-1. GRTL's Laminated Glass Beam Response as a Function of Shear Modulus

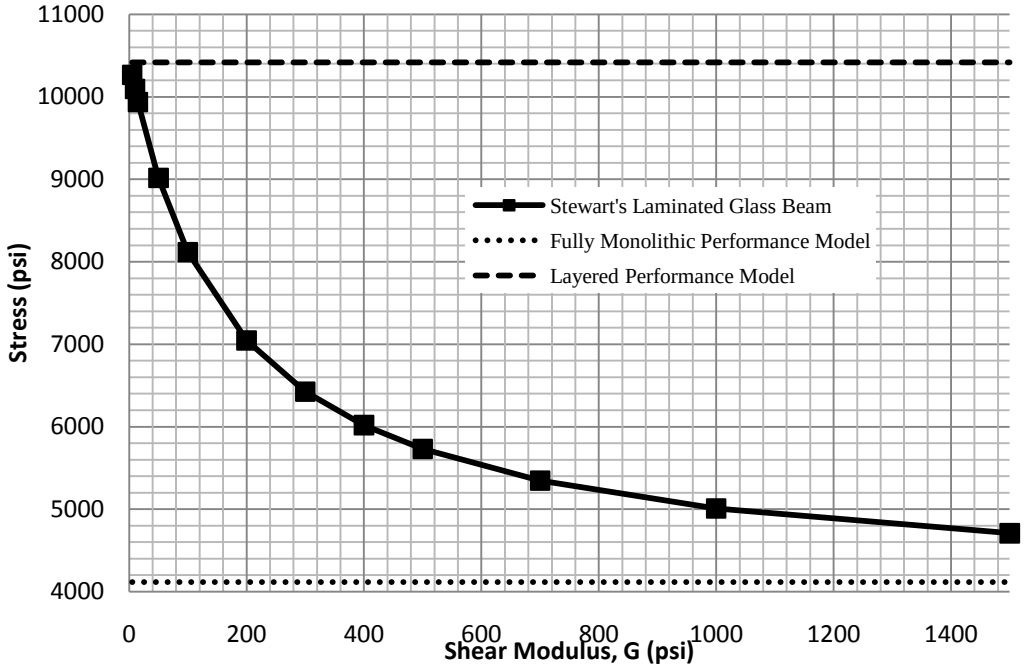

FIG. 6-2. Stewart's Laminated Glass Beam Response as a Function of Shear Modulus

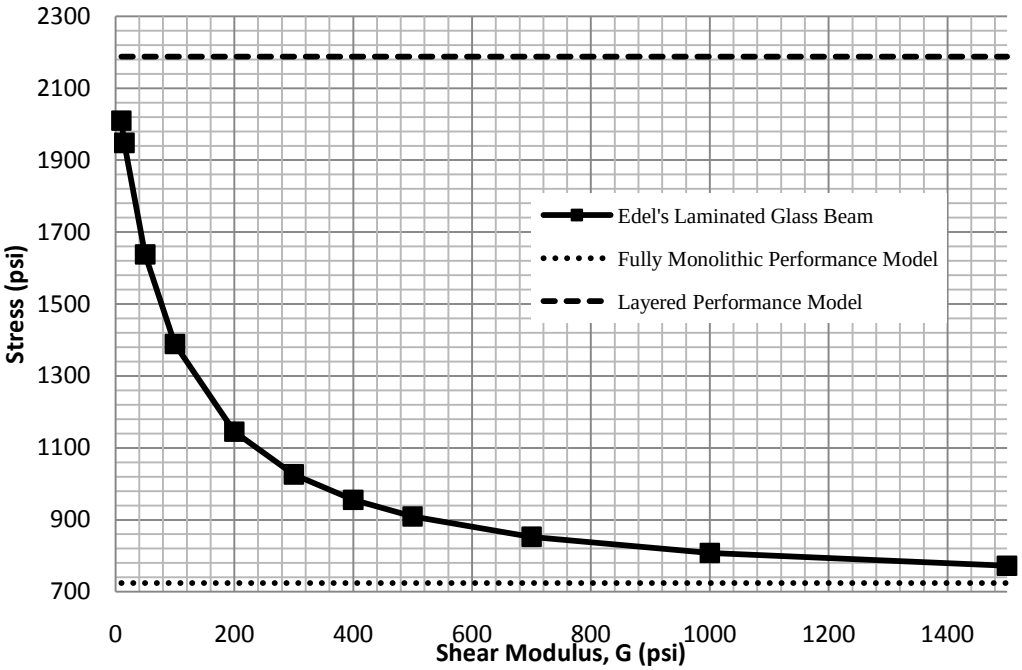

FIG. 6-3. Edel's Laminated Glass Beam Response as a Function of Shear Modulus

These data collected through finite element analyses and reported experimental data may then be coupled using the interpolation techniques described in Chapter V. Cross-plots of these data will estimate the shear modulus as a function of temperature for the laminated glass beams that were tested.The resulting cross-plotted data are presented in Fig 6-4 and 6-5 for experiments by the GRTL and Stewart, respectively.

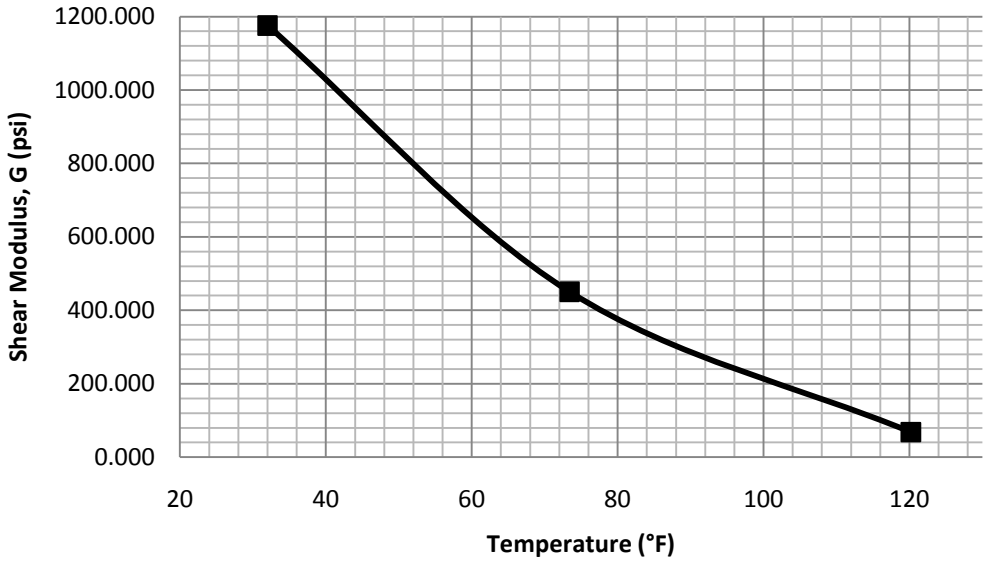

FIG. 6-4. GRTL's Laminated Glass Beam Shear Modulus as a Function of Temperature

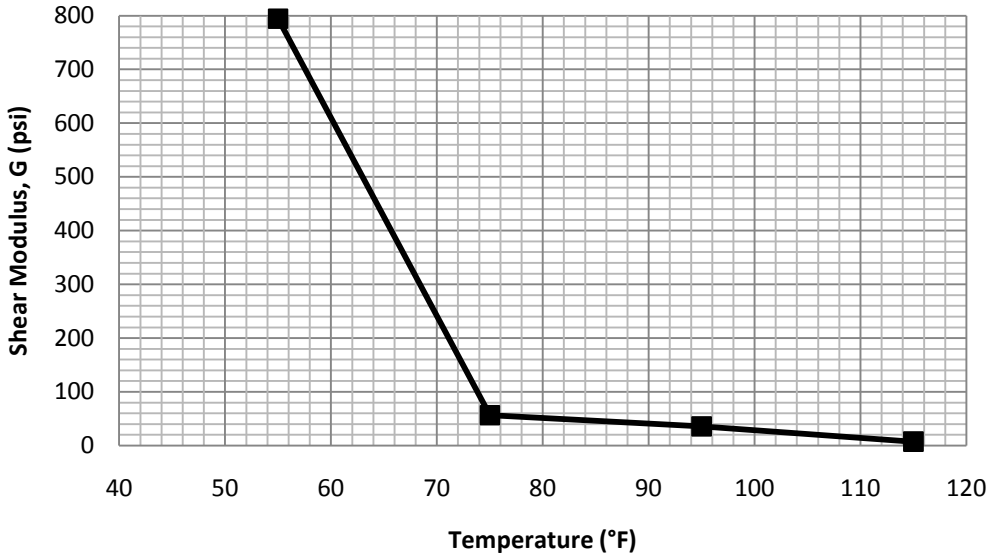

Fig. 6-5. Stewart's Laminated Glass Beam Shear Modulus as a Function of Temperature

Fig. 6-6 shows the relationship between shear modulus and temperature for a 60 s load duration from data presented by Edel. In addition, these data are compared to the shear modulus derived from experiments conducted herein on the same laminated glass beam tested over a decade earlier. Upon examination of the tabulated data (Table 6-2), it appears that PVB may lose stiffness with age for temperatures above room temperature through 120 °F. However, it must

be remembered that the decade old PVB beams were not exposed to thermal cycles and ultraviolent light exposure typical to those in architectural glazing applications.

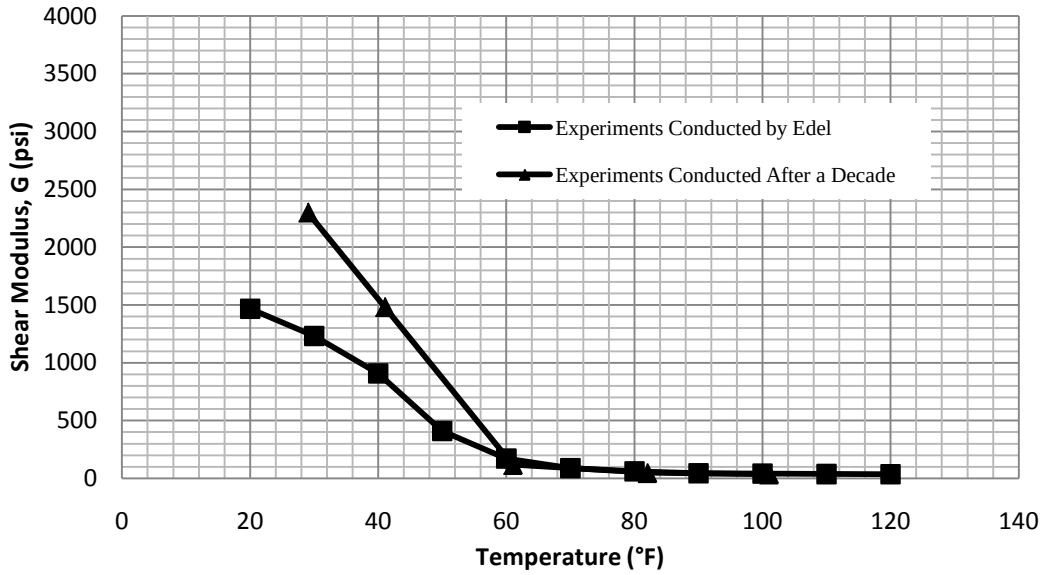

FIG. 6-6. Edel's Laminated Glass Beam Shear Modulus as a Function of Temperature

TABLE 6-2. Edel's Laminated Glass Beam Shear Modulus as a Function of Temperature

Experiments Conducted by Edel		Experiments Conducted After a Decade	
***T* (°F)**	***G* (psi)**	***T* (°F)**	***G* (psi)**
20	1466.577	-	-
30	1231.320	29	2301.304
40	907.858	41	1483.972
50	409.061	-	-
60	171.098	61	118.911
70	88.611	-	-
80	60.619	82	48.871
90	43.527	-	-
100	41.533	101	37.152
110	37.426	-	-
120	35.079	122	22.921

Fig. 6-7 presents a summary of the relationship between shear modulus and temperature for PVB, including previous experiments and those conducted herein. From these data it is seen that in the critical temperature ranges of room temperature to 120 °F that the shear modulus curves from most of the data appear to cluster reasonable closely with the obvious exception of the data produced by the GRTL. At the usual design temperature of 120 °F shows that the shear modulus for PVB varies in a range of approximately 10 to 70 psi. The lower value is associated with the research conducted by Stewart. The largest value is associated with experiments conducted by the GRTL. The experiments conducted herein, match closely with those of DuPont and Edel. These values range from approximately 35 to 42 psi at 120 °F.

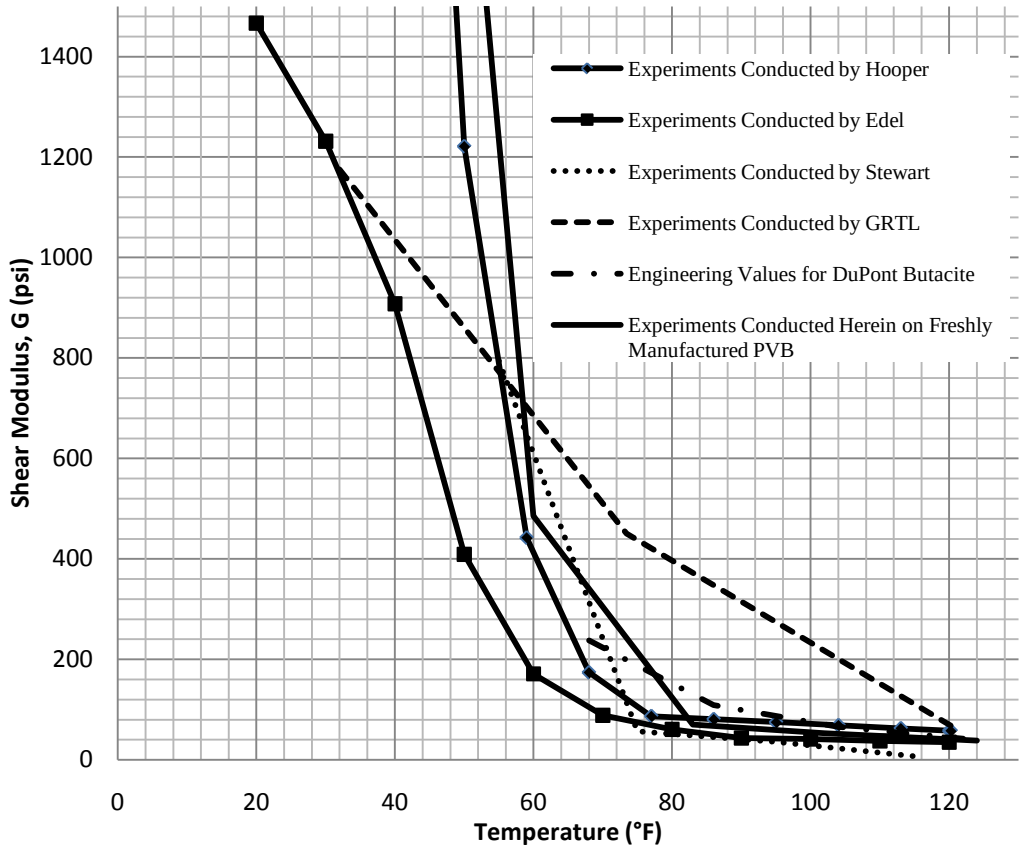

FIG. 6-7. Summary for PVB Laminated Glass Beam Shear Modulus as a Function of Temperature

CHAPTER VII

CONCLUSIONS

The purpose of this thesis was to develop a standard procedure that allows for the shear modulus of typical laminated glass interlayers to be deduced from straight-forward physical experiments using small laminated glass beams. These beams are tested in a configuration that is representative of laminated glass layups used in common architectural glazing applications. In addition, the beam test procedure is conducted at stress levels and load durations meaningful with respect to glass plates exposed to wind loadings.

The research conducted herein shows that it is possible to estimate the in situ shear modulus for common laminated glass interlayers using simple beam tests on relatively small beams. The development of this procedure required the design of an environmental testing chamber in which stress data were collected through a set of controlled physical experiments on laminated glass beams. Then, finite element analyses were used to determine the variation of the corresponding theoretical stress for the laminated glass beam as a function of interlayer shear modulus. These data were then used to derive a relationship for the variation of shear modulus as a function of temperature and load duration.

The procedure has been demonstrated on three different types of interlayer materials and geometries: freshly manufactured PVB, PVB that was manufactured over 10 years ago, and freshly manufactured SGP. In addition, this procedure was applied to the results from various research presented in the literature.

The major conclusions that can be drawn from this research are as follows:

1. This research demonstrates that it is possible to determine the interlayer shear modulus as a function of temperature and load duration using simple beam tests.
2. This test procedure appears to be more sensitive for estimating shear moduli as the laminated glass beam performance approaches the layered performance model.
3. Based on the limited amount of data presented herein, it appears that PVB may lose stiffness with age for temperatures from room temperature to about 120 °F. However, it must be remembered that the decade old PVB beams were stored in a temperature controlled unit without exposure to ultraviolent light or thermal cycling. If these two effects were taken into account, this conclusion might not hold up. How-

ever, if this assumption holds to further scrutiny, there are major implications for the design of laminated glass.

4. Most of the PVB shear moduli data reviewed or calculated appear to cluster in a relatively small range at temperatures from room temperature to 120 °F, except for the data extracted from the GRTL beam experiments.
5. Most of the PVB shear moduli data reviewed or calculated appear to cluster in a relatively small range at the customary laminated glass design temperature of 120 °F including data extracted from the GRTL beam experiments.
6. Based on the limited amount of data generated in this thesis, SGP appears to be stiffer than PVB for all temperatures tested.
7. The SGP data collected in this research agree more closely with the original SGP data presented by DuPont than data published more recently by DuPont.

It should be noted, that the purpose of this thesis was to present a procedure to determine the shear modulus for laminated glass interlayers and not to develop a full range of interlayer shear moduli for design purposes. Careful considerations should be taken when applying shear modulus results presented herein to the design of laminated glass.

Further research should be conducted to optimize this procedure. A comprehensive program needs to be developed that collects data from multiple laminated glass beams and can be used to estimate the interlayer shear modulus for the design of laminated glass. In addition, the observation regarding the stiffness reduction with age of the interlayer deserves additional scrutiny. Research should continue until sufficient data has been collected for the design of laminated glass.

REFERENCES

American Society for Testing and Materials (ASTM) (1989). "Standard practice for determining the minimum thickness of annealed glass required to resist a specified load." Annual Book of ASTM Standards, E-1300-89.

American Society for Testing and Materials (ASTM) (1994). "Standard practice for determining the minimum thickness and type of glass required to resist a specified load." Annual Book of ASTM Standards, E-1300-94.

American Society for Testing and Materials (ASTM) (2002). "Standard practice for determining load resistance of glass in buildings." Annual Book of ASTM Standards, E-1300-02.

American Society of Mechanical Engineers (ASME) (1963). "Engineering with glass." *Journal of Mechanical Engineering*, 85(3), 30-37.

Beason, W.L. (1980). "A failure prediction model for window glass." Ph.D. dissertation, Texas Tech Univ., Lubbock, Texas.

Beason, W.L., and Lingnell, A.W. (2000). "Emerging uses for window glass." *Emerging materials for civil infrastructure: state of the art*, R. A. Lopez-Anido and T. R. Naik, eds., ASCE, 190-216.

Beason, W.L., Meyers, G.E., and James, R.W. (1984). "Hurricane related window glass damage in Houston." *Journal of Structural Engineering*, 110(12), 2843-2857.

Beer, F.P., Johnston, E.R., and DeWolf, J.T. (2002). *Mechanics of materials*, McGraw-Hill, New York.

Behr, R.A., Minor, J.E., and Linden, M.P. (1986). "Load duration and interlayer thickness effects on laminated glass." *Journal of Structural Engineering*, 112(6), 1441-1453.

Behr, R.A., Minor, J.E., and Norville, H.S. (1993). "Structural behavior of architectural laminated glass." *Journal of Structural Engineering*, 119(1), 202-222.

Behr, R.A., Minor, J.E., Linden, M.P., and Vallabhan, C.V. (1985). "Laminated glass units under uniform lateral pressure." *Journal of Structural Engineering*, 111(5), 1037-1050.

Bennison, S.J., Qin, M.H.X., and Davies, P.S. (2008). "High-performance laminated glass for structurally efficient glazing." *HKIE/IStructE Joint Structural Division Annual Seminar: Innovative Light-weight Structures and Sustainable Facades*, Hong Kong.

Bennison, S.J., Smith, C.A., Duser, A.V., Jagota, A. (2002). "Structural performance of laminated glass made with a "stiff" interlayer." *The use of glass in buildings*, V.L. Block, eds., ASTM International, Pennsylvania, 57-65.

BOCA Basic/National Building Code (Boca) (1984). "Building enclosures, walls and wall thickness." Building Officials and Code Administrators International, Inc., Illinois, 249-254.

Brandrup, J., and Immergut, E.H. (1989). *Polymer handbook*, John Wiley and Sons, Inc., New York, 210-2, 258.

Callister, W.D. (2007). *Materials science and engineering: an introduction*, John Wiley and Sons, Inc., New York.

Chia, C. Y. (1980). *Nonlinear analysis of plates*, McGraw-Hill, New York.

Dice, J.A. (1992). "Development of a design procedure for architectural laminated glass window units." MS thesis, Texas A&M Univ., College Station, Texas.

DuPont Company (2004). "Engineering values for DuPont SentryGlas Plus." *Presentation to American Society of Testing and Materials (ASTM)*. (Private collection, M.S. Brackin)

Edel, M.T. (1997). "The effect of temperature on the bending of laminated glass beams." MS thesis, Texas A&M Univ., College Station, Texas.

Fariss, R.H. (1993). "Fifty years of safer windshields." *Chemtech*, 23(9), 38-43.

Gere, J.M. (2006). *Mechanics of materials*, Thompson, Canada.

Gere, J.M., and Timoshenko, S.P. (1997). *Mechanics of materials*, PWS Publishing Company, Massachusetts.

Hooper, J.A. (1973). "On the bending of architectural laminated glass." *International Journal of Mechanical Science (Great Britain)*, 15, 309-323.

Libbey Owens Ford Company (LOF) (1980). "Strength of glass under wind loads." File: #1 – Strength of Glass, ATS-109, Toledo, Ohio.

McLellan, G., and Shand, E. (1984). *Glass engineering handbook*, McGraw-Hill, New York.

Minor, J.E., and Reznik, P.L. (1990). "Failure strengths of laminated glass." *Journal of Structural Engineering*, 116(4), 1030-1039.

Norville, H.S., King, K.W., and Swofford, J.L. (1998). "Behavior and strength of laminated glass." *Journal of Structural Engineering*, 124(1), 46-53.

Pantelides, C.P., Horst, A.D., and Minor, J.E. (1991). "Experimental evaluation of architectural glazing products for tall buildings." *Proceedings of the Ninth Structures Congress*, 350-353.

SAFLEX (1989). "Polyvinyl butyral interlayer." Monsanto Company, Missouri.

Somayaji, S. (2001). *Civil engineering materials*, Prentice Hall, New Jersey.

Standard Building Code (SBC) (1985). "Glass." Southern Building Code Congress International, Inc. (SBCCI), Birmingham, Alabama, 345-348.

Stewart, R.A. (1991). "Laminated glass test results." *Presentation to American Society of Testing and Materials (ASTM) Task Group E06.51.13*. (Private collection, M.S. Brackin)

Timoshenko, S., and Woinowsky-Krieger, S. (1959). *Theory of plates and shells*, McGraw-Hill, New York, Toronto, London.

Ugural, A.C., and Fenster, S.K. (2008). *Advanced strength and applied elasticity*, Prentice Hall, New Jersey.

Uniform Building Code (UBC) (1982). "Glass and glazing." International Conference of Building Officials, 683-687.

Vallabhan, C.V., Das, Y.C., and Ramasamudra, M. (1992). "Properties of PVB interlayer used in laminated glass." *Journal of Materials in Civil Engineering*, 4(1), 71-76.

Vallabhan, C.V., Magdi, M., Asik, M., and Bailey, J.R. (1993). "Analysis of laminated glass units." *Journal of Structural Engineering*, 119(5), 1572-1585.

Vallabhan, C.V., Minor, J.E., and Nagalla, S.R. (1987). "Stresses in layered glass units and monolithic glass plates." *Journal of Structural Engineering*, 113(1), 36-43.

Young, J.F., Mindess, S., Gray, R.J., and Bentur, A. (1998). *The science and technology of civil engineering materials*, Prentice Hall, New Jersey.

APPENDIX A

ENVIRONMENTAL TESTING CHAMBER

To account for the effect temperature has on the stiffness of laminated glass interlayers, it is necessary to test the laminated glass beams in an environmentally controlled chamber. The environmental testing chamber held the laminated glass beams at a constant ambient temperature for the duration of loading and data collection. The environmental testing chamber was developed using a modified commercial vertical freezer.

A commercial vertical freezer was used to provide an insulated chamber. As well, the freezer had the capability of reaching temperatures below 0 °F. The freezer was modified by installing an apparatus for heating the chamber. Heating of the insulated chamber was achieved through the use of two 5-kilowatt heating strips and a low speed circulation blower. The use of heat strips allowed the chamber to reach uniform chamber temperatures in excess of 120 °F.

A digital, 24 volt, commercial thermostat control was used to maintain the chamber temperature. This device is shown in Fig. A-1. The thermostat had a temperature range capability from -30 to 220 °F. In addition, the thermostat had the ability to maintain the chamber temperature within a specified temperature differential. The temperature differential could range from 1 to 30 °F or °C. For the purposes herein, the temperature differential was set to 1 °F for all experiments.

FIG. A-1. 24 Volt Commercial Thermostat Control

Fig. A-2 shows the 24 volt contactors, relays, transformers, and time delays, used to maintain the desired chamber temperature. For the purposes herein the environmental testing chamber was setup for a testing temperature range of 30 to 120 °F.

FIG. A-2. 24 Volt Electronic Temperature Control System

Designed as a commercial freezer, little modifications were needed for cooling the chamber. The internal thermostat was disabled to allow the thermostat to control the chamber's temperature. Air flow for the freezer evaporator fan is shown in Fig. A-3. A uniform temperature is achieved throughout the chamber during cooling stages.

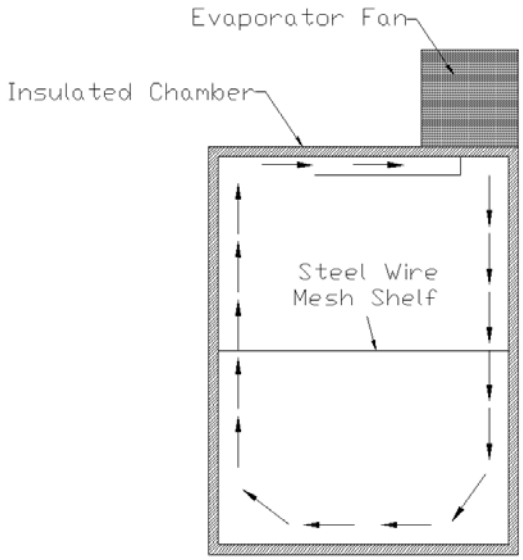

FIG. A-3. Environmental Testing Chamber Cooling Stage Air Flow

The freezer was modified to achieve chamber heating by removing a single door (Fig. A-4) and mounting an external heating device. The external heating device was made of ¾ in. plywood and housed two 5-kilowatt heating strips and a low speed circulation blower. This device is shown in Fig. A-5 through A-7.

FIG. A-4. Environmental Testing Chamber with a Single Door Removed

FIG. A-5. Low Speed Circulation Blower Setup

FIG. A-6. 5-Kilowatt Heating Strip Assembly

FIG. A-7. Externally Mounted Heating Device Assembly

The installation of this external heating device allowed for uniform temperature and air movement throughout the chamber during the heating stage. To make the chamber efficient the external heating device was insulated and sealed using foil tape and rubber duct sealant. The device was insulated using residential sheathing with an R-value of 3.0. Sealing the device pre-

vented the escape of conditioned air and slowed heat flow within the chamber. The insulation and sealant process is shown in Fig. A-8 and A-9.

FIG. A-8. Heating Device Insulation and Foil Tape

FIG. A-9. Heating Device Rubber Duct Sealant

During experiments, one gallon jugs filled with water were used as ballast inside the chamber to store energy. This allowed the freezer to rapidly recover the energy lost during beam

setup and exchange. Shown in Fig. A-10, ballast were placed in fashion as to surround the beam being tested. Further, this ensures minimal temperature variation during data collection.

FIG. A-10. Ballast of Water Used to Store Energy

To visually inspect the laminated glass beam during data collection, a quadruple glazed window was installed (Fig. A-11). The insulated window is comprised of four 10 in., square, single strength glass plates. The glass plates were incased by a 2x6 in., southern pine, wooden frame with three equally spaced air pockets between the glass plates. The wood case had four notched grooves into which the glass plates fit. Each grove was filled with silicone before the glass plate was inserted. The bottom space between each plate was filled with a moisture absorbing material approximately a ¼ in. deep. This eliminated issues of fogging from condensation due to the high temperature differentials. A simple 100 watt incandescent light fixture was used to illuminate the chamber for increased visibility through the viewing window.

FIG. A-11. Quadruple Glazed Viewing Window

APPENDIX B
CALCULATIONS

FULLY MONOLITHIC PERFORMANCE MODEL FOR DECADE OLD PVB

$$I_{total} = \frac{1}{12}bh^3 = \frac{1}{12}(6\ in)(0.317\ in)^3 = 0.015927507\ in^4$$

$$Gage\ Factor\ (GF) = \left(1 - \frac{offset}{L/2}\right) = \left(1 - \frac{2}{11}\right) = .8181$$

$$M_{gage} = \frac{PL}{4}(GF) = \frac{(25.7619\ lbs.)(22\ in)}{4}(.8181) = 115.93\ in\ lbs.$$

$$\sigma = \frac{Mc}{I} = \frac{(115.93\ in\ lbs.)(\frac{0.317\ in}{2})}{0.015927507\ in^4} = 1153.64\ psi$$

LAYERED PERFORMANCE MODEL FOR DECADE OLD PVB

$$I_{glass\ plate} = \frac{1}{12}bh^3 = \frac{1}{12}(6\ in)(0.129\ in)^3 = 0.001073345\ in^4$$

$$Gage\ Factor\ (GF) = \left(1 - \frac{offset}{L/2}\right) = \left(1 - \frac{2}{11}\right) = .8181$$

$$M_{gage} = \frac{PL}{4}(GF) = \frac{(12.88095\ lbs.)(22\ in)}{4}(.8181) = 57.96\ in\ lbs.$$

$$\sigma = \frac{Mc}{I} = \frac{(57.96\ in\ lbs.)(\frac{0.129\ in}{2})}{0.001073345\ in^4} = 3483.22\ psi$$

FULLY MONOLITHIC PERFORMANCE MODEL FOR FRESHLY MANUFACTURED PVB

$$I_{total} = \frac{1}{12}bh^3 = \frac{1}{12}(4\ in)(0.243\ in)^3 = 0.004782969\ in^4$$

$$Gage\ Factor\ (GF) = \left(1 - \frac{offset}{L/2}\right) = \left(1 - \frac{2}{11}\right) = .8181$$

$$M_{gage} = \frac{PL}{4}(GF) = \frac{(9.681\ lbs.)(22\ in)}{4}(.8181) = 43.56\ in\ lbs.$$

$$\sigma = \frac{Mc}{I} = \frac{(43.56\ in\ lbs.)(\frac{0.243\ in}{2})}{0.004782969\ in^4} = 1106.65\ psi$$

LAYERED PERFORMANCE MODEL FOR

FRESHLY MANUFACTURED PVB

$$I_{glass\ plate} = \frac{1}{12}bh^3 = \frac{1}{12}(4\ in)(0.107\ in)^3 = 0.000408348\ in^4$$

$$Gage\ Factor\ (GF) = \left(1 - \frac{offset}{L/2}\right) = \left(1 - \frac{2}{11}\right) = .8181$$

$$M_{gage} = \frac{PL}{4}(\ GF) = \frac{(4.8405\ lbs.)(22\ in)}{4}(.8181) = 21.78\ in\ lbs.$$

$$\sigma = \frac{Mc}{I} = \frac{(21.78\ in\ lbs.)\left(\frac{0.107\ in}{2}\right)}{0.000408348\ in^4} = 2853.82\ psi$$

FULLY MONOLITHIC PERFORMANCE MODEL FOR

FRESHLY MANUFACTURED SGP

$$I_{total} = \frac{1}{12}bh^3 = \frac{1}{12}(4\ in)(0.347\ in)^3 = 0.013927308\ in^4$$

$$Gage\ Factor\ (GF) = \left(1 - \frac{offset}{L/2}\right) = \left(1 - \frac{2}{11}\right) = .8181$$

$$M_{gage} = \frac{PL}{4}(GF) = \frac{(37.49044\ lbs.)(22\ in)}{4}(.8181) = 168.71\ in\ lbs.$$

$$\sigma = \frac{Mc}{I} = \frac{(168.71\ in\ lbs.)(\frac{0.347\ in}{2})}{0.013927308\ in^4} = 2101.67\ psi$$

LAYERED PERFORMANCE MODEL FOR

FRESHLY MANUFACTURED SGP

$$I_{glass\ plate} = \frac{1}{12}bh^3 = \frac{1}{12}(4\ in)(0.129\ in)^3 = 0.000715563\ in^4$$

$$Gage\ Factor\ (GF) = \left(1 - \frac{offset}{L/2}\right) = \left(1 - \frac{2}{11}\right) = .8181$$

$$M_{gage} = \frac{PL}{4}(GF) = \frac{(18.74522\ lbs.)(22\ in)}{4}(.8181) = 84.35\ in\ lbs.$$

$$\sigma = \frac{Mc}{I} = \frac{(84.35\ in\ lbs.)(\frac{0.129\ in}{2})}{0.000715563\ in^4} = 7603.52\ psi$$

LOAD VARIATION FROM WEIGHT BASKET, PARTIAL CHAIN LINKS, AND NYLON RECOIL HOSE

$$I_{monolithic} = \frac{1}{12}bh^3 = \frac{1}{12}(4\ in)(0.225\ in)^3 = 0.003796875\ in^4$$

$$\sigma = \varepsilon * E = (19.5\ \mu\varepsilon)(10.4 * 10^{-6}\ psi) = 202.8\ psi$$

$$Gage\ Factor\ (GF) = \left(1 - \frac{offset}{L/2}\right) = \left(1 - \frac{2}{11}\right) = .8181$$

$$M_{max} = \frac{\sigma I}{c(GF)} = \frac{(202.8\ psi)(0.003796875\ in^4)}{(\frac{0.225\ in}{2})(.8181)} = 8.3655\ in\ lbs.$$

$$P = \frac{4 * M_{max}}{L} = \frac{4(8.3655\ in\ lbs.)}{22\ in} = 1.521\ lbs.$$

¼ MONOLITHIC GLASS PLATE BENDING THEORY

$$P_{Large\ Brick} = 4.49618\ lbs.$$

$$I_{monolithic} = \frac{1}{12}bh^3 = \frac{1}{12}(4\ in)(0.225\ in)^3 = 0.003796875\ in^4$$

$$Gage\ Factor\ (GF) = \left(1 - \frac{offset}{L/2}\right) = \left(1 - \frac{2}{11}\right) = .8181$$

$$M_{gage} = \frac{PL}{4}(GF) = \frac{(4.49618\ lbs.)(22\ in)}{4}(.8181) = 20.23\ in\ lbs.$$

$$\sigma = \frac{Mc}{I} = \frac{(20.23\ in\ lbs.)(\frac{0.225\ in}{2})}{0.003796875\ in^4} = 599.49\ psi$$

$$\varepsilon = \frac{\sigma}{E} = \frac{599.49\ psi}{10.4 * 10^6\ psi} = 57.64\ \mu\varepsilon$$

APPENDIX C

EXPERIMENTAL EFFORT DATASHEETS

TABLE C-1. Freshly Manufactured PVB Laminated Glass Beam 30 °F Datasheet

Time (S)	µЄ	T *(°F)*
3	107	30
5	109	30
10	108	30
60	108	30
300	108.5	29
600	109	29
1200	109	29
2400	109.5	29
3600	110	29

TABLE C-2. Freshly Manufactured PVB Laminated Glass Beam 40 °F Datasheet

Time (S)	µЄ	T *(°F)*
3	110	40
5	106	40
10	107	40
60	108	40
300	108	41
600	109	40
1200	109	40
2400	111	40
3600	112	40

TABLE C-3. Freshly Manufactured PVB Laminated Glass Beam 60 °F Datasheet

Time (S)	µЄ	T *(°F)*
3	112	60
5	113	60
10	115	60
60	125	60
300	141	60
600	150	60
1200	159.5	60
2400	169.5	59
3600	175	59

TABLE C-4. Freshly Manufactured PVB Laminated Glass Beam 80 °F Datasheet

Time (S)	µЄ	T *(°F)*
3	160	83
5	164	83
10	168	83
60	176	84
300	181	83
600	184	82
1200	185	84
2400	196	79
3600	189	83

TABLE C-5. Freshly Manufactured PVB Laminated Glass Beam 100 °F Datasheet

Time (S)	µЄ	T *(°F)*
3	176	102
5	177	102
10	178	102
60	184	103
300	189	96
600	189	104
1200	191	100
2400	196	98
3600	192	104

TABLE C-6. Freshly Manufactured PVB Laminated Glass Beam 120 °F Datasheet

Time (S)	µЄ	T *(°F)*
3	184	124
5	188	124
10	192	124
60	199	124
300	207	124
600	210	124
1200	214	124
2400	216	125
3600	220	126

TABLE C-7. Decade Old PVB Laminated Glass Beam 30 °F Datasheet

Time (S)	µЄ	T *(°F)*
3	125	29
5	122	29
10	122	29
60	123	29
300	124	30
600	125.5	30
1200	127.5	30
2400	130	31
3600	132	30

TABLE C-8. Decade Old PVB Laminated Glass Beam 40 °F Datasheet

Time (S)	µЄ	T *(°F)*
3	125	41
5	123	41
10	124	41
60	128	41
300	137	41
600	143	41
1200	153	41
2400	165	41
3600	173	41

TABLE C-9. Decade Old PVB Laminated Glass Beam 60 °F Datasheet

Time (S)	µЄ	T *(°F)*
3	152	61
5	165	61
10	181	61
60	218	61
300	244	61
600	253	61
1200	261	60
2400	268	60
3600	271	60

TABLE C-10. Decade Old PVB Laminated Glass Beam 80 °F Datasheet

Time (S)	µЄ	T *(°F)*
3	240	82
5	245	82
10	251	82
60	260	82
300	267	83
600	269	84
1200	275	82
2400	278	83
3600	284	80

TABLE C-11. Decade Old PVB Laminated Glass Beam 100 °F Datasheet

Time (S)	µЄ	T *(°F)*
3	265	101
5	263	101
10	266	101
60	274	101
300	281	103
600	286	102
1200	290	102
2400	293	102
3600	295	102

TABLE C-12. Decade Old PVB Laminated Glass Beam 120 °F Datasheet

Time (S)	µЄ	T *(°F)*
3	268	122
5	276	122
10	280	122
60	291	122
300	301	121
600	305	122
1200	309	122
2400	312	122
3600	315	122

TABLE C-13. Freshly Manufactured SGP Laminated Glass Beam 40 °F Datasheet

Time (S)	**µЄ**	**T** *(°F)*
3	214	41
5	214	41
10	219	41
60	220	41
300	220	42
600	221	41
1200	221	41
2400	221	40
3600	222	40

TABLE C-14. Freshly Manufactured SGP Laminated Glass Beam 60 °F Datasheet

Time (S)	µЄ	T *(°F)*
3	225	60
5	219	60
10	221	60
60	222	60
300	222	60
600	223	60
1200	223	60
2400	223	61
3600	223.5	60

TABLE C-15. Freshly Manufactured SGP Laminated Glass Beam 80 °F Datasheet

Time (S)	με	T *(°F)*
3	222	82
5	224	82
10	222	82
60	223	81
300	224	81
600	225	82
1200	227	82
2400	227	82
3600	230	81

TABLE C-16. Freshly Manufactured SGP Laminated Glass Beam 100 °F Datasheet

Time (S)	με	T *(°F)*
3	227	102
5	224	102
10	224	102
60	227	102
300	231	102
600	234	102
1200	240	102
2400	247	102
3600	252	102

TABLE C-17. Freshly Manufactured SGP Laminated Glass Beam 120 °F Datasheet

Time (S)	με	T *(°F)*
3	229	120
5	244	120
10	249	120
60	264	120
300	284	124
600	297	124
1200	304	125
2400	317	123
3600	322	124

VITA

Michael Scott Brackin

Safety & Structural Systems Division

Texas Transportation Institute

Texas A&M University System

3135 TAMU

College Station, Texas, 77843-3135

Michael Scott Brackin received his Bachelor of Science degree in Civil Engineering from Texas A&M University in December 2008. Upon graduation, he began academics for a Master of Science degree in Civil Engineering, specializing in Structural Engineering, at Texas A&M University. During his tenure at Texas A&M University, Mr. Brackin worked for Texas Transportation Institute's (TTI) Road Side Safety and Structural Division. While at TTI, his time was spent designing roadside safety systems and structures through the use of finite element analysis. His scope of work included classified projects for the Department of Homeland Security and Department of State. Mr. Brackin received his Master of Science degree in Civil Engineering, specializing in Structural Engineering, on May 2010.